

Some pages of this thesis may have been removed for copyright restrictions.

If you have discovered material in AURA which is unlawful e.g. breaches copyright, (either yours or that of a third party) or any other law, including but not limited to those relating to patent, trademark, confidentiality, data protection, obscenity, defamation, libel, then please read our [Takedown Policy](#) and [contact the service](#) immediately

RETINAL VESSEL ANALYSIS:
FLICKER REPRODUCIBILITY,
METHODOLOGICAL STANDARDISATIONS
AND PRACTICAL LIMITATIONS

ANGELOS KALITZEOS
Doctor of Philosophy

ASTON UNIVERSITY
September 2013

©Angelos Kalitzeos, 2013
Angelos Kalitzeos asserts his moral right to be identified as the author of this thesis

This copy of the thesis has been supplied on condition that anyone who consults it is understood to recognise that its copyright rests with its author and that no quotation from the thesis and no information derived from it may be published without proper acknowledgement.

Aston University

Retinal Vessel Analysis: Flicker Reproducibility, Methodological Standardisations
and Practical Limitations

Angelos Kalitzeos

Doctor of Philosophy

2013

Thesis Summary:

The Retinal Vessel Analyser (RVA) is a commercially available ophthalmoscopic instrument capable of acquiring vessel diameter fluctuations in real time and in high temporal resolution. Visual stimulation by means of flickering light is a unique exploration tool of neurovascular coupling in the human retina. Vessel reactivity as mediated by local vascular endothelial vasodilators and vasoconstrictors can be assessed non-invasively, *in vivo*. In brief, the work in this thesis

- deals with interobserver and intraobserver reproducibility of the flicker responses in healthy volunteers
- explains the superiority of individually analysed reactivity parameters over vendor-generated output
- links in static retinal measures with dynamic ones
- highlights practical limitations in the use of the RVA that may undermine its clinical usefulness
- provides recommendations for standardising measurements in terms of vessel location and vessel segment length and
- presents three case reports of essential hypertensives in a 5-year follow-up.

Strict standardisation of measurement procedures is a necessity when utilising the RVA system. Agreement between research groups on implemented protocols needs to be met, before it could be considered a clinically useful tool in detecting or predicting microvascular dysfunction.

Keywords: Cardiovascular Disease, Autoregulation, Blood Pressure, Endothelial Function

Contents

List of Figures	7
List of Tables	9
1 Overview of principal literature	11
1.1 The Heart	11
1.1.1 Cardiac Anatomy and Physiology	11
1.1.2 Conduction System	11
1.2 Cardiovascular System	12
1.2.1 Blood Flow	12
1.2.2 Arterial Blood Pressure	13
1.2.3 Regulation of Blood Pressure	14
1.2.3.1 Mean Arterial Blood Pressure and Pulse Pressure	15
1.3 Diagnostic Tests and Procedures	16
1.3.1 Ambulatory BP Monitoring	16
1.3.1.1 Ambulatory Arterial Stiffness Index	17
1.3.2 Electrocardiography	17
1.3.2.1 Ambulatory ECG Monitoring	19
1.3.2.2 Heart Rate Variability	20
1.3.3 CardioTens 24-hour ECG and BP monitoring	23
1.4 Hypertension	24
1.4.1 Definition and Classification of Hypertension	24
1.4.2 Management of Hypertension	25
1.5 Peripheral Circulation	25
1.6 The Eye	26
1.6.1 Retinal Vasculature	26
1.6.2 Posterior Eye Haemodynamics	27
1.7 Qualitative Retinal Analysis	27
1.7.1 The Keith-Wagener-Barker Classification	28

Contents

1.8	Quantitative Retinal Analysis	29
1.8.1	Assessing Retinal Structure	29
1.8.1.1	Arterio-Venous Ratio	29
1.8.1.2	Vessel Tortuosity Index	31
1.8.1.3	Bifurcation Angles and Junction Exponents	33
1.8.1.4	Length-to-Diameter Ratio	34
1.8.2	Assessing Retinal Vessel Dynamics	34
1.8.2.1	Retinal Vessel Analyser	34
1.8.2.2	Flicker Provocation	36
1.8.2.3	Dynamic Response Analysis	37
1.8.2.4	Other External Provocations	39
1.8.3	Retinal Oximetry	39
1.8.4	Visual Field Testing	40
1.9	Nailfold Capillaroscopy	40
1.9.1	Measurement Principle	41
1.9.2	CapiScope Capillaroscopy System	41
2	Retinal Vessel Analyser: Reproducibility	43
2.1	Background	43
2.1.1	Motivation and Research Rationale	44
2.1.2	Aims	44
2.2	Subjects and Methods	45
2.2.1	Interobserver Reproducibility	45
2.2.2	Intraobserver Reproducibility	45
2.2.3	Standardisations Applied	45
2.2.4	Inclusion and Exclusion Criteria	45
2.2.5	Study Protocol	46
2.2.5.1	Intraocular Pressure Measurement	46
2.2.5.2	Blood Pressure and Pulse Assessment	46
2.2.5.3	Retinal Vessel Functional Assessment	46
2.2.5.4	Retinal Vessel Structural Assessment	47
2.2.6	Outcome Measures	48
2.2.7	Dynamic Parameters	48
2.2.8	Static Parameters	50
2.2.9	Statistics and Data Analysis	50

Contents

2.3	Results	50
2.3.1	Interobserver Reproducibility	50
2.3.1.1	Subjects	50
2.3.1.2	Retinal Vessels' Absolute Diameters	50
2.3.1.3	Inbuilt Dynamic Flicker Response Analysis	51
2.3.1.4	Independent Dynamic Flicker Response Analysis	51
2.3.1.5	Comparison Between Inbuilt and Independent Analysis	52
2.3.1.6	Averaged Flicker Responses	57
2.3.2	Intraobserver Reproducibility	57
2.3.2.1	Subjects	57
2.3.2.2	Retinal Absolute Diameters	59
2.3.2.3	Inbuilt Dynamic Flicker Response Analysis	59
2.3.2.4	Independent Dynamic Flicker Response Analysis	59
2.3.2.5	Comparison Between Inbuilt and Independent Analysis	63
2.3.2.6	Averaged Flicker Responses	65
2.3.2.7	Static Retinal Vessel Parameters	65
2.3.2.8	Multiple Regression Analysis	65
2.4	Discussion	67
2.4.1	Interobserver Reproducibility Study	67
2.4.2	Intraobserver Reproducibility Study	68
2.5	Conclusions	71
3	Location and Length Influence on Vessel Reactivity	73
3.1	Background	73
3.1.1	Motivation and Research Rationale	74
3.2	Subjects and Methods	75
3.2.1	Data Collection	75
3.2.2	Data Processing	76
3.2.2.1	Analysis per Location	76
3.2.2.2	Analysis per Segment's Length	77
3.2.3	Data and Statistical Analysis	77
3.3	Results	78
3.3.1	Baseline Characteristics	78
3.3.2	Comparison Across Vessel Segments	78
3.3.3	Flicker Responses Variability as a Function of Location	80
3.3.4	Comparison Between Segment Lengths	80

Contents

3.4	Discussion	84
3.4.1	Measurement Location Considerations	84
3.4.2	Measurement Length Considerations	90
3.5	Conclusions	91
4	Essential Hypertension: Case Reports	92
4.1	Introduction and Motivation	92
4.2	Ethical Approval	92
4.3	Methods and Subjects	92
4.3.1	Day 1 - Ambulatory BP and ECG Monitoring	92
4.3.1.1	Outcome Measures	93
4.3.2	Day 2 - Eye examinations	93
4.3.2.1	Intraocular Pressure Measurement	93
4.3.2.2	Retinal Functional Analysis	93
4.3.2.3	Outcome Measures	93
4.3.3	Data Analysis	94
4.4	Results	94
4.4.1	Sample	94
4.4.2	24hr BP and ECG Monitoring	94
4.4.3	Retinal Functional Assessment	94
4.5	Discussion	95
	Bibliography	99
	Acronyms	114
	Appendix	116

List of Figures

1.1	Primary physiologic factors affecting certain physical factors.	14
1.2	Graphical representation of the blood pressure wave.	16
1.3	Two complete, normal ECG cycles.	19
1.4	Modified three-electrode bipolar lead system.	20
1.5	The time series of R-R intervals, i.e. tachogram.	21
1.6	Power Spectral Density of the tachogram in Figure 1.5.	23
1.7	Set-up window of the CardioVisions software.	24
1.8	Normal fundus image of a left eye, ONH centered, 30°.	26
1.9	Normal fundus image of a right eye, macula centered, 50°.	26
1.10	Concentric AVR measurement rings as defined by the ARIC study.	31
1.11	Schematic representation of the standard flicker measurement protocol.	36
1.12	A typical, normal arterial and venular flicker response.	38
2.1	Typical measurement location.	47
2.2	Measurement of the Arterio-Venous Ratio.	48
2.3	Illustration of bifurcation angles measurement using ImageJ.	49
2.4	Illustration of tortuosity measurement using ImageJ.	49
2.5	Arteriolar diameter fluctuation and responses across all three flickers.	54
2.6	Arteriolar reaction and constriction times across all three flickers.	55
2.7	Venular diameter fluctuation and responses across all three flickers.	56
2.8	Venular reaction times across all three flickers.	56
2.9	Arteriolar diameter fluctuation and responses across all three flickers.	62
2.10	Arteriolar reaction and constriction times across all three flickers.	63
2.11	Venular diameter fluctuation and responses across all three flickers.	64
2.12	Venular reaction times across all three flickers.	64
3.1	RVA's measuring window.	75
3.2	Illustration of measured locations.	77
3.3	Maximum Dilation Response and MABP Correlation.	82

List of Figures

3.4	Comparison between segment length: Arteries.	85
3.5	Comparison between segment length: Veins.	86
4.1	5 years follow-up: Subject JH.	96
4.2	5 years follow-up: Subject JW.	96
4.3	5 years follow-up: Subject TR.	97

List of Tables

1.1	Statistical measures of HRV used in time domain analysis.	21
1.2	Geometrical measures of HRV used in time domain analysis.	22
1.3	Classification of hypertension based on blood pressure levels.	24
1.4	Keith-Wagener-Barker hypertension classification system.	28
1.5	Vendor-supplied software vessel response classification scheme.	37
2.1	Sample demographics and baseline characteristics.	51
2.2	Comparison of absolute arteriolar and venular diameters.	52
2.3	Inbuilt Dynamic Flicker Response Analysis.	52
2.4	Independent Dynamic Flicker Response Analysis.	53
2.5	Reaction and Constriction Time Response Analysis.	55
2.6	Inbuilt and Independent Analysis Comparison.	57
2.7	Independent Dynamic Flicker Response Analysis.	58
2.8	Reaction and Constriction Time Response Analysis.	58
2.9	Sample baseline characteristics.	58
2.10	Comparison of absolute arteriolar and venular diameters.	59
2.11	Inbuilt Dynamic Flicker Response Analysis.	59
2.12	Independent Dynamic Flicker Response Analysis.	60
2.13	Reaction and Constriction Time Response Analysis.	61
2.14	Inbuilt and Independent Flicker Analysis Comparison.	63
2.15	Independent Dynamic Flicker Response Analysis.	66
2.16	Reaction and Constriction Time Response Analysis.	66
2.17	Static Retinal Vessel Parameters.	66
3.1	Vessel Segments Absolute Diameters and Baseline Characteristics.	78
3.2	Extended Vessel Segments Analysis: Flicker Responses.	79
3.3	Extended Vessel Segments Analysis: Reaction Times.	81
3.4	Extended Vessel Segments Analysis: Averaged Flicker Responses.	81
3.5	Extended Vessel Segments Analysis: Averaged Reaction Times.	82

List of Tables

3.6	Parameters' Variability as a Function of Location.	83
3.7	Comparison of Long and Short Segments.	83
3.8	Diameter Deviation Between Long and Short Segments.	87
4.1	Blood Pressure and Heart Rate Variability Parameters.	95
4.2	RVA parameters across a five-year follow up.	97

Chapter 1

Overview of principal literature

1.1 The Heart

1.1.1 Cardiac Anatomy and Physiology

The circulatory system of an adult individual contains a volume of approximately 5 litres of blood (Rogers, 2010). The body organ responsible for its circulation to every tissue is the heart. Anatomically, the heart consists of four muscular chambers; the right and left atria (superiorly) and the right and left ventricles (inferiorly). These are pairwise interconnected via two valves; the tricuspid and the mitral valve respectively. Exteriorly to the heart, these chambers are connected to the largest blood vessels of the human body; the vena cavæ (the superior and the inferior) and the aorta. Oxygen-deprived blood is fed to the heart via the vena cavæ, entering into the right atrium. Blood flow continues through the tricuspid valve into the right ventricle, while the valve opens and the atrium contracts (atrial systole). In turn, as soon as the right ventricle fills with blood, it contracts as well (ventricular systole). At the same time another valve, the pulmonary valve, opens up to let blood through to the pulmonary arteries to be pumped into the lungs. In the lungs, carbon dioxide is released and oxygen is absorbed. Now, oxygen-rich blood returns to the heart via the pulmonary veins and correspondingly passes through the left atrium, the mitral valve and into the left ventricle. This occurs at the same time as a new contraction is taking place in the heart's right atrium-ventricle. The final valve that opens simultaneously with left ventricular contraction is the aortic valve. Here, blood is pumped into the aorta to be distributed further out towards the body's organs and tissues.

1.1.2 Conduction System

The aforementioned muscle contractions are driven by a series of electrical impulses (action potentials) generated by a group of specialised cells in the right atrium, the cardiomyocytes. The tissue that comprises these cells is called the Sinoatrial (SA) node, also known as the

heart's "natural pacemaker". The conduction pathway of the heart is made up of the following specialised heart tissues: the Atrioventricular (AV) node, the bundle of His, the right and left bundle branches and the Purkinje fibres, successively. Finally, the actual contraction function is performed by the contractile cells of the heart. These provide the necessary kinetic and potential energy for blood to propagate through the circulatory system.

Cardiac function is altered by neural activation. The heart is innervated by both the Sympathetic Nervous System (SNS) (adrenergic) and the Parasympathetic Nervous System (PNS) (cholinergic). The two systems work in tandem; the former is known to be the accelerator of the heart, whereas the latter serves as the heart's decelerator. Epinephrine and norepinephrine are the two main chemical mediators that increase Heart Rate (HR), AV conduction and contractility, via the SNS. The overall effect of sympathetic contribution is to increase Cardiac Output (CO), Systemic Vascular Resistance (SVR) and arterial Blood Pressure (BP). The time necessary for the SNS to actuate these effects is in the order of 15 seconds (Clifford et al., 2006). This compensating mechanism is particularly important during exercise, emotional stress and haemorrhagic shock. On the other hand, parasympathetic innervation of the heart is controlled by the vagus nerve. Parasympathetic activity therefore is sometimes termed vagal activity. In contrast with the SNS, the vagus nerve acts quickly, carrying impulses that lower HR and decelerate or block AV conduction, via acetylcholine release, within a second.

1.2 Cardiovascular System

1.2.1 Blood Flow

The flow of fluids with viscosity (η) through rigid, cylindrical tubes of length (L) and radius (r) in hydraulic systems obey the Poiseuille-Hagen law (Pournaras et al., 2008) that expresses the relation between the fluid flow (Q) and the pressure difference (or else perfusion pressure) (ΔP):

$$Q = \frac{\Delta P \pi r^4}{8 \eta L} = \frac{\Delta P}{R} \quad (1.1)$$

The above expression assumes long, straight tubes, a Newtonian fluid and steady, laminar flow conditions. Despite the fact that these assumptions are not entirely true for the human vascular system, the flow, pressure and resistance relationships still remain applicable. Hence, in analogy to electrical circuits and Ohm's law, the rate of blood flow (Q) is inversely proportional to vascular resistance (R). From Equation (1.1):

$$R \propto \frac{\eta L}{r^4} \quad (1.2)$$

In health, blood viscosity does not fluctuate, assuming constant haematocrit and temperature, thus it can be considered constant (Klabunde, 2011). Similarly, vessel length is constant. Therefore, the major determinant of resistance to blood flow through a blood vessel is its calibre (diameter is directly proportional to radius), since it is proportional to $1/r^4$ (Equation (1.2)). This means that a potential halving of blood vessel radius increases resistance 16-fold and vice versa. It is evident that subtle vessel calibre fluctuations can yield marked changes in vascular resistance and consequently in blood flow.

Due to their small diameter (i.e. less than $200\mu\text{m}$), arterioles are termed resistance vessels and may regulate local blood flow in their surrounding tissues (Klabunde, 2011). The extrinsic regulation is mediated via a twofold pathway; the Autonomic Nervous System (ANS) and the endocrine system. At rest, arterioles receive a baseline level of autonomic stimulation which makes them slightly constricted, known as the vascular tone. Vasodilation is reached by decrease of sympathetic stimulation below baseline levels and vasoconstriction by increase above the baseline. Other mechanisms controlling vasomotor response, intrinsic to the vessels this time, take the form of metabolic and myogenic control; the former is incurred by metabolite accumulation according to the rate of metabolic activity and the latter by smooth muscle relaxation or contraction. Metabolic regulation is mainly mediated by vascular endothelial cells and local neural tissue surrounding the vessels, which release vasoactive molecules. The most potent vasodilator is known to be Nitric Oxide (NO) and conversely endothelin-1 is the most potent vasoconstrictor (Haefliger et al., 1993). The myogenic responses for blood flow vascular autoregulation are mediated by pericytes and smooth muscle cells. Myogenic vascular tone is a function of artery wall stretch and depends on the presence of calcium in the extracellular space (Bevan et al., 1986).

1.2.2 Arterial Blood Pressure

The arterial vascular network is considered to be physically determined by its elastic characteristics (compliance) and the blood volume circulating in it. The arterial volume in turn depends on the inflow rate from the heart into the arteries (CO) and the outflow rate from the arteries through the resistance vessels (arterioles) into tissues and body organs (Figure 1.1). In the resting state, these peripheral organs are supplied with blood according to their metabolic needs. From the law of conservation of mass, given that the vascular system is a closed-loop circuit, if the heart pumps blood at a higher rate than it is fed through veins, then the arterial walls need to expand, giving a pressure rise and vice versa.

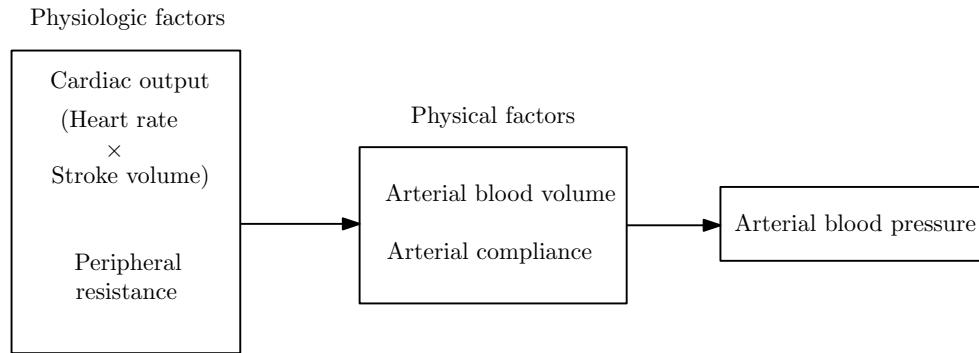


Figure 1.1: Primary physiologic factors affecting certain physical factors which, in turn, determine arterial blood pressure. Adapted from Berne and Levy (1997) (p. 142)

Arterial BP is the force of blood against artery walls due to the pumping of the heart. BP is defined by the two extremes of systemic BP, namely systolic and diastolic pressure. Systolic Blood Pressure (SBP) is the highest measured value obtained during ventricular contraction (during a heartbeat), whereas Diastolic Blood Pressure (DBP) is the lowest measured value obtained during ventricular relaxation (between heartbeats). BP is measured in millimeters of mercury (mmHg). Automatic, digital BP devices using the oscillometric measurement method are clinically used. Measurement is performed by occluding the artery of an extremity (arm, wrist, finger, or leg) with an inflatable cuff (Beevers et al., 2001).

1.2.3 Regulation of Blood Pressure

In physiologic conditions, whenever the sympathetic system is activated, the body down-regulates parasympathetic activity and vice versa. These two branches of the ANS are rarely completely activated or deactivated; instead the body adjusts their levels of activation appropriately to its needs. On that basis, the ANS makes HR adjustments via sensors located throughout the body. These sensors include the baroreceptors which exist in all mammalian arteries and sense the arterial pressure. They are a type of mechanoreceptor and respond to arterial wall stretching, in a negative feedback loop fashion. If arterial pressure (mean, pulse or both, see Section 1.2.3.1) rises abruptly, then vessel walls passively dilate in order to accommodate this pressure rise. Consequently, the baroreceptors get activated and fire action potentials to a degree proportional to the change in pressure. The baroreceptor firing has an inhibitory effect on sympathetic outflow and a boosting effect on vagal outflow, hence driving BP down. Also, these autonomic changes cause vasoconstriction (increased SVR) and decreased CO. The reduction in CO results from both a decreased HR and a reduced force of AV contraction, dropping arterial BP. The reverse action is taking place in case of a sudden pressure drop, sustaining arterial BP at normal levels at all times. This is known as the baroreceptor

reflex or simply baroreflex, one of the body's mechanisms capable of maintaining homoeostasis. Baroreflex sensitivity is now a prognostic factor in cardiology; it is significantly altered during certain disease states (La Rovere et al., 1988).

1.2.3.1 Mean Arterial Blood Pressure and Pulse Pressure

When BP is clinically measured, the systolic and diastolic values are recorded. But two additional ways of characterizing BP are important to consider. Physiologically, the pressure that is primarily regulated and considered a better indicator of perfusion (than SBP) to vital organs, is the Mean Arterial Blood Pressure (MABP). MABP, measured in mmHg, is the pressure in the arteries averaged over a single cardiac cycle duration and can be approximated from the following empirical formula:

$$\text{MABP} \approx \frac{2}{3}\text{DBP} + \frac{1}{3}\text{SBP} \quad (1.3)$$

Since the heart spends more time in the relaxing state (diastole) than in the contracting state (systole), DBP has a greater effect on MABP. For example, if systolic pressure is 120 mmHg and diastolic pressure is 80 mmHg, then MABP is approximately 93 mmHg using the above calculation. A MABP of at least 60 mmHg is necessary to perfuse the coronary arteries, brain, and kidneys. Factors that determine MABP are CO and SVR, according to the following relationship (based on Equation (1.1)) :

$$\text{MABP} \approx \text{CO} \cdot \text{SVR} \quad (1.4)$$

As the left ventricle ejects blood into the aorta, the aortic pressure increases. The maximal change in aortic pressure during systole represents the aortic pulse pressure. Pulse Pressure (PP) is defined as the difference between arterial systolic and diastolic pressures. Thus, Equation (1.3) can be rewritten as:

$$\text{MABP} \approx \text{DBP} + \frac{1}{3}\text{PP} \quad (1.5)$$

Using the same numeric example as previously (SBP/DBP equal to 120/80 mmHg) then PP equals to 40 mmHg. The rise in aortic pressure from its diastolic to systolic value is determined by the compliance of the aorta as well as the ventricular Stroke Volume (SV). The stroke volume is the amount of blood injected into arteries by each heart beat:

1 Overview of principal literature

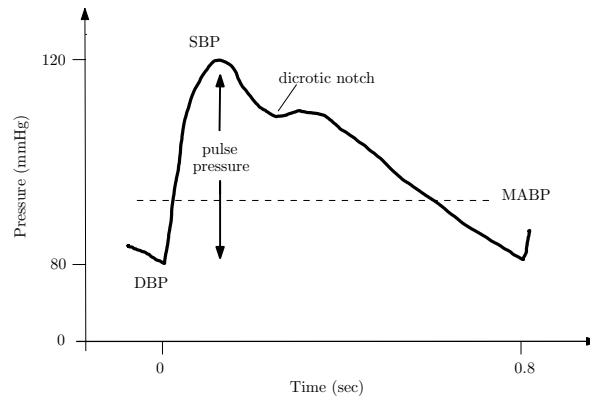


Figure 1.2: Graphical representation of the BP wave. $SBP - DBP = PP$. The dicrotic notch is caused by the aortic valve closure. MABP is defined according to Equation (1.3). Duration of a cardiac cycle is approximately 800 msec.

$$SV = \frac{CO}{HR} \quad (1.6)$$

The greater the stroke volume the heart pumps out, the greater the change in aortic pressure. Compliance is simply a measure of the capacity of the arterial system to accommodate further increases in volume ($\Delta\text{volume} / \Delta\text{pressure}$). At given stroke volumes, the pressure increase is determined by the vessel compliance. Flexible arteries that expand easily have high compliance, contrary to stiff arteries. The aorta's walls, being the most compliant vessel walls throughout the arterial system, expand to accommodate the increase in blood volume with ventricular ejection. The more compliant a vessel, the smaller the pressure change during cardiac cycles (i.e. smaller PP). Aortic compliance decreases with age or disease (e.g. arteriosclerosis) due to structural changes, thereby producing age-dependent increases in PP. In general, both an abnormally high PP and MABP are risk factors for cardiovascular disease (Dart and Kingwell, 2001).

1.3 Diagnostic Tests and Procedures

1.3.1 Ambulatory BP Monitoring

Since BP is depending on factors such as age, gender, time of day (Millar-Craig et al., 1978), diet, cardiac cycle (Knudtson et al., 2004; Chen et al., 1994), stress and physical activity (Anuradha et al., 2011) it is evident that isolated, clinic BP measurements have inherent limitations and may not be representative of the true BP in many patients. The white-coat effect, referring to a BP increase occurring at the time of a clinic visit and attenuating soon thereafter, may be an additional obstacle to true BP assessment (Pickering et al., 2002). An alternative

method of measuring BP in clinical practice is self-monitoring or home monitoring. Multiple measurements at home enable a better estimate of the average or true pressure, it is cost-effective and usually eliminates the white-coat effect (Verberk et al., 2007). Nevertheless, it is prone to measurement bias due to unreliable procedures when obtaining BP.

Portable BP monitors that can be fitted for durations of 24 to 48 hours and can obtain and record regular BP readings have become widely accepted as a clinically useful tool for diagnosing and managing Hypertension (HT) (Waeber et al., 2007). Rather than measuring BP when patients are remaining under artificial clinic conditions, BP behaviour is recorded during their usual daily activities. Ambulatory Blood Pressure Monitoring (ABPM) offers a wealth of BP related information that no other method can provide. Mapping of diurnal variation of BP, calculating arterial stiffness indices and pinpointing transient BP events would not be achieved without the advent of ABPM. Measurement frequency during a typical 24-h period is generally not recommended to be greater than every 15 minutes (which could interfere with routine activities), neither less frequent than every 30 minutes (which could give an inadequate amount of measurements). Pieces of evidence from cardiovascular event-based, longitudinal studies have been made available, that ABPM improves cardiovascular risk stratification over and beyond traditional risk factors, including conventional clinic BP measurement (Verdecchia, 2000).

1.3.1.1 Ambulatory Arterial Stiffness Index

Another surrogate marker of arterial stiffness derived from ABPM that may predict cardiovascular mortality is the Ambulatory Arterial Stiffness Index (AASI) (Dolan et al., 2006). AASI is derived graphically by plotting DBP against SBP readings from unedited 24-hour recordings and obtaining the slope of the regression line. AASI is then calculated as one minus the regression slope. It is a novel measure which has been shown to be an integrated measure, which is characteristic for an individual and reflects the combined effects of left ventricular ejection, active and passive components of arterial stiffness, and the reflection of the arterial pulse wave (Li et al., 2006). Prior to the introduction of AASI, researchers were using PP as a measure of arterial stiffness. However, PP only reflects a static difference between systolic and diastolic pressure and does not exploit the dynamic relation between diastolic and systolic blood pressure throughout the whole day as AASI does.

1.3.2 Electrocardiography

The electrical activity of the heart can be monitored in a non-invasive manner by means of an electrocardiograph. Changes occurring in the membrane potential of cardiac muscle cells during consecutive cardiac cycles are added up to produce an Electrocardiogram (ECG). ECG

recordings provide a plethora of information about cardiac structure and function over time. It is widely used in clinical practice to diagnose heart disorders including cardiac arrhythmias. A number of electrodes are attached to the skin at pre-specified positions sensing the electrical currents which propagate from the heart's surrounding tissue to the skin surface. These weak, at first, electrical currents are transmitted to an ECG device, amplified and transformed into ECG traces that represent the heart's systole-diastole cycle. A schematic representation of an ECG tracing is shown in Figure 1.3.

Cardiac cells at rest are considered polarised. When a stimulus occurs (SA node firing), ions cross the cell membrane and cause an action potential resulting in atrial contraction. This is called depolarisation and is represented by the P wave. The electrical impulse arrives at the AV node where it is delayed by 40 milliseconds. Albeit minute, this delay is critical: it allows the atria to fully contract and eject blood into the ventricle. At the same time, it keeps the ventricle from contracting too quickly, allowing adequate time to complete its filling phase. On the ECG, this brief period of no electrical activity is depicted by a straight (isoelectric) line between the P wave and the beginning of the QRS complex. The impulse is then propagated down to the ventricle through the bundle of His, right and left bundle branches and Purkinje fibres yielding ventricular contraction (QRS complex). Finally, the ventricle returns to its relaxed state (T wave); this is called repolarisation. HR can be determined from the R-R interval, which is the time between consecutive QRS complexes. Here, the term HR refers to the rate of ventricular contractions. In some abnormal conditions atrial and ventricular rates differ, so it is important to distinguish between the two. Atrial HR is determined by measuring the P-P intervals.

Obtaining an ECG waveform is possible by means of one or more leads simultaneously. A lead provides a view of the heart's electrical activity between a positive and a negative pole. Intuitively, these are called bipolar. Connecting these two poles by an imaginary line defines the lead's axis, which refers to the direction of the electrical current flowing through the heart. The ECG output consists of an upward deflection if electrical current is heading towards the (+) electrode and vice versa. All bipolar leads need a third electrode as well, known as the ground. This is placed on the sternum bone to prevent electrical interference from reducing the ECG signal's quality. Electrode terminals are color-coded for easier identification and placement.

Since the heart is a three-dimensional organ and ECG electrodes may only be placed superficially on the skin, there are two different planes that electrical activity can be probed from. These are the frontal and the horizontal planes. Conventionally, for the frontal plane there are six limb leads, 3 bipolar (I, II, III) and 3 unipolar (avR, avL, avF) and for the horizontal plane there are six chest (alternatively called precordial) leads, all unipolar (V_1 to V_6). Different leads provide different diagnostic information. Unipolar leads require only one electrode.

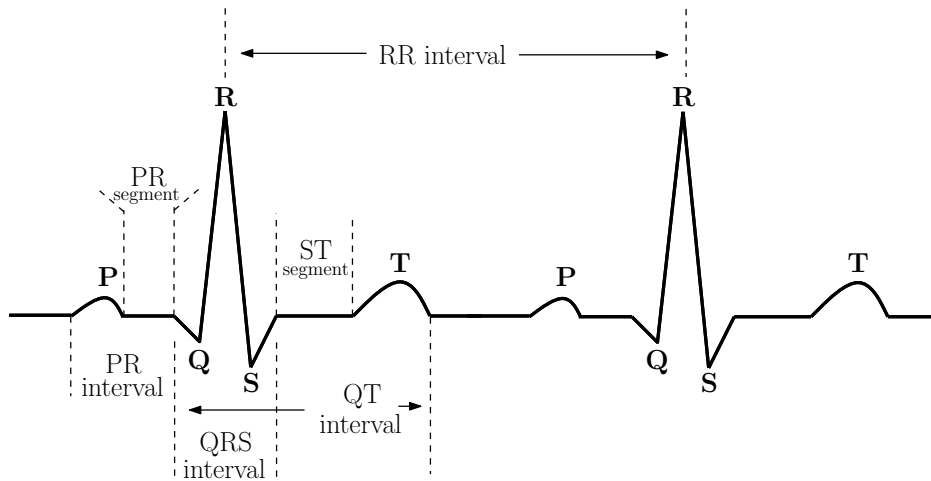


Figure 1.3: Two complete, normal ECG cycles with waves, intervals and segments shown.

Combining more than one lead and omitting others is normal clinical practice on a per patient basis.

An ECG may be recorded for a short time period (for example, 5 minutes), so the output can be manually processed from hard copy printouts of the ECG strip created. Alternatively, longer recordings (24 or 48 hour) demand digital storage on solid state disks and specialised software for analysis and interpretation.

1.3.2.1 Ambulatory ECG Monitoring

Norman J. Holter, an American biophysicist, developed the first clinical prototype of a portable ECG recorder in 1962 (Barold, 2005). Since then, the term Holter monitoring is a synonym of Ambulatory Electrocardiography (AECG). There are two types of AECG monitors. Continuous ones that typically record for 24 or 48 hours and intermittent ones that are used for long periods of time (weeks to months) to provide shorter, intermittent recordings on demand (alternatively termed event recorders).

Ambulatory cardiac monitoring overcomes the limitations of one-off ECG recordings as it is designed to identify transient cardiac disturbances occurring throughout the patient's daily routine, thus deemed free of bias of a controlled laboratory setting. It also makes possible the examination of cardiac autonomic function by measuring Heart Rate Variability (HRV) (see Section 1.3.2.2). According to the Seventh Report of the Joint National Committee clinical situations in which AECG monitoring may be useful are white-coat hypertension, evaluation of nocturnal BP changes and hypotensive symptoms associated with antihypertensive medications or autonomic dysfunction. Modern AECG monitors have an autonomy of storage

capacity and running time of digitally recording more than 100.000 QRS complexes (for a 24h period) and at the same time are compact and lightweight to carry on. Modified three-electrode bipolar leads have been developed for the case of AECG. Some of these electrode placements are shown in Figure 1.4.

All modified bipolar lead placements shown in Figure 1.4 have the plus electrode in position V_5 . That is, the fifth intercostal space at the left anterior axillary line. The Central Back (CB_5) lead has the negative electrode at the right scapula bone. The Central Manubrium (CM_5) lead has the negative lead at the manubrium sterni. Lastly, the CC_5 lead has the negative electrode at the fifth intercostal space at the right anterior axillary line (alternatively, this is the V_5R position). Typically, combinations of two or three bipolar leads are used, which amounts to five or seven electrodes in total, respectively. Signals are recorded in separate channels per electrode pair.

The aforementioned modified ambulatory leads offer maximised P-wave height for the diagnosis of atrial arrhythmias and increased ECG sensitivity for the detection of anterior myocardial ischaemia. Particularly, a study has exemplified the use of the CM_5 lead as being the most useful one for ambulatory monitoring (Quyyumi et al., 1986).

1.3.2.2 Heart Rate Variability

The balance between the two reciprocal activities of the ANS (SNS and PNS) is evidenced in the beat-to-beat changes of the cardiac cycle. HRV is concerned with the oscillation (i.e. variability) in the interval between consecutive heart beats, which may contain indicators of current disease, or signs about impending cardiovascular disease. It can be quantitatively and non-invasively evaluated either by time domain or by frequency domain methods (Malliani, 2005). Comparisons of the sympatho-vagal balance can be made between pathological and physiological conditions, different types of activity (rest, exercise) and to analyse circadian rhythms (day-night changes).

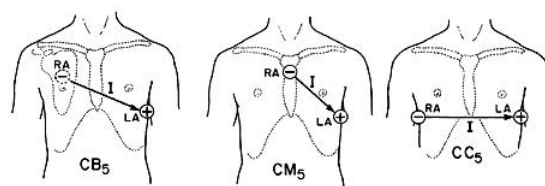


Figure 1.4: Modified three-electrode bipolar lead system: CB_5 , CM_5 , CC_5 . Ground electrode is not shown. LA stands for Left Arm, RA stands for Right Arm.

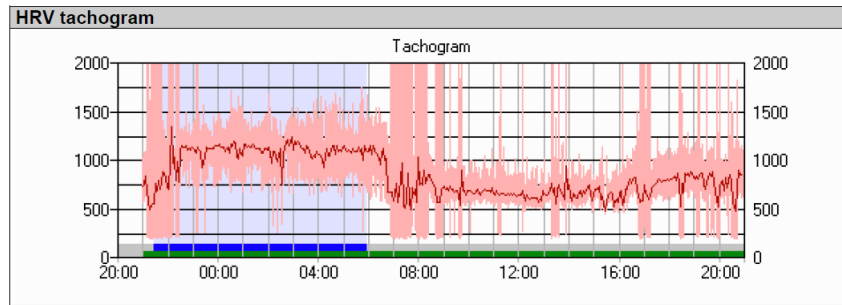


Figure 1.5: The time series of R-R intervals obtained is represented graphically as a tachogram. The horizontal axis of the diagram indicates the time and the vertical axis shows the RR distance in msec (average of 15 seconds). One data line shows the minimum and maximum RR intervals. See also Figure 1.6.

In case of time domain HRV analysis, the so-called Normal-to-Normal (NN) intervals are determined. These are all intervals between normal (sinus) beats. Assuming a 24-hour AECG recording, the variables that can be calculated to estimate an overall HRV are either of statistical nature (Table 1.1) or of geometrical nature (Table 1.2). The list of variables in the aforementioned tables is not exhaustive (Malik et al., 1996). SDNN estimates (and similarly other HRV measures) depend on the length of the recording period. As such, valid comparisons are only to be carried out between values derived from ECG recordings of comparable durations.

The series of NN intervals can also be plotted accordingly to derive useful clinical correlates. The geometrical time domain methods are derived from various approaches implemented to characterize the variability of these plot patterns. To perform such calculations, either the sample density distribution of NN intervals is constructed (assigning the number of equally long NN intervals to each value of their duration) or a (2D or 3D) Lorenz/Poincaré plot of NN intervals (each NN interval is plotted against its next one) (Hnatkova et al., 1995). Such geometrical methods require the NN intervals sequence to be appropriately binned on their time scale to permit the construction of smoothed histograms. The reason that these bins are

Variable	Units	Description
SDNN	msec	Standard Deviation of all NN intervals
SDANN	msec	Standard Deviation of the Averages of NN intervals calculated over 5 minutes ECG segments
RMSSD	msec	(Square) Root of the Mean of the Sum of the Squares of Differences between successive NN intervals

Table 1.1: Statistical measures of HRV used in time domain analysis.

selected to be of approximately 8 milliseconds (see Table 1.2) is simply because it corresponds to the typical sampling frequency of commercial AECG monitors (128 Hz).

Taking a step further from time domain into frequency domain analysis, spectral information from an R-R tachogram can be decomposed and periodicities may be identified. Power spectra of R-R variability from AECG recorders have been shown to provide markers of sympathetic and vagal function. In humans, three main spectral components are distinguished in a Power Spectral Density (PSD) plot (Figure 1.6). The Very Low Frequency (VLF) component (0.003 - 0.04 Hz) that depends primarily on the presence of parasympathetic outflow (Taylor et al., 1998). The Low Frequency (LF) component (0.04 - 0.15 Hz) which is believed to be due to baroreceptor mediated BP control and relates to both sympathetic and parasympathetic function and the High Frequency (HF) component (0.15 - 0.4 Hz) which is correlated with respiratory driven vagal input to the SA node, reflecting parasympathetic nervous system activity (Kamath and Fallen, 1993). Measurement of VLF, LF and HF power components is made in absolute values of power (msec^2). Alternatively, LF and HF specifically may also be reported in normalised units (nu) which represent the relative value of each component in proportion to the total power minus the VLF component (Pagani et al., 1986). The LF/HF ratio is an index of sympatho-vagal balance (Lombardi et al., 1996). High values for the ratio suggest predominance of sympathetic nervous activity and vice versa.

In 24 hour AECG recordings of normal subjects, despite the fact that LF and HF components account for approximately only 5% of the total spectral power (see Figure 1.6), these two are the spectral components mostly referred to in literature. LF and HF can increase under different conditions. In healthy subjects, an increased LF is observed during 90° head tilt, standing, mental stress and moderate exercise, whereas increased HF is induced by controlled respiration and cold stimulation of the face (Malik et al., 1996).

The role of the ANS in essential HT (see Section 1.4) is an important area of investigation. A significant amount of studies have investigated the clinical value of HRV in various cardiovascular

Variable	Units	Description
HRV triangular index	n/a	Total number of all NN intervals divided by the maximum height of the histogram of all NN intervals measured on a discrete scale of 7.8125 msec bins (1/128 sec)
TINN	msec	Width of the base of the triangular interpolation (the minimum square difference is used to find such a triangle) of the maximum height of the histogram of all NN intervals

Table 1.2: Geometrical measures of HRV used in time domain analysis.

1 Overview of principal literature

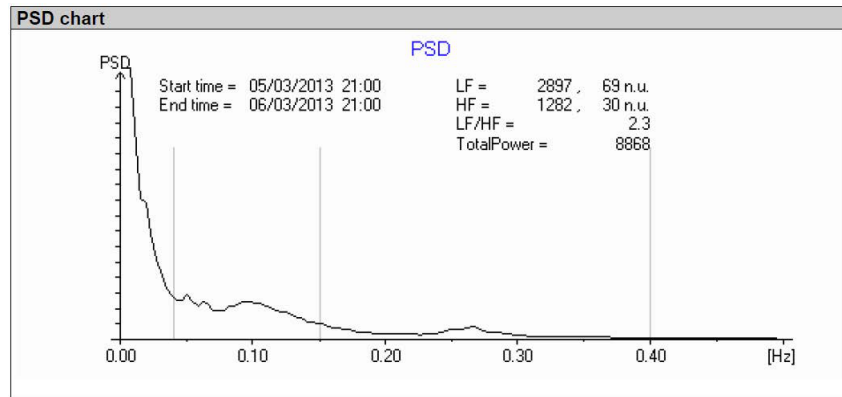


Figure 1.6: Power Spectral Density of the tachogram in Figure 1.5. Horizontal axis represents frequency in Hz and the vertical axis shows the PSD. The input range, total power, LF and HF power components and LF/HF ratio are displayed, too. The grey vertical lines on the chart mark the VLF, LF and HF components (0-0.04 Hz, 0.04-0.15 Hz, 0.15-0.4 Hz, respectively).

diseases, including HT. Among those studies, an increased LF component during night-time rest has been found in hypertensives compared to normotensives, accompanied by blunting of circadian patterns (Guzzetti et al., 1991). Complementary evidence of reduced parasympathetic cardiac control was found a few years later between a group of hypertensives and both normal and borderline hypertensive groups (Langewitz et al., 1994).

1.3.3 CardioTens 24-hour ECG and BP monitoring

CardioTens (Meditech Ltd, Hungary) is a commercially available combined ambulatory BP and ECG monitor. The device can be used either as an independent ABPM device if only the BP cuff is attached to it, or as an AECG if only the ECG electrodes are attached or as a dual recorder incorporating both functions simultaneously. The incorporated ABPM device is validated by the British Hypertension Society and performs within the recommendations of the Association for the Advancement of Medical Instrumentation (Barna et al., 1998). It uses a proprietary Meditech algorithm for determining BP which is equivalent to that obtained by a trained observer using the cuff/stethoscope auscultation method Korotkoff phase V, within the limits prescribed by the American National Standard for Electronic or Automated Sphygmomanometers (White et al., 1993). Readings can be taken at frequent, pre-programmed time intervals.

The AECG part of the device can perform routine AECG registration via two independent channels, producing an ECG strip with two leads (CM_5 and CC_5) of 30 seconds duration every 5 minutes, continuously for up to 48 hours. It features a sampling rate of 200 Hz, adequate to precisely locate the peak of QRS complexes, and an analog-to-digital converter

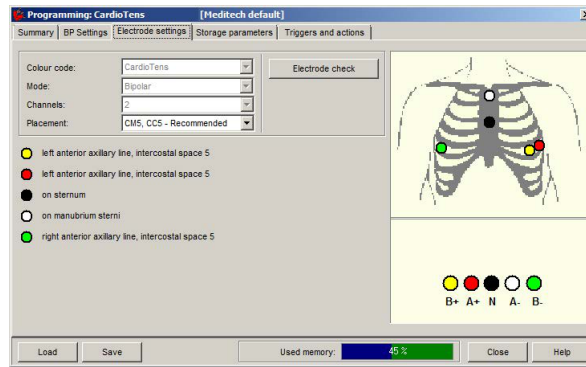


Figure 1.7: Set-up window of the CardioVisions software for confirming correct electrode placement and checking ECG signal in real-time. Channel A (red, white) corresponds to lead CC_5 , channel B (yellow, green) corresponds to CM_5 and N electrode is the ground.

of 12 bits. PSD processing in CardioVisions uses four-minute Hann-windowed samples. If the input range is longer than this four-minute unit, PSD is calculated by averaging adjacent, non-overlapping four-minute samples. Individual spectral components can be automatically determined, together with their center frequency and associated power, i.e. area.

1.4 Hypertension

1.4.1 Definition and Classification of Hypertension

Diagnosis and treatment of hypertension is essentially based on the outcome of casual, indirect BP readings, although ambulatory or BP recordings at home might eventually become preferable to minimise the bias of white-coat HT. A systolic and/or diastolic BP measurement persistently higher than normal values - for a given age group - is defined as HT. According to the latest and most relevant (for the European population) guidelines jointly published (Mancia et al., 2007) by the European Society of Hypertension and the European Society of Cardiology, normotensives and hypertensives are distinguished as in Table 1.3.

Category	Systolic BP (mmHg)		Diastolic BP (mmHg)
Optimal	<120	and	<80
Normal	120-129	and/or	80-84
High normal (Pre-Hypertension)	130-139	and/or	85-89
Grade 1 HT (mild)	140-159	and/or	90-99
Grade 2 HT (moderate)	160-179	and/or	100-109
Grade 3 HT (severe)	≥ 180	and/or	≥ 110

Table 1.3: Classification of HT based on BP levels in adults (Mancia et al., 2007). In case of SBP and DBP falling into different categories, the higher value is considered for classification.

HT diagnosed in the vast majority of the population is of an unknown cause (i.e. idiopathic). This condition is called primary or essential HT. In both developed and developing countries, essential hypertension affects 25–35% of the adult population, and up to 60–70% of those beyond their seventh decade of life (Staessen et al., 2003). HT in the rest of hypertensive patients, results secondarily from renal disease, endocrine disorders, or other identifiable causes and this type is called secondary hypertension.

Malignant Hypertension (MHT) is the most severe form of HT, and is defined clinically as the presence of severe hypertension in association with ocular disease (Shantsila et al., 2010).

1.4.2 Management of Hypertension

Guidelines have been published from the World Health Organisation and the International Society of Hypertension on management of HT (Whitworth, 2003). More recently, the British Hypertension Society working party, in light of the latest peer-reviewed publications, has also published relevant guidelines (Williams et al., 2004).

Non-pharmacological strategies can reduce BP (Williams et al., 2004). These entail reduction of alcohol consumption, lowering of salt intake, adopting a diet rich in fresh fruits and vegetables and restriction of caloric intake. Less effective for BP reduction but helpful also towards reducing cardiovascular risk in general, are regular dynamic exercise and abstaining from smoking.

Antihypertensive drug treatment diminishes the complications of HT. The three broad classes of drugs used to treat primary HT are diuretics (to reduce blood volume), vasodilators (to decrease SVR), and cardioinhibitory drugs (to decrease CO). Irrespective of the mechanisms that may operate to initiate and sustain HT, its treatment is important because it increases the risk of further complications such as coronary artery disease, stroke and renal disease.

1.5 Peripheral Circulation

Although the site of routine BP measurement focuses attention on the haemodynamics of large conduit arteries, namely the brachial artery from the upper arm, it is accepted that HT is a systemic condition involving the vascular tree as a whole. As such, various non-invasive clinical tools have been developed to assess microvascular function and structure. Described in the following sections are two such vascular beds that can be affected by generalised systemic disturbances or, in fact, be the ones that undergo pathological changes prior to systemic disease: the retinal circulation and the nailfold microcirculation.

1.6 The Eye

The eye is an easily accessible, transparent “window” to peripheral microvasculature that can be examined non-invasively *in vivo*. Two vascular beds exist in the posterior eye; the choroidal (part of the uveal layer) and the retinal. On one hand, retinal blood vessels supply nutrients and oxygen to the neural retina, namely retinal ganglion cells and their axons, as well as to the anterior part of the Optic Nerve Head (ONH). On the other hand, the choroidal plexus, is the most perfused tissue of any other tissue in the body per unit weight (Nickla and Wallman, 2010). Hence, the maintenance of normal fundus vascular structure and function is of high importance. In the following sections, retinal circulation features are described along with current clinical and laboratory investigative techniques on retinal structure and function.

1.6.1 Retinal Vasculature

The main vessels of the eye comprise the Central Retinal Artery (CRA) and the Central Retinal Vein (CRV). These enter and exit the globe respectively within the ONH, bifurcate at the optic disk into superior and inferior branches and then further divide into temporal and nasal branches (Figure 1.8). Mapping the retina into four quadrants yields the respective superior temporal, superior nasal, inferior temporal and inferior nasal vessel branches. The temporal parts of these vessel branches form the superior arcade, composed of the superior temporal artery and vein and the inferior arcade, composed of the inferior temporal artery and vein. In terms of fundus photography the temporal half of the retina is the target that is documented, including the ONH and the macula (Figure 1.9). Stokoe and Turner (Stokoe and Turner, 1966) reported that the temporal side of the fundus contained wider vessels and were more predictable in their branching than the nasal one, when they were trying to obtain comparable vessel pairs (arteries and veins) for their study.



Figure 1.8: Normal fundus image of a left eye, ONH centered, 30°.

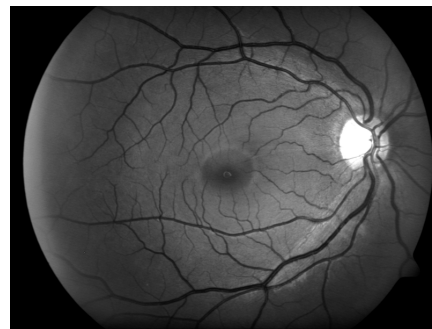


Figure 1.9: Normal fundus image of a right eye, macula centered, 50°.

Whilst termed retinal arteries and veins, retinal vessels after they bifurcate for the first time distal to the ONH are in fact arterioles and venules respectively, if accurate terminology is used. Namely, the CRA begins to change markedly in its structure after passing through the lamina cribrosa of the sclera, losing a big part of its internal elastic lamina and its muscular coat (Scheie, 1953). After the first bifurcation distal to the ONH, the arterioles and venules have no elastic lamina and the muscle fibers lose continuity. Then, arterioles gradually branch off to form smaller arteriole daughter vessels and terminal arterioles, which feed into the capillary bed as they extend towards the peripheral retina. Pre-capillary arterioles and post-capillary venules are linked through anastomotic capillaries.

1.6.2 Posterior Eye Haemodynamics

Blood circulation of the posterior eye and especially choroidal blood flow depend on perfusion pressure. Mean Ocular Perfusion Pressure (OPP) driving blood through the eye is the mean blood pressure in the ophthalmic artery entering the orbit minus the pressure in the veins returning to the heart. The venous pressure is approximately equal to Intraocular Pressure (IOP), while there is a pressure drop of a factor of $2/3$ between the brachial artery and the ophthalmic artery (Pournaras et al., 2008), thus:

$$\text{meanOPP} \simeq \frac{2}{3}\text{MABP} - \text{IOP} \quad (1.7)$$

Retinal blood vessels are not innervated; rather their dilation and constriction depend on autoregulation (Dorion, 1998). The main regulators of retinal blood flow are the vascular endothelium cells, the neural and the glial cells. Experimentally, autoregulation of the retinal microcirculation is assessed by provocation methods, which are extensively described in Sections 1.8.2.2 to 1.8.2.4.

The choroid, in contrast, does not exhibit autoregulation of blood flow. This, however, does not mean that the choroid is a passive, non-reactive vascular region. An intensive autonomous innervation by the SNS permits central regulation of the choroidal blood flow. This is important, for example, for protecting the choroid from hyperperfusion in patients with increased BP.

1.7 Qualitative Retinal Analysis

The quest for early detection of systemic vascular disease by means of ophthalmologic examination has surely been long-lasting and is still ongoing. One of the earliest reports “*on ophthalmoscopic evidence of general arterial disease*” dates back to 1898 (Gunn, 1898).

Markus Gunn first precisely defined a number of signs of the retinal vessels that are typical of retinal arteriosclerosis and demonstrated their close relation to cerebral vascular disease. Specifically, these signs have been further investigated by Moore (Moore, 1916) and comprised of a) irregularity of the lumen of retinal arteries, b) arterial tortuosity, c) increased arteriolar light reflex, d) loss of arterial wall translucency, e) venular blood flow obstruction where they are crossed by arteries (this condition was later termed as “arteriovenous nipping”) and f) retinal oedema.

1.7.1 The Keith-Wagener-Barker Classification

By early 1900’s, investigators had identified two distinct types of essential HT; the benign and the malignant form of the disease. However, it was apparent that this grouping was rather crude and did not facilitate all cases. In 1939, Keith et al. (1939) attempted to relate retinal vascular changes to survival rates in the hypertensive population aiming towards increased accuracy of prognosis in the general population. To avoid descriptive terms that could cause confusion, they used numbered groups. The so-called Keith-Wagener-Barker classification system appears in Table 1.4.

Their results were based on identifying a combination of structural changes: qualitative retinal observations and quantitative measurements of peripheral arterioles of the pectoralis major muscle. The 219 hypertensive patients included in their study were followed up for a period of 5 to 9 years and were grouped on the basis of the ophthalmoscopic characteristics of each group (Table 1.4). The resulting survival curves were distinct for each of the four groups having a gradually increasing steepness from benign to malignant hypertension. Despite the inherent limitations of their study, described not only by later publications (Chasis, 1974) but by the authors themselves too, the Keith-Wagener-Barker classification scheme has been widely adapted (Walsh, 1982) in prognosticating for survival.



Table 1.4: Keith-Wagener-Barker hypertension classification system (Walsh, 1982).

1.8 Quantitative Retinal Analysis

1.8.1 Assessing Retinal Structure

Digital retinal images are taken by means of fundus cameras. These images can be post-processed in order to yield a breadth of quantitative values towards the ultimate goal of vascular network characterisation and risk stratification. These quantitative metrics are discussed below.

1.8.1.1 Central Retinal Arteriolar, Venular Equivalent and Arterio-Venous Ratio

The arteriole and venule widths and their ratio have long been regarded as signs of hypertensive disease (Kagan et al., 1967). In 1974, Parr and Spears (Parr and Spears, 1974a,b) paved the way towards the long-sought transition from qualitative and subjective grading of retinal images to quantitative and objective measurements by summarising the calibre of all retinal arteries as the equivalent width of the CRA. That way, comparison of the arterial widths of different eyes was made possible, independently of the complexity and pattern of branching. They recruited normotensive young adults and measured the diameter of all arterioles (parent-daughter pairs) from the edge of the ONH outward to about 30°. The rationale behind this zone selection is that at that distance from the optic disk the retinal arteries and veins are rather arterioles and venules respectively (i.e. they have lost their internal elastic lamina and their muscle layer is not continuous (Scheie, 1953)) and according to studies (Parr, 1974) it has been suggested that these vessels are more readily affected from pathological conditions, like HT. Then, they investigated the relationship between individual trunk vessels and their corresponding branches and calculated a model that best fit their experimental data. Next, they confirmed their model with an independent group of subjects. This empirically derived formula calculated the width (in μm) of a parent artery from the widths of its two branches:

$$W_{\text{artery}} = \sqrt{(0.87W_1^2 + 1.01W_2^2 - 0.22W_1W_2 - 10.76)} \quad (1.8)$$

where W_{artery} is the parent trunk arteriole diameter, W_1 the narrower and W_2 the wider branch. Successive calculations from the outer peripheral retina towards the ONH yielded a single value of the width of the CRA, the Central Retinal Artery Equivalent (CRAE). This mathematical relationship compared remarkably better than both the sum of the widths and the sum of the squares of the widths of all arteries entering the retina, that since that time had been used as a measure of the general calibre of these vessels. After corroborating the original Parr formula, Hubbard et al. (1992) adapted this approach to deliver an analogous formula for venules that calculated the width (in μm) of a parent vein from the widths of its two branches:

$$W_{\text{vein}} = \sqrt{(0.72W_1^2 + 0.91W_2^2 + 450.05)} \quad (1.9)$$

where, respectively, W_{vein} is the parent trunk venule diameter, W_1 the narrower and W_2 the wider branch. Likewise, the general venular calibre is summarised in a value termed the Central Retinal Vein Equivalent (CRVE). Hence, the Arterio-Venous Ratio (AVR) could be obtained as per following equation:

$$\text{AVR} = \frac{\text{CRAE}}{\text{CRVE}} \quad (1.10)$$

AVR is dimensionless, thus has advantages over absolute vessel width measurements. Apart from the fact that - by definition - it represents a generalised vessel calibre, rather than isolated vessel diameters, it additionally does not require to take into consideration any scaling differences between different refractive errors of eyes, as these are cancelled out. Correction for refraction is surely important for quantifying absolute retinal vessel widths without errors, but this is not the case when using the AVR (Wong et al., 2004; Patton et al., 2005).

Hubbard and his colleagues modified Parr's methodology in a way to make it more attractive to use in large population studies, like the Atherosclerosis Risk In Communities (ARIC) study (Hubbard et al., 1999) in which they first tested its validity and reproducibility. They first defined a ring-shaped measurement zone, concentric to the optic disk and half to one Disk Diameter (DD) away from it (Figure 1.10). Then, instead of identifying the pairs of every branch vessel and the corresponding parent trunk as in the Parr method, they arbitrarily matched the largest vessel with the smallest one, then the next largest with the next smallest and so on, until all vessels coursing through that measurement zone were accounted for and the central retinal equivalents (CRAE, CRVE) were calculated and from these, AVR. In case the number of vessels to be combined is odd, the remaining single vessel is carried on to the next iteration. A comparison between the modified ARIC method with the original Parr method showed no statistically significant differences between AVR values, hence its use was deemed appropriate.

Four years later, Knudtson et al. (2003), essentially members of the previous ARIC study, suggested revised formulæ, as well as methodology, for summarising retinal vessel diameters, proving their superiority over the Parr-Hubbard formulæ and methodology. The major advantage of the revised formulæ over the previous ones is that they do not contain constant values, thus can be solved for various measurement units (eg. number of pixels) and are not constrained for vessel widths in micrometers only, being virtually independent of image scale. Regarding the methodology, instead of measuring all vessels lying within the measurement zone, they only include the six largest of them in their formulæ. Investigating the relationship



Figure 1.10: Concentric AVR measurement rings as defined by the ARIC study (Hubbard et al., 1999). The grid is composed of three circles concentric with the ONH: the innermost circumscribing the average optic disc, the middle one including the area from the disc margin to half DD from the margin and the outer one including the area from half DD to 1 DD from the disc margin.

between the number of vessels taken into the measurements and the resulting CRAE and CRVE they found a strong increasing trend that falsified the final result. Therefore, restricting the measured vessels at six at all times their methodology proved more robust and at the same time reduced the process time of the calculations. Several studies implemented the use of these revised formulæ (Taarnhøj et al., 2006; Cheung et al., 2010).

Of course, the various approaches of different investigators are not ceasing to evolve, complicating the quest for standardisation. Patton et al. (Patton et al., 2006) proposed another revised formula that incorporates an asymmetry factor of the retinal arteriolar branching. Various formulæ for calculating AVR have been tested and compared (Hemminki et al., 2007) and more recently newer methods have emerged as well that incorporate extended measurement zones (Cheung et al., 2010).

1.8.1.2 Vessel Tortuosity Index

In healthy subjects, blood vessels follow a fairly straight course or are only slightly, in an arc-fashion, curved. One can find different definitions of tortuosity indices in the literature (Kalitzeos et al., 2013). The most easily implemented and widely used, the tortuosity index, T , is calculated as the ratio of the actual length of the vessel segment L (arc length) to the straight line distance between two branching points, D (chord length).

$$T = \frac{L}{D} \quad (1.11)$$

The bending of a vessel influences its local flow haemodynamics and may result in adverse clinical consequences. Thus, quantifying tortuosity could be used as an indicator of retinal morphological changes, either on a local extent if specific vessels are chosen or globally if the total vascular tree is analysed.

Early investigations (Moore, 1916) on the signs of arteriosclerosis were rather contained in including tortuosity of the arteries as one of them, because of its wide variability under physiological conditions and its rare occurrence. Various theories have been described (Bracher, 1982) and tube models tested (Kylstra et al., 1986) to try to elucidate the aetiology of vessel tortuosity. In vascular disease the vessel wall loses its elasticity and the lumen is narrowed, impeding blood flow, as previously described (Section 1.2.3.1). As a result of the force of BP upon a tube which has lost its carrying power, the vessel then becomes tortuous (Bracher, 1982; Gunn, 1898). Leatham (Leatham, 1949) stated that tortuosity of retinal arterioles was not believed to be a sign of hypertension because it occurred randomly in both aged, normotensives individuals as well as hypertensives. Adding to the uncertainty of accessing general vessel tortuosity during ophthalmoscopy, the subjective characterisation such as “not noticeably tortuous”, “moderately tortuous” and “markedly tortuous” was making its usefulness even more dubious.

Later investigators incorporated manipulation of fundus photographs with the use of bulky, but quite accurate devices such as profile projectors (Lotmar et al., 1979). Absolute and relative measurement of retinal arterial tortuosity was made possible by subdividing a vessel into a series of circular arcs of individual curvature and measuring the chord lengths and arrow height of these arcs. The sequence of chords is considered to represent the vessel in its “non-twisted” form. It is easy to understand that such a technique was entirely manual to perform, thus time-consuming, error-prone and difficult to reproduce. Others (Kylstra et al., 1986) defined tortuosity as merely the sum of the height of the arcs that make up the tortuous vessel.

The course of arterioles from projected fundus images on a digitising table was measured from two normotensive age groups (Williams, 1982). Measurement of a single arteriole (~3mm long), representative of all arterioles in the posterior pole region was performed by calculating the distance of its actual path length and the distance of the line connecting its first and last point. The tortuosity index is the ratio between them as previously mentioned (Equation (1.11)). An absolutely straight vessel would have an index of 1, whereas one that has an actual course 30% longer than its straight line course would have a tortuosity of 1.3. Differences between old and young age groups were not significant and other investigators confirmed the same outcome (Taarnhøj et al., 2008), although their methodology differed significantly.

The above definition of the tortuosity index has been described as unsuitable for its weakness to distinguish between vessels with equal path lengths and different degree of bending, so a number of novel indices have been proposed (Azegrouz et al., 2006; Dougherty and Varro, 2000; Hart et al., 1999). Advances in computer-assisted methods (Wallace, 2007; Cheung et al., 2010; Dougherty et al., 2010) have pushed current methodologies forward and qualitative studies are currently an exception to the rule (Taarnhøj et al., 2008).

1.8.1.3 Bifurcation Angles and Junction Exponents

A vessel branching can be described geometrically in terms of its junction exponent, χ , and its bifurcation angle ω , which is the angle between two daughter vessels. The junction exponent provides an index of the relative widths of the parent d_0 and daughter d_1, d_2 vessels through the equation:

$$d_0^\chi = d_1^\chi + d_2^\chi \quad (1.12)$$

where d_1 is the wider branch and d_2 the narrower one. It has been suggested that, in an “ideal” vascular network, there is an optimal way that vessels at bifurcation junctions can be interconnected, in order for fastest transport of blood to be achieved for the least amount of biological work (Murray, 1926). In other words, it is implied that deviations from optimal vascular architecture may be associated with vascular damage. These theoretical, optimal values were calculated to be $\chi = 3$ and $\hat{\omega} \approx 75^\circ$, so Equation (1.12) is written:

$$d_0^3 = d_1^3 + d_2^3 \quad (1.13)$$

Assumptions made when deriving Equation (1.13) include laminar blood flow and constant blood viscosity. Comparison of experimental results to theoretical values have followed, although in scarce numbers. Zamir and colleagues (Zamir et al., 1979) introduced two non-dimensional parameters in order to make comparisons of relative diameters of branches rather than absolute diameters: the area ratio β and the asymmetry ratio α ; in that way differences of magnification between images was not an issue. Even so, results followed the trend of the theoretical values, but scattered significantly.

Few studies have considered comparing healthy subjects with hypertensives. Average bifurcation angles from both normotensives and hypertensives varied considerably from theoretical values (Stanton et al., 1995), but at the same time the sample size was small and only arteries were measured. Bifurcation angle values declined with increasing age. Regarding junction exponents, both groups had similar values, declined with age and were always smaller than the theoretical value of 3. Another study’s results (Houben et al., 1995), followed an almost identical trend for arterial bifurcation angles between hypertensives and normals showing significant

differences. Their attempt to measure vein bifurcation angles as well, yielded insignificant differences.

In a rather small sample, the effect of oxygen and carbon dioxide inhalation was tested in normotensives and hypertensives (Chapman et al., 2000). Neither bifurcation angles, nor junction exponents differed significantly between the two BP groups and parent arteriolar diameters were comparable. Hypertensive patients had a less marked arteriolar constriction when breathing oxygen than controls and breathing carbon dioxide resulted in increased arteriolar diameters in healthy subjects, but not in the hypertensive group. No alterations in junction exponents in either groups were noted.

Comparison of branching angles between individuals with atherosclerosis and healthy subjects showed no significant difference (Chapman et al., 2002). Instead of using junction exponents, the same group introduced a novel optimality parameter that performed better in terms of reliability and showed significant difference between the two groups. Recently, another study (Witt et al., 2010) proposed a parameter referred to as optimality ratio, that appears promising.

1.8.1.4 Length-to-Diameter Ratio

The Length-to-Diameter Ratio (LDR) is another structural, dimensionless quantity that may describe the retinal vascular bed. As the name suggests, it is defined as the ratio of the length of a vessel, between two branching points, to its diameter over that segment (King et al., 1996). Its clinical usefulness has not been extensively assessed as yet (Chapman et al., 2002; Hughes et al., 2006).

1.8.2 Assessing Retinal Vessel Dynamics

All structural parameters described in the previous sections are extracted from measurements based on static fundus images which essentially are a snapshot of the constantly changing retinal circulation. The opportunity to monitor microvasculature over a period of time might elucidate more complex functional principles.

1.8.2.1 Retinal Vessel Analyser

The Retinal Vessel Analyser (RVA) is a commercially available (Imedos Systems, Germany) ophthalmoscopic instrument capable of acquiring vessel diameter fluctuations in real time. These diameter changes happen physiologically due to the pulsatile nature of blood flow and additionally may be altered by means of external provocation. RVA comprises a mydriatic fundus camera, a Charged-Coupled Device (CCD) video camera and a personal computer that uses dedicated software to control and adjust the measurement parameters. Versatility is a

key aspect of RVA, being easily extendible with a flicker module for vascular reactivity testing (Section 1.8.2.2), an oxygen module for Oxygen Saturation (OSat) mapping (Section 1.8.3), an electrocardiograph or a BP monitoring interface for synchronisation with the cardiac cycle (Blum et al., 1999) and with a video recorder for offline post-processing of the recorded sessions.

At the system's heart is a Carl Zeiss FF450^{plus} mydriatic fundus camera capable of acquiring both full color and red-free (530-600 nm) retinal images 20°, 30° or 50° wide. Still images can be recorded at a resolution of 1360×1024 pixels, while video sequences are displayed at a lower resolution of 640×480 pixels. To achieve an optimum contrast for visualisation of the retinal blood vessels a special green filter is intercepted in the illumination pathway of the fundus camera. Thus, green light enters the subject's eye via its pharmacologically dilated pupil. Since, retinal blood vessels containing haemoglobin have different absorption spectra from the surrounding tissue, the integrated vessel tracker registers with the red blood cells column and follows it throughout the course of time making both temporal and spatial diameter analysis possible. Consequently, a data matrix of vessels' diameters is obtained at the end of a measuring session. Temporal resolution of the RVA system is 40 msec (i.e. 25 diameter readings per second), while spatially it assesses one mean diameter value every 10 Measuring Units (MU); where one MU corresponds to one micron for the standard Gullstrand eye and assuming relaxed accommodation. Calculation of relative values, for example baseline versus stimulation values, minimises the influence of deviation of individual eyes from the Gullstrand eye model, as well as from optical errors.

Although subject compliance is crucial for taking quality measurements, small eye and/or head movements, as well as transient shadows or reflections are unavoidable. To overcome these practical issues, the RVA encompasses adaptive algorithms that can compensate for a reasonable amount of such disturbances (Muench et al., 1995). The view obtained from the fundus camera is simultaneously acquired from the 3-CCD video camera (JVC, KY-F70BU), displayed on the computer's monitor and optionally recorded on video tape at the same time.

Regarding continuous baseline vessel diameter recordings, short term and day to day reproducibility of the RVA system have been found to be higher for veins than arteries for a five minute long measurement session (Polak et al., 2000). Nevertheless, short term reproducibility was reported to be excellent with Intraclass Correlation Coefficient (ICC) values of 0.98 for veins and 0.96 for arteries and slightly lower for day to day sessions (0.90 and 0.87, respectively). Similarly high reproducibility values for baseline (i.e. constant illumination) diameter measurements have been reported a few years later as well (Pache et al., 2002).

1.8.2.2 Flicker Provocation

Contrary to extraocular blood vessels, intraocular retinal vessels are not innervated (Brown and Jampol, 1996), thus depend on local autoregulatory factors for actively regulating blood flow (see Section 1.6.2). The autoregulation mechanism, that maintains constant blood flow despite changes in arterial perfusion pressure or metabolic demands of the surrounding tissue, is an undoubtful and well documented phenomenon (Johnson, 1986). Retinal vessels are capable of responding to such changes by either vasodilation or vasoconstriction, accordingly (see Section 1.2.1). Despite the complex association between endothelial function and Cardio-Vascular Disease (CVD) progress (Luscher, 1994), impaired retinal vascular reactivity has been described in a number of pathological conditions; hypertension amongst them (Panza et al., 1990; Delles et al., 2004).

Following animal studies, Formaz and collaborators (Formaz et al., 1997) proved an increase in retinal vessel diameters induced by diffuse luminance flicker illumination in the human retina. Since then, many studies have exploited retinal flicker provocation as a tool to assess vascular reactivity in health and disease (Heitmar and Summers, 2012). Interrupting the illumination path of the RVA system with an optoelectronic shutter, light is modulated with a rectangular bright-dark (on/off) wave to produce a flicker stimulus over the entire 30° angle field of the camera. This flicker stimulus has a 12.5 Hz frequency, well within the range of frequencies (10-20 Hz) where the human visual system's sensitivity for luminance flicker is at its maximum (Lee et al., 1990). For a PAL standard CCD video camera of a frame rate of 25 Hz, every other frame is a dark image, thus halving the amount of collected data points during the flicker cycles.

Across literature there are reports of various flicker protocols being implemented. Prior to the adaptation of the embedded RVA flicker module, research groups used their own implementations of external flicker stimuli (Polak et al., 2002). These used not only different flicker frequencies (8 Hz), but also different baseline/flicker durations and amount of flicker repeats. Since 2006, the standard and most widely used flicker protocol is the one shown in Figure 1.11, using the 12.5 Hz flicker frequency. Starting off with a baseline of 50 seconds, the first flicker period of 20 seconds starts. The pattern of 80 seconds of recovery (i.e. baseline illumination) and 20 seconds of flicker is then repeated two times and the measurement concludes at the 350 seconds mark, or put differently, in five minutes and fifty seconds.



Figure 1.11: Schematic representation of the standard flicker measurement protocol.

For practical reasons of avoiding artificially variable baseline vessel diameters, it is common practice to discard the first 20 seconds of every measurement session from subsequent analysis.

A typical response of a pair of retinal vessels to the RVA flicker session is shown in Figure 1.12. Arteries and veins follow distinct reaction paths, owing to the functional and structural differences between each vessel type. For the artery, with each flicker initiation the vessel responds with vasodilatation, relying on the principles of neurovascular coupling (Riva et al., 2005). After flicker cessation, artery diameter decreases below baseline values (reactive constriction) and returns to the range of initial diameter values approximately 10-40 seconds post flicker cessation. Essentially, the choice of 20 seconds flicker duration and 80 seconds of recovery time thereafter is empirically based on a compromise between gaining a marked vessel response and allowing enough time to vessels for their diameters to return back to initial values (Nagel et al., 2005). Veins, on the other hand, do not undergo a constriction phase as arteries do and additionally show a sustained vasodilation phase, characteristic of their larger vessel compliance and their nature of being reservoir vessels.

1.8.2.3 Dynamic Response Analysis

Analysis of the retinal arteriolar and venular responses similar to the one in Figure 1.12 can be performed either by utilising the RVA software-generated output or by independently processing raw data. The RVA software summarises the three flicker provocations into one average and reports the following four parameters: A_{\max} , A_{\min} , A_{peak} (maximum arterial dilation, constriction and difference between the two, respectively) and V_{\max} (maximum venular dilation). For statistical purposes, these responses are calculated from an arbitrarily chosen time window, that encompasses 6 seconds: 3 seconds before flicker cessation and 3 seconds after (Kotliar et al., 2004). Then, the software automatically generates a report, classifying the vessel responses according to values from Table 1.5, as “normal”, “narrowed”, “unremarkable” or “undetectable” reaction.

Arteries	Normal Mean	Normal Standard Deviation (SD)
A_{\max} (%)	6.9	± 2.8
A_{\min} (%)	-2.7	± 1.4
A_{peak} (%)	9.6	± 3
Veins		
V_{\max} (%)	6.5	± 2.5

Table 1.5: Classification scheme of vessel response to flicker used by the in-built RVA software. Based on these values (Nagel et al., 2005), RVA generates a report of a “normal”, “narrowed”, “unremarkable” or “undetectable” reaction.

1 Overview of principal literature

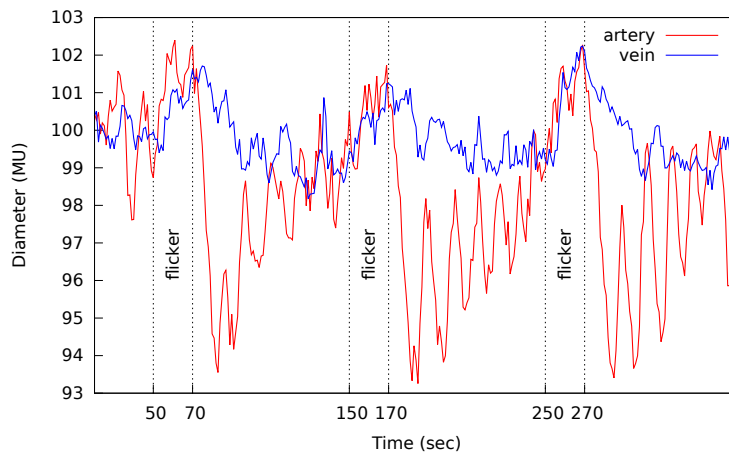


Figure 1.12: A typical, normal arterial (red) and venular (blue) response from flicker provocation following the standard protocol shown in Figure 1.11. Dotted vertical lines indicate the presence of the flicker stimulus. The first 20 seconds have been discarded prior to plotting the graphs.

In terms of analysing raw data output independently of the RVA software, there are various approaches as well as measurement parameters calculated. The basic distinction between approaches is choosing to report on an averaged response across all three (or as many as possible) flicker repeats or choosing to analyse them separately. Irrespectively of that choice, the parameters used to characterise an arteriolar and venular response to flicker provocation are the following:

- Baseline Diameter Fluctuation (BDF), the maximum amplitude (peak-to-peak) for arterioles and venules, 30 seconds prior to (each) flicker start
- Maximum Dilation (MD), the maximum 1-second diameter for arterioles and venules, within 50 seconds after (each) flicker start
- Maximum Constriction (MC), the minimum 1-second diameter for arterioles, within 50 seconds after (each) flicker start
- Dilation Amplitude (DA), the difference between MD and MC for arterioles
- Baseline-Corrected Flicker Response (bFR), the difference between DA and BDF for arterioles (Nagel et al., 2004)
- Reaction Time (RT), the time needed (in seconds) to reach MD for arterioles and venules
- Constriction Time (CT), the time needed (in seconds) to reach MC for arterioles
- ΔD , the difference between MD and the 1-second vessel diameter prior to flicker start for arterioles or venules (a measure of vessel dilatory capacity) (Heitmar et al., 2010)

- Average Peak Ratio (APR), the ratio of DA over BDF for arterioles (a measure of vessel elasticity) (Heitmar et al., 2011a)

All diameter values are reported as a % change (i.e. normalised) to the initial (i.e. prior to the first flicker) mean baseline diameter. Similarly to the MD and MC parameters, others have defined a 4 seconds time window (calculating the median), i.e. 2 seconds before and 2 seconds after the time point of the maximum/minimum dilation/constriction diameter and have termed it “mean maximal dilation/constriction”, respectively (Kotliar et al., 2011b). Also, the area under the reaction curve during baseline and during/after flicker has been calculated, essentially providing an average diameter (Gugleta et al., 2012).

1.8.2.4 Other External Provocations

The first report on the results of external provocation with the RVA system by means of isometric exercise was performed in 1999 (Blum et al., 1999) on 40 healthy volunteers with encouraging results for the feasibility of retinal functional assessment. Other techniques that temporarily alter retinal blood flow to assess vascular reactivity include the use of an oculo-oscillo dynamograph (Nagel and Vilser, 2004; Kotliar et al., 2008) and gas mixtures inhalation (Blum et al., 2001; Kiss et al., 2002; Resch et al., 2005; Wimpissinger et al., 2004; Jean-Louis et al., 2005). A combination of stimulation techniques is also possible; performing an isometric exercise (Bek et al., 2008; Jensen et al., 2011) or temporarily elevating IOP by means of an episcleral suction cup (Garhöfer et al., 2005) and at the same time stimulating the retina with flickering light.

1.8.3 Retinal Oximetry

Measurement of retinal oxygen consumption may provide important clinical information about the metabolic state of the retina. Differences between the oxygen delivered to the retina via arterioles and drained away from it via venules can be quantified, if the total OSat in these vessels is measured. Such information can be used to complement our understanding on retinal function in health and disease.

Dual-wavelength oximetry uses digitally recorded retinal images obtained simultaneously at two distinct wavelengths to determine retinal vessel OSat. A dual band-pass filter at a sensitive (610 nm) and a non-sensitive (548 nm, isosbestic) wavelength is replacing the optoelectronic shutter in the previously described RVA camera system (Section 1.8.2.1). Oxyhemoglobin (HbO₂) and deoxyhemoglobin (Hb) absorb light equally at the isosbestic wavelength, whereas there is a considerable absorbance variation at the sensitive wavelength. Since it is practically impossible to measure neither transmittance nor absorption of light in the retina, in order

to determine OSat, reflection must be exploited instead. Thus, Optical Density (OD) can be calculated based on the retinal reflectance of the retinal vessels (I_{int}) and that of the surrounding tissue (I_{ext}), measured as grayscale pixel values:

$$\text{OD} = \log \frac{I_{\text{ext}}}{I_{\text{int}}} \quad (1.14)$$

The Optical Density Ratio (ODR) is the ratio between the ODs of the two sampled wavelengths, which has been found to be linearly related to OSat after compensation for vessel diameter and fundus pigmentation (Hammer et al., 2008). Reliability and reproducibility of the technique has been recently evaluated in healthy volunteers with promising results (Lasta et al., 2012; Man et al., 2013).

1.8.4 Visual Field Testing

Visual Field (VF) testing (or else perimetry) is an additional ancillary test for following functional changes of many retinal diseases, alongside its frequent use in glaucoma management and in diagnosis of neurological disorders. Static automated perimetry is the most common method of clinical VF testing. It involves determining the dimmest stimulus that can be seen at a series of pre-determined test point locations. The Humphrey Field Analyser II (Carl Zeiss Meditec, Germany) is an advanced, commercially available perimeter intended to identify visual field defects. It incorporates widely accepted testing algorithms, especially the Swedish Interactive Thresholding Algorithm (SITA), which offer very high accuracy and a relatively short test time. The test of choice for examining the central visual field is the 30-2 SITA Standard pattern which comprises 76 test point locations covering the central 30° field with a grid of points 6° apart. Two quantitative global indices that summarise visual field status are the mean deviation and the pattern standard deviation, both measured in decibels. The former shows how much, on average, the whole field deviates from normal while the latter reflects irregularities in the field, such as those caused by localised defects. These can be used in research to sort eyes into groups of varying disease states.

1.9 Nailfold Capillaroscopy

Structural evaluation of the morphology, distribution and number of capillaries is deemed necessary to investigate microvessel rarefaction at a peripheral level. Capillary rarefaction occurs in many tissues in patients with essential HT and has been shown to contribute to an increased peripheral vascular resistance (Serne et al., 2001). It is yet unknown whether abnormalities in these vessels are a cause or consequence of elevated BP (Noon et al., 1997). Rarefaction may be caused by a structural (anatomic) lack of capillaries, functional non-

perfusion, or both. Conjunctival (Harper et al., 1978) and nailfold (Noon et al., 1997; Antonios et al., 1999) capillary density have been found significantly smaller in hypertensives than in normotensives. Common techniques used to assess cutaneous microvascular function include capillaroscopy, venous occlusion plethysmography, and laser Doppler anemometry (Yvonne-Tee et al., 2006).

The nailfold plexus is one of only a few locations on the human body where capillaries advance close enough to the skin surface to become easily detectable *in vivo*. They lie in hairpin-like loops parallel to the skin surface. Each loop consist of an arterial and a venous limb. Using laser Doppler anemometry blood cell velocities can be measured within single skin capillaries, not only from the nailfold area, but also in the sublingual and lip skin. Of course, the nailfold area causes no discomfort to the patient and is easier to minimise involuntary movements, thus it is the preferred microvascular sampling site.

1.9.1 Measurement Principle

When a narrow beam of laser light is focused onto an arterial or venous limb of a capillary loop, a fraction of the laser light is backscattered by red blood cells, shifting the frequency of light according to the Doppler effect. The frequency shift is directly proportional to the speed of the blood column. Impaired haemodynamic patterns and functional activity of the nailfold capillaries have been reported after topical temporary cooling of the area. The test is being performed by rapidly decompressing CO₂ and directing it to the fingertip by means of a tube. The nailfold capillaries are being observed and blood velocity is recorded before, during and after the cooling phase. Flow stop is defined as velocity below 0.05 mm/sec for longer than 5 seconds (Mahler et al., 1987). Prolonged stop of flow, a condition termed vasospasm, characterised hypertensives contrary to normotensives in a study (Gasser and Bühler, 1992). This finding has been interpreted as a reduced functional reserve at a capillary level in HT.

1.9.2 CapiScope Capillaroscopy System

The CAM₁ Laser Doppler Capillary Anemometer (KK Technology, England) is a commercially available video capillaroscopy system that can measure blood cell velocity (Stücker et al., 1996). It uses a low power, near-infrared (780 nm) laser for detecting the necessary Doppler shift. The use of this wavelength has several advantages: it exhibits a deeper penetration depth, the measurement is less affected by the oxygenation of blood and it is also less dependent on skin color, as melanin has a low absorption in the near-infrared. Actual sample depth is typically less than 100µm. The laser beam is focused via the objective down to a 10 microns diameter spot in the centre of the field of view. Illumination is provided by 8 LEDs emitting green light (525 nm) to maximize the contrast between the erythrocytes and the surrounding tissue. A

CCD camera (Model XC-75CE, Sony, Japan) needs to be focused so that the object plane and the laser focal point match to get a clear view. The camera output is fed to a computer monitor.

The CAM1 system provides an approximately $\times 220$ magnified image of the nailfold plexus with a resolution of 640×480 pixels. The device can be positioned appropriately onto the limb of a capillary loop using an XYZ micropositioner stage. The laser beam is reflected by blood cells at the focal point moving parallel to the tissue surface. This gives the laser light a Doppler shift directly proportional to the velocity of the reflecting blood cells. Acoustic feedback control with sound from the Doppler shift provides real time audible cues via the computer speakers during the entire measurement. This allows the operator to obtain the point of maximum signal strength more readily. The Doppler shifted laser signal is collected by the objective and internal optoelectronics and processed in real time by means of the accompanied CapiScope software producing a velocity trace (in absolute units of mm/s). This system can be used to measure velocities ranging from 0.02 to 14.6 mm/s. The velocity trace can be saved along with an image or video sequence of the capillary being measured, onto the hard drive of the computer, for offline post-processing.

Chapter 2

Retinal Vessel Analyser: Reproducibility

2.1 Background

During the early years of introduction of the RVA (Chapter 1) into the scientific setting, it was merely used to observe and record retinal vessel diameters under constant illumination (baseline conditions) over time. A few studies, as mentioned in Section 1.8.2.1, have reported on the device's reproducibility and sensitivity under such conditions with excellent results. However, with the introduction of flicker stimulation and the possibility to probe retinal reactivity, a completely different regime of measurements (dynamic reaction) was characterising RVA's main function. Unfortunately, subsequent studies utilising flicker measurements described the accuracy of the system by referring to the reproducibility and sensitivity of the non-relevant early studies.

Studies actually reporting on reproducibility of the flicker responses are either irrelevant to the current hardware and protocol or incomplete. An early study reported Coefficient of Variation (CV) values of 25% but it was unclear whether this was for arteries, veins, or combined (Polak et al., 2002). A later study reported CV values of 15.2% for arteries and 20.3% for veins (Garhöfer et al., 2003). However, both studies at that time were using a prototype RVA system and a flicker frequency of 8 Hz. Nagel et al. (2006a) were the first to report short-term (1 hour) and long-term (1 month) variability of flicker responses but had the following limitations: they measured only one parameter (maximum vessel dilation), they did not state how they defined that parameter and also they averaged responses over the three flicker cycles within each session. Reproducibility of the values calculated with the inbuilt RVA analysis have been reported in healthy Asian individuals (Nguyen et al., 2009) using non-standard measures (Pearson correlation coefficients). The only report - using the current RVA system and the current protocol - on CV values among both baseline and reaction diameters has been published

only recently, with low CV values for MD and MC and moderate CV values for RT (Heitmar et al., 2010).

2.1.1 Motivation and Research Rationale

The RVA in its current implementation is a fairly new research tool in retinal functional assessment since it was introduced no earlier than 2006 (Nagel et al., 2006a). A few years later, several experts in the field published a feature review on the RVA and its applicability, highlighting several “unresolved open questions” (Garhöfer et al., 2010). The insufficiency of reproducibility data of flicker responses was the main one.

The nature of such measurements, being related to microvasculature haemodynamics, is inherently variable. Thus, protocols should be strictly adhered to and standardisation procedures should always be meticulously observed. Otherwise, external factors might mask or exaggerate the true flicker responses. On that basis, detailed reproducibility analysis by means of the ICC is performed: comparisons between examiners are reported for the first time and the intraobserver (or else intersession) reproducibility analysis from Heitmar et al. (2010) is expanded upon with a greater amount of parameters tested across arteries and veins on a flicker per flicker breakdown, as well as on averaged flicker cycles.

Lastly, the vendor-generated flicker-reaction report classifies responses according to an obsolete flicker protocol (Nagel et al., 2005) and its inbuilt parameters are defined on a rather narrow time window of 6 seconds (3 seconds prior to flicker cessation and 3 seconds after) (Section 1.8.2.3). Recent studies utilising different parameter definitions (Heitmar et al., 2010) have reported values of maximum dilation and/or constriction to be occurring outside this time frame, thus rendering the appropriateness of the RVA-generated parameters ambivalent. Thus, comparison between the inbuilt and independent analysis output is being performed.

2.1.2 Aims

The aims of this study were the following:

- to quantify and test the interobserver and intraobserver reproducibility of the RVA system for the independently analysed dynamic retinal vessel reactivity parameters (BDF, DA, MD, MC, bFR, ΔD , APR, RT, CT) on a per flicker analysis.
- to quantify and test the reproducibility of the inbuilt software-generated parameters of A_{\max} , A_{\min} , A_{peak} and V_{\max} and to compare them with their counterparts: arterial MD, MC, DA and venular MD, respectively.

- to quantify the static retinal vessel parameters of tortuosity, branching angles and AVR as processed from fundus photos obtained with the same RVA system.

2.2 Subjects and Methods

2.2.1 Interobserver Reproducibility

Measurements were performed by two Examiners for 13 healthy volunteers (5 males, 8 females) under identical conditions. Both Examiners had comparable experience with the RVA device and adhered to the detailed protocol described in Section 2.2.5. The sequence of data collection between Examiner 1 and Examiner 2 was arbitrarily selected. A break of at least five minutes was allowed between the two sessions per subject. All measurements took place within 6 months.

2.2.2 Intraobserver Reproducibility

Measurements were performed by a single examiner for 30 healthy volunteers (15 males, 15 females) on two occasions under identical conditions. All measurements adhered to the detailed protocol described in Section 2.2.5.

2.2.3 Standardisations Applied

The vessel length selection was governed by each individual's angioarchitecture, but was always kept as long as possible. Nevertheless, when selecting vessel segments for a measurement in real time, no two pairs can be selected to be precisely equally long. Thus, in order to standardise comparisons and to eliminate potential influence of the segment length measured between examiners (interobserver reproducibility study) as well as between sessions (intraobserver reproducibility study) the following procedure was followed: for every pair of vessel segments that underwent comparison, the longer one was truncated to exactly the same length as the shorter one. This was possible by processing the raw data matrix output of the RVA. Moreover, for the repeated measurement throughout the intraobserver reproducibility study, the repetition feature of the software was used, which automatically measures exactly the same location as in the previous one. In some cases this was not possible due to registration issues, but the location was manually matched as closely as possible.

2.2.4 Inclusion and Exclusion Criteria

All participants conformed with the following criteria:

- aged at least 18 years old

- had no history of systemic disease or any current relevant manifestation
- were medication-free
- had clear optical media
- had no history of epilepsy

They were given a minimum of 24 hours to decide on their participation and to ask any questions, after receiving a written description of the study protocol. The tenets of the Declaration of Helsinki were observed, and institutional review board approval was granted. Written informed consent was obtained from every participant prior to the measurements.

2.2.5 Study Protocol

At least 12 hours prior to their morning visits, participants were asked to abstain from smoking, from consuming products containing alcohol or caffeine, as well as from taking up any sort of considerable physical activity, whereas they were instructed not to fast. Room temperature was maintained constant during all measurements (21-24 °C).

2.2.5.1 Intraocular Pressure Measurement

Non-contact tonometry was performed to assess IOP by means of a validated (Ogbuehi and Almubrad, 2008) device (Pulsair EasyEye, Keeler Ltd., UK). Three readings were obtained from each eye and the average value was recorded.

2.2.5.2 Blood Pressure and Pulse Assessment

All participants remained seated for at least 20 minutes to ensure stable haemodynamic conditions prior to the start of the examination. BP was measured from the brachial artery of the forearm using a validated (Rogoza et al., 2000), automated oscillometric digital BP monitor (UA-767, A&D Instruments Ltd., UK). Three consecutive readings of SBP, DBP and HR were recorded. MABP was calculated as previously defined (Equation (1.3)).

2.2.5.3 Retinal Vessel Functional Assessment

Details on the measuring principle of the RVA have been described earlier (Section 1.8.2.1). One arbitrarily selected eye was examined. One drop of Tropicamide (1% w/v, Bausch & Lomb, UK) was instilled to achieve pupil dilation necessary for getting unobstructed view of the posterior pole. As soon as full pupil dilation was reached, the dynamic retinal vessel assessment commenced. The fellow eye was covered to achieve good fixation. During the examination, subjects were encouraged to blink normally (to maintain a sufficiently wet cornea) and to

maintain steady fixation at the internal target, the tip of a needle. This was placed accordingly in order to position the desired vessel segments centrally as viewed on the computer monitor. The measurement location selected was 1-2 DD away from the ONH (Garhöfer et al., 2010) (Figure 2.1). First, the arterial vessel segment was selected, then the venular one and as soon as the software registered successfully the corresponding positions the measurement session started automatically. In case the contrast between the vessels and the background tissue was not adequate, or other degradations affecting video quality appeared, the measurement was aborted and restarted. The standard flicker protocol of 50 seconds baseline, 20 seconds flicker and 80 seconds of recovery was applied (Figure 1.11). The software used throughout the data capturing sessions was the vendor-supplied Retinal Vessel Analyser (V4.16.006.2).

2.2.5.4 Retinal Vessel Structural Assessment

Following the RVA assessment, the camera was set to take monochromatic and color fundus images from the same, previously dilated eye. The vendor-supplied software - Visualis (V2.62.003.1) - was used for capturing the fundus photos. A series of images were obtained as follows:

- for AVR calculation: one monochromatic image with the ONH centered at 30° and one color RGB image (for reference)
- for tortuosity and branching angles: one monochromatic image with the macula centered at 50° that included the superotemporal and inferotemporal quadrants

The desired topology was achieved by instructing the subject to follow a blinking red fixation Light-emitting Diode (LED) light with the fellow, unobstructed eye. The images were digitally stored in Tagged Image File Format (TIFF) format (lossless) for subsequent analysis.



Figure 2.1: Typical measurement location. Letter A in the red circle represents the arterial vessel segment and letter V in the blue circle represents the venular vessel segment.

For the AVR measurement, the vendor-supplied software was used for analysis, namely VesselMap 2 (V3.01.003.0). The CRAE and the CRVE were semi-automatically obtained from each subject according to the ARIC protocol (Hubbard et al., 1999). The quotient of these values was automatically calculated to derive AVR. At least four arteries and four veins were selected for the AVR measurement, depending on individual angioarchitecture. Whenever images were captured on two occasions, average AVR values were calculated (Figure 2.2).

For the measurement of branching angles (Figure 2.3) and tortuosity values (Figure 2.4) ImageJ (Version 1.47v) (Abramoff et al., 2004) was used on monochromatic fundus images for increased contrast and, hence, greater accuracy. First and second order major bifurcations of one representative artery and one representative vein were selected distal to the ONH for branching angles and the vessel segment linking those two bifurcations defined the location of tortuosity measurements. The line coursing through the vessels measured the arc length, whereas the straight line corresponded to the chord length. The ratio of the two equalled the tortuosity index. All bifurcation angle and arc/chord length measurements were repeated three times and their averages went into subsequent analyses.

2.2.6 Outcome Measures

2.2.7 Dynamic Parameters

The following parameters (as defined in Section 1.8.2.3) were measured and compared (between examiners and between sessions, for inter- and intraobserver reproducibility respectively) for all three flicker cycles (henceforth designated with numbers 1, 2 and 3) by means of raw RVA output data processing: BDF, bFR, MD, MC, DA, RT, CT, ΔD and APR. Absolute arteriolar and venular diameters were recorded in MU and compared across Examiners and across measurement sessions. Also, the RVA generated parameters of A_{\max} , A_{\min} , A_{peak} and

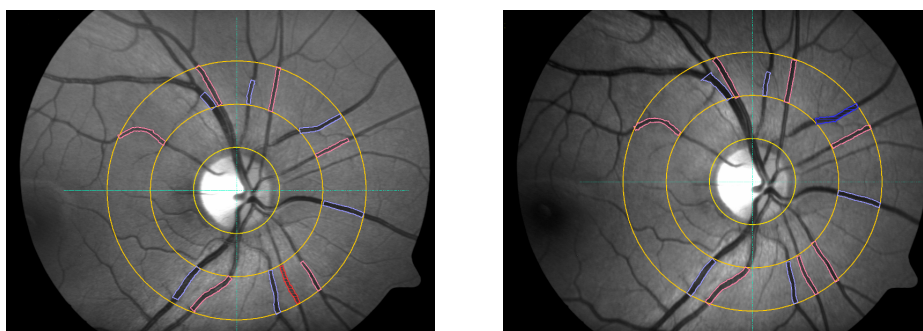


Figure 2.2: Measurement of AVR of a right eye by manually selecting arteries (red) and veins (blue) coursing through the outer ring (left). Measurement of AVR of the same eye from a subsequent visit (right). See also Figure 1.10 on page 31.

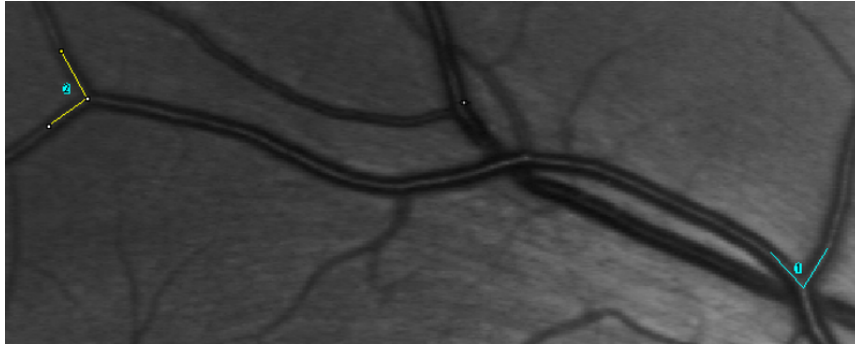


Figure 2.3: Illustration of bifurcation angles measurement using ImageJ. Values reported are in degrees. The angle marked in green represents the proximal measurement site and the angle marked in yellow represents the distal measurement site. The two bifurcation angles define the vessel segment taken for tortuosity measurements (see Figure 2.4).

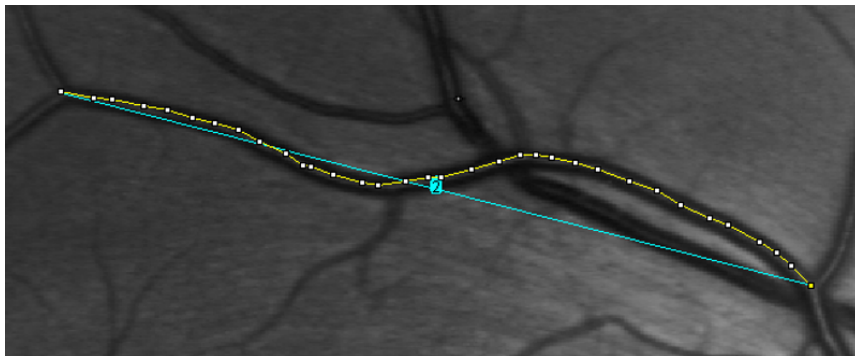


Figure 2.4: Illustration of tortuosity measurement using ImageJ, of the same vessel segment as in Figure 2.3. Values reported are dimensionless. The yellow line marks the arc length and the green line marks the chord length.

V_{\max} are reported and compared to their counterparts: arterial MD, MC, DA and venular MD, respectively.

2.2.8 Static Parameters

CRAE, CRVE and corresponding AVR values, tortuosity indices (see Equation (1.11)) and bifurcation angles for both arteries and veins are reported according to the previously described protocols (Section 2.2.5.4) for the intraobserver cohort (n=30) only (Table 2.17).

2.2.9 Statistics and Data Analysis

SPSS (Version 13.0 Chicago, SPSS Inc.) was used for statistical analysis and Graphpad Prism (Version 6.03) for plotting purposes. Normality tests were performed on all continuous data by means of the Shapiro-Wilk test, to determine distribution. In case of normal distributions, data are expressed as means (SD) and groups are compared by Student's paired *t*-tests. Non-normally distributed data are expressed as medians (Inter-Quartile Range (IQR)), compared by the Mann-Whitney U test. IQR is calculated as the difference between the third and first quartiles. For multiple comparisons across the three flicker cycles, the non-parametric Friedman test was performed. Forward stepwise multiple linear regression analysis was used to test if any of the static or dynamic variables significantly predicted maximum dilation responses. For all calculations, a P value of < 0.05 was considered significant. Reproducibility was tested by means of the ICC (Shrout and Fleiss, 1979). Box-and-whiskers plots shown indicate the median and the IQR, whereas whiskers are drawn down to the 5th percentile and up to the 95th. Points below and above the whiskers are drawn as black filled dots, indicating outliers, where applicable.

2.3 Results

2.3.1 Interobserver Reproducibility

2.3.1.1 Subjects

Characteristics of the participants (n=13) for the interobserver reproducibility part of this study are shown in Table 2.1. Mean (\pm SD) age of the healthy volunteers cohort was 29 (\pm 7) years old.

2.3.1.2 Retinal Vessels' Absolute Diameters

The retinal arteriolar and venular absolute diameter values followed a normal distribution. Hence, values are expressed as means (SD). No statistically significant difference was found between Examiners of the absolute arterioles and venules diameters that each one selected for

Subject	Age (years)	Gender	IOP (mmHg)	SBP (mmHg)	DBP (mmHg)	MABP (mmHg)	HR (pulses/min)
1	20	f	12	113	80	91	85
2	22	m	11	111	64	79	76
3	22	f	11	107	61	77	78
4	24	f	10	102	73	83	64
5	24	m	15	137	97	110	68
6	24	m	15	144	88	107	64
7	24	f	14	89	62	71	77
8	28	f	13	127	75	93	76
9	30	f	10	107	67	80	68
10	34	f	11	117	83	94	61
11	37	f	14	102	76	84	62
12	38	m	7	115	77	89	83
13	42	m	10	121	81	95	62

Table 2.1: Demographics and baseline characteristics of subjects (n=13) included in the interobserver study. Subjects are sorted by age in ascending order. For acronyms, see page 114.

the assessment of the retinal microvascular reactivity to flicker light. P values are shown in Table 2.2.

2.3.1.3 Inbuilt Dynamic Flicker Response Analysis

The parameters A_{\max} , A_{\min} , A_{peak} for arterioles and V_{\max} for venules generated from the RVA software (averaged across all three flicker cycles) are shown in Table 2.3 per Examiner. Since these values followed a normal distribution, a parametric Student's *t*-test was performed to check for differences.

2.3.1.4 Independent Dynamic Flicker Response Analysis

All dynamic response parameters tested for interobserver reproducibility were not normally distributed. Thus, values shown are medians (IQR). Statistical significance was sought using the Mann-Whitney U test. Box-and-whisker diagrams were plotted for BDF, MD, MC, DA, bFR, ΔD , APR, RT and CT for arteries (Figures 2.5 to 2.6) and for BDF, MD, ΔD and RT for veins (Figures 2.7 to 2.8) for all three flickers. The difference of MC of arterioles of the second and third flicker cycles between examiners was statistically significant ($p=0.044$ and $p=0.029$, respectively). Statistically significant difference was also found between the MD response of arteries during the last (third) flicker ($p=0.034$) (Table 2.4).

The time points of maximum dilation and maximum constriction for arteries (RT, CT) and for maximum dilation for veins (RT) are shown in Table 2.5. Comparisons across Examiners

2 Retinal Vessel Analyser: Reproducibility

Subject	Examiner 1 Arteriolar Diameter (MU)	Examiner 2 Arteriolar Diameter (MU)	Examiner 1 Venular Diameter (MU)	Examiner 2 Venular Diameter (MU)
1	107.8	107.6	177.5	168.6
2	161.1	158.1	150.4	149.1
3	128	127.5	118.8	116.3
4	118.1	116.2	144.6	146.2
5	85.2	83.9	141.3	142.5
6	119.1	119.2	155.6	157
7	144.2	142.2	156.3	164.2
8	108.2	112.8	141.7	138.3
9	125.8	133.2	125	126.8
10	111.9	111.9	141.7	140.1
11	127.3	131.3	114.5	110.3
12	94.8	95.4	171.4	174.4
13	126.4	128.4	179.4	175.2
Mean (SD)	119.8 (19.7)	120.5 (19.5)	147.5 (20.7)	146.8 (20.9)
ICC	0.994		0.990	
p value	0.38		0.55	

Table 2.2: Comparison of absolute arteriolar and venular diameters between Examiners. MU stands for Measurement Units. Student's paired *t*-tests were performed.

revealed a difference only for the arterial RT during the second flicker cycle ($p=0.029$). Across flicker cycles within Examiners, no statistically significant differences were found. Finally, non-parametric comparisons using the Mann Whitney U test between arterial and venular RT revealed differences only for Examiner 2 (flickers 2 and 3), with the veins needing longer time to reach maximum dilation compared to their arterial counterparts.

2.3.1.5 Comparison Between Inbuilt and Independent Analysis

To compare the inbuilt RVA software analysis with the one independently calculated from raw data, the three flicker responses as per Table 2.4 were averaged. Then, the two were

Parameter (%)	Examiner 1	Examiner 2	ICC	p value
A_{\max}	2.9 (1.9)	2.9 (1.7)	0.926	0.979
A_{\min}	-0.6 (0.9)	-0.7 (1.7)	0.714	0.634
A_{peak}	3.5 (2.3)	3.7 (2.9)	0.938	0.599
V_{\max}	3.5 (3.3)	3.5 (2.7)	0.871	1.000

Table 2.3: Inbuilt RVA dynamic flicker response parameters compared between examiners ($n=13$). Values are expressed as means (SD) % change to baseline diameter. Student's paired *t*-tests were performed. For definitions, see Section 1.8.2.3 on page 37.

2 Retinal Vessel Analyser: Reproducibility

Parameter	Examiner 1 Arterioles	Examiner 2	ICC	p value (across Examiners)
BDF ₁ (%)	3.9 (1.6)	3.5 (3.1)	0.358	0.920
BDF ₂ (%)	4 (4.1)	4.3 (2.8)	0.734	0.920
BDF ₃ (%)	3.9 (6.5)	3.8 (1.8)	0.728	0.840
<i>Friedman test (within Examiner)</i>	0.771	0.074		
MD ₁ (%)	104.8 (2.4)	103.6 (2.3)	0.790	0.243
MD ₂ (%)	105.7 (3.8)	104 (2.1)	0.491	0.081
MD ₃ (%)	105.7 (3.6)	103.2 (1.9)	0.487	0.034
<i>Friedman test (within Examiner)</i>	0.230	0.735		
MC ₁ (%)	96.6 (2.5)	95.7 (3.7)	0.411	0.287
MC ₂ (%)	96.9 (2.5)	94.5 (3.6)	-0.297	0.044
MC ₃ (%)	96.8 (2.2)	95.2 (2.9)	-0.749	0.029
<i>Friedman test (within Examiner)</i>	0.397	0.302		
DA ₁ (%)	9.1 (6)	8.6 (6.6)	0.943	0.840
DA ₂ (%)	9.5 (4.6)	9.3 (5.6)	0.873	1.000
DA ₃ (%)	9.4 (4.6)	8.6 (5.6)	0.742	0.762
<i>Friedman test (within Examiner)</i>	0.058	0.058		
bFR ₁ (%)	3.8 (6)	2.8 (5)	0.897	0.920
bFR ₂ (%)	3.3 (3.1)	3.4 (5.3)	0.475	0.960
bFR ₃ (%)	4.4 (4.4)	4.6 (3.7)	0.595	0.614
<i>Friedman test (within Examiner)</i>	0.735	0.230		
ΔD ₁ (%)	5.4 (3.7)	3.4 (2.7)	0.648	0.223
ΔD ₂ (%)	5.6 (2.9)	4.2 (1.1)	0.380	0.579
ΔD ₃ (%)	3.7 (3.7)	3.9 (2.5)	0.559	0.880
<i>Friedman test (within Examiner)</i>	0.726	0.926		
APR ₁	1.9 (1.3)	1.6 (1.4)	0.532	0.880
APR ₂	1.9 (1)	1.7 (0.9)	0.094	0.650
APR ₃	1.7 (2)	2.4 (1)	0.512	0.362
<i>Friedman test (within Examiner)</i>	0.923	0.084		
Venules				
BDF ₁ (%)	1.9 (2.5)	2 (1.3)	0.260	0.840
BDF ₂ (%)	2.8 (2.5)	2.2 (1.2)	0.187	0.418
BDF ₃ (%)	2.9 (2.4)	2.7 (1.1)	0.227	0.287
<i>Friedman test (within Examiner)</i>	0.368	0.375		
MD ₁ (%)	104.3 (3.2)	103.5 (2.7)	0.642	0.579
MD ₂ (%)	104 (4.2)	104 (4.4)	0.686	0.362
MD ₃ (%)	104 (5.2)	103 (3.2)	0.117	0.418
<i>Friedman test (within Examiner)</i>	0.657	0.867		
ΔD ₁ (%)	3.8 (2.7)	3.6 (2.1)	0.545	0.511
ΔD ₂ (%)	4.2 (2.6)	4.2 (4.3)	0.535	1.000
ΔD ₃ (%)	3.5 (2.8)	3.3 (2.6)	0.117	0.687
<i>Friedman test (within Examiner)</i>	0.284	0.838		

Table 2.4: Independently analysed RVA dynamic flicker response parameters compared between examiners (n=13). Values are expressed as medians (IQR). Mann Whitney U tests were performed for across Examiners comparisons and Friedman tests were performed for within Examiner comparisons. Statistical significance is denoted in bold. For acronyms, see page 114.

2 Retinal Vessel Analyser: Reproducibility

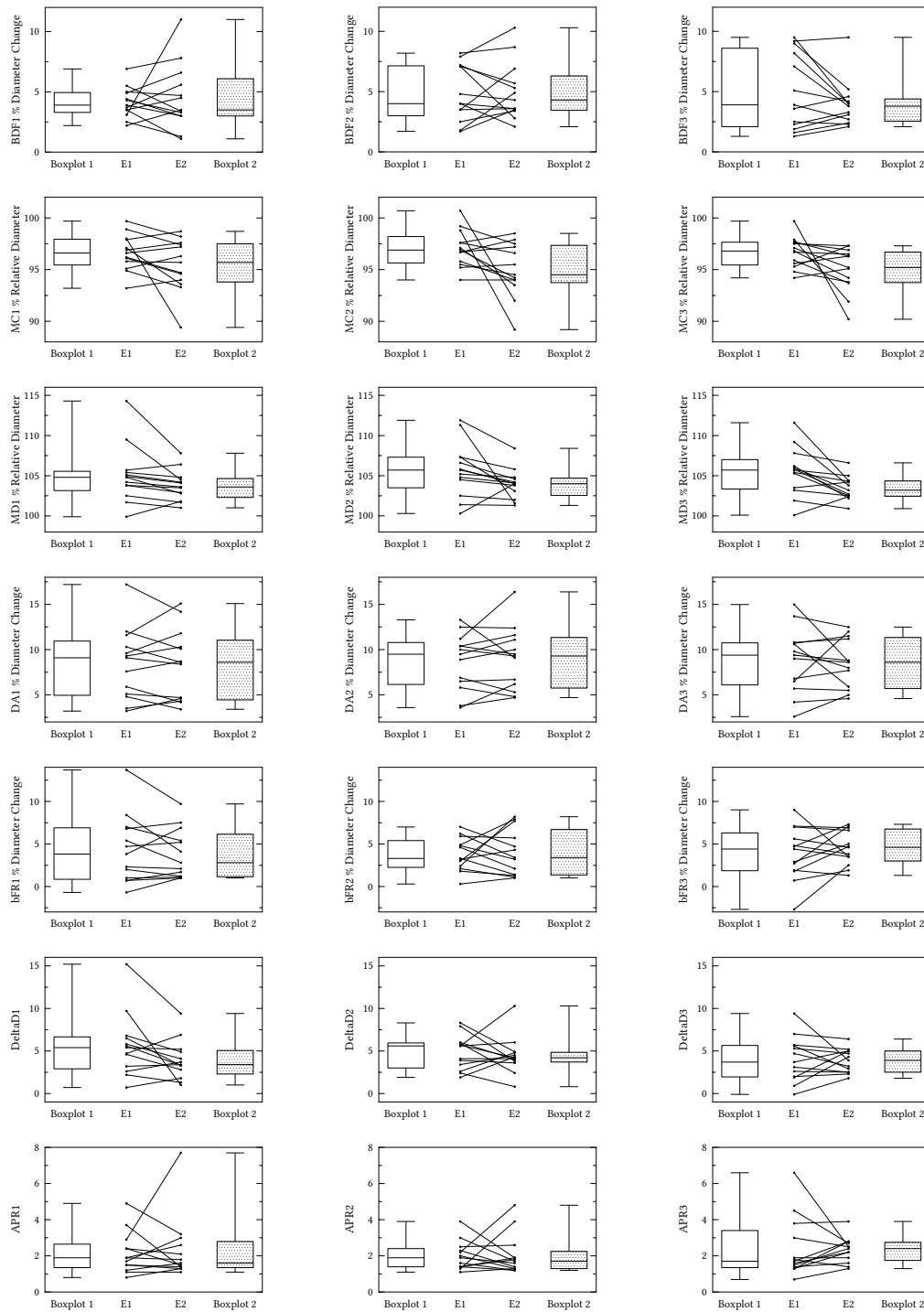


Figure 2.5: Combined box-and-whisker and “Examiner 1 - Examiner 2” comparison scatterplots (joined with straight lines) showing arteriolar diameter fluctuation and flicker responses (n=13) across all three flickers. See Table 2.4 for numerical values. For acronyms, see page 114.

2 Retinal Vessel Analyser: Reproducibility

Parameter	Examiner 1 Arterioles	Examiner 2 Arterioles	ICC	p value (across Examiners)
RT1 (seconds)	19 (17)	17 (13)	0.531	0.336
RT2 (seconds)	21 (10)	15 (7.5) [†]	0.275	0.029
RT3 (seconds)	19 (18)	15 (8.5) [‡]	0.541	0.390
<i>Friedman test (within Examiner)</i>	0.584	0.767		
CT1 (seconds)	35 (5)	34 (9.5)	-0.533	0.448
CT2 (seconds)	34 (33)	36 (11)	-0.472	0.479
CT3 (seconds)	35 (9.5)	35 (6)	0.778	0.960
<i>Friedman test (within Examiner)</i>	0.783	0.439		
Venules				
RT1 (seconds)	19 (8.5)	19 (10.5)	0.178	0.960
RT2 (seconds)	23 (11)	20 (9.5) [†]	0.829	0.311
RT3 (seconds)	19 (12)	22 (8) [‡]	-0.264	0.362
<i>Friedman test (within Examiner)</i>	0.162	0.144		

Table 2.5: Independently analysed RVA dynamic response parameters (n=13) compared between examiners. Values are expressed as medians (IQR). Mann Whitney U tests were performed for across Examiners and across vessel type (arteries-veins) comparisons and Friedman tests were performed for within Examiner comparisons. † signifies borderline statistically significant difference (p=0.05) between arteries and veins for flicker 2. ‡ signifies statistically significant difference (p=0.002) between arteries and veins for flicker 3. For acronyms, see page 114.

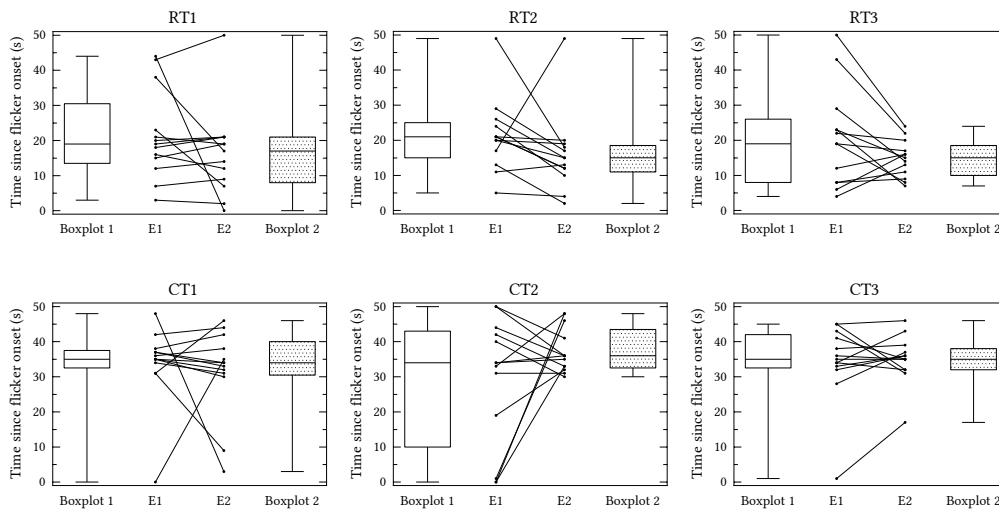


Figure 2.6: Combined box-and-whisker and “Examiner 1 - Examiner 2” comparison scatterplots (joined with straight lines) showing arteriolar reaction and constriction times (n=13) across all three flickers. See Table 2.5 for numerical values. For acronyms, see page 114.

2 Retinal Vessel Analyser: Reproducibility

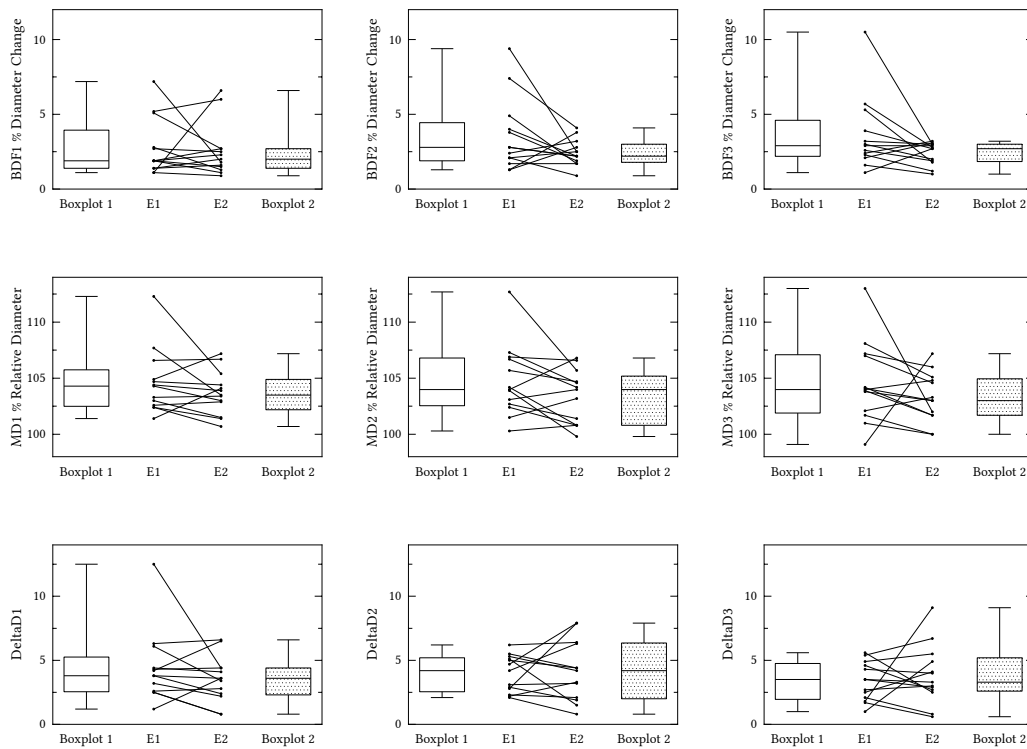


Figure 2.7: Combined box-and-whisker and “Examiner 1 - Examiner 2” comparison scatterplots (joined with straight lines) showing venular diameter fluctuation and flicker responses (n=13) across all three flickers. See Table 2.4 for numerical values. For acronyms, see page 114.

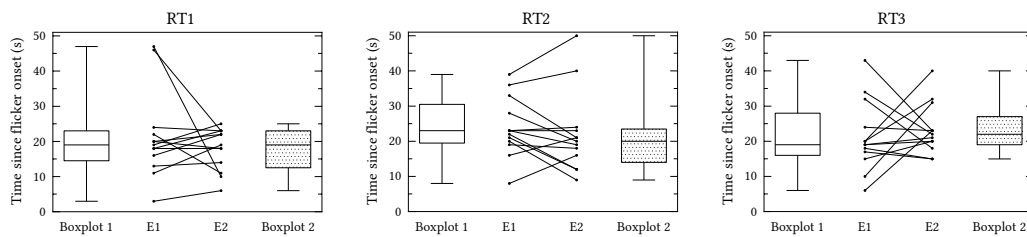


Figure 2.8: Combined box-and-whisker and “Examiner 1 - Examiner 2” comparison scatterplots (joined with straight lines) showing venular reaction times (n=13) across all three flickers. See Table 2.5 for numerical values. For acronyms, see page 114.

compared using a parametric Student's *t*-test and the results are shown in Table 2.6. For Examiner 1, all arterial parameters calculated by means of the vendor-supplied RVA software were significantly underestimated, compared to the respective independently analysed ones. The statistical significance of venular maximal dilation response was borderline ($p=0.051$). For Examiner 2, maximal arterial constriction ($p<0.001$) and arterial dilation amplitude ($p=0.001$) were found to be significantly different between the two.

2.3.1.6 Averaged Flicker Responses

All previously calculated parameters were tested for reproducibility on a per flicker basis. Since the majority of research groups are performing averaging across the three flicker cycles, we are also presenting reproducibility results of all previously calculated parameters, this time with averaged values, collapsing data across all flicker repetitions (Tables 2.7 to 2.8). Averaged values followed a normal distribution, hence parametric tests were performed to check for differences.

2.3.2 Intraobserver Reproducibility

2.3.2.1 Subjects

Baseline characteristics of the participants ($n=30$) for the intraobserver reproducibility part of this study are shown in Table 2.9. Mean (\pm SD) age of the healthy volunteers cohort was 31 (\pm 9) years old.

Parameter (%)	Examiner 1	p value	Examiner 2	p value
A_{\max}	2.9 (1.9)	0.025	2.9 (1.7)	0.140
MD (arteries)	5.4 (3.1)		3.7 (1.5)	
A_{\min}	-0.6 (0.9)	<0.001	-0.7 (1.7)	<0.001
MC	-3.2 (1.4)		-4.8 (2.3)	
A_{peak}	3.5 (2.3)	<0.001	3.7 (2.9)	0.001
DA	8.6 (3.2)		8.6 (3.2)	
V_{\max}	3.5 (3.3)	0.051	3.5 (2.7)	0.834
MD (veins)	4.6 (3)		3.4 (1.9)	

Table 2.6: Comparison ($n=13$) between inbuilt (see Table 2.3) and independent flicker analysis (see Table 2.4). Values are expressed as means (SD) % change to baseline diameter. Student's paired *t*-tests were performed. Statistical significance is denoted in bold. For definitions, see Section 1.8.2.3 on page 37.

2 Retinal Vessel Analyser: Reproducibility

Parameter	Examiner 1	Examiner 2	ICC	p value
	Arterioles			
BDF (%)	4.6 (2)	4.4 (2.2)	0.762	0.732
MD (%)	105.4 (3.1)	103.7 (1.5)	0.645	0.022
MC (%)	96.8 (1.4)	95.1 (2.3)	-0.114	0.057
DA (%)	8.6 (3.2)	8.6 (3.2)	0.924	0.964
bFR (%)	3.9 (2.1)	4.1 (2.3)	0.842	0.789
Δ D (%)	4.8 (1.8)	4 (1.1)	0.769	0.050
APR	2.1 (0.7)	2.2 (1.1)	0.529	0.883
Venules				
BDF (%)	3.2 (1.9)	2.4 (0.9)	0.385	0.142
MD (%)	104.6 (3.1)	103.4 (1.9)	0.545	0.154
Δ D (%)	3.9 (1.6)	3.8 (1.7)	0.671	0.937

Table 2.7: Independently analysed RVA dynamic flicker response parameters (n=13) compared between measurement sessions, averaged across all three flicker cycles. Values are expressed as means (SD). Student's paired *t*-tests were performed. Statistical significance is denoted in bold. For acronyms, see page 114.

Parameter	Examiner 1	Examiner 2	ICC	p value (across Examiners)
	Arterioles			
RT (seconds)	21 (9)	15 (7)	0.401	0.050
CT (seconds)	32 (8)	34 (6)	0.275	0.421
Venules				
RT (seconds)	22 (6)	21 (5)	-0.299	0.634

Table 2.8: Independently analysed RVA dynamic response parameters (n=13) compared between examiners, averaged across all three flicker cycles. Values are expressed as means (SD). Student's paired *t*-tests were performed. Statistical significance is denoted in bold. For acronyms, see page 114.

Parameter	Measurement 1	Measurement 2	p value
IOP (mmHg)	13 (3)	12 (3)	0.061
SBP (mmHg)	113 (14)	113 (15)	0.856
DBP (mmHg)	72 (11)	72 (11)	0.747
MABP (mmHg)	86 (11)	86 (11)	0.765
HR (pulses/min)	70 (9)	70 (8)	0.922

Table 2.9: Baseline characteristics of subjects (n=30) participating in the intraobserver study. Values are expressed as means (SD). Student's paired *t*-tests were performed. For acronyms, see page 114.

2.3.2.2 Retinal Absolute Diameters

Comparing the absolute arteriolar diameter between measurement sessions revealed no statistically significant difference. On the other hand, absolute venular diameters were significantly different. Nevertheless, ICC values for both vessel types showed excellent reproducibility (See Table 2.10).

Vessel Type	Measurement 1	Measurement 2	ICC	p-value
Arteries (MU)	117 (17)	117 (18)	0.967	0.876
Veins (MU)	147 (20)	144 (19)	0.970	0.025

Table 2.10: Comparison of absolute arteriolar and venular diameters (n=30) between the two measurement sessions. Values are expressed as means (SD). Student's paired *t*-tests were performed. Statistical significance is denoted in bold.

2.3.2.3 Inbuilt Dynamic Flicker Response Analysis

The parameters A_{\max} , A_{\min} , A_{peak} for arterioles and V_{\max} for venules generated from the RVA software (averaged across all three flicker cycles) are shown in Table 2.11 for each measurement session. Non-parametric Mann Whitney U tests for significance testing were performed, since values failed to indicate normal distributions.

2.3.2.4 Independent Dynamic Flicker Response Analysis

Similarly to the interobserver analysis, all dynamic response parameters tested for intraobserver reproducibility were not normally distributed. Thus, values shown are medians (IQR). Statistical significance was checked using the Mann-Whitney U test. Box-and-whisker diagrams were plotted for BDF, MD, MC, DA, bFR, ΔD , APR, RT and CT for arteries (Figures 2.9 to 2.10) and for BDF, MD, ΔD and RT for veins (Figures 2.11 to 2.12) for all three flickers. Outliers are shown with black filled dots, where applicable.

Parameter (%)	Measurement 1	Measurement 2	ICC	p value
A_{\max}	3.5 (3.1)	2.8 (3.1)	0.818	0.297
A_{\min}	-0.95 (1.6)	-0.6 (1.1)	0.101	0.711
A_{peak}	4.6 (4.1)	3.4 (3.6)	0.732	0.375
V_{\max}	3.3 (3.4)	2.6 (4)	0.837	0.539

Table 2.11: Inbuilt RVA dynamic flicker response parameters compared between measurement sessions (n=30). Values are expressed as medians (IQR) % change to baseline diameter. Mann Whitney U tests were performed for across measurements comparisons. For definitions, see Section 1.8.2.3 on page 37.

2 Retinal Vessel Analyser: Reproducibility

Parameter	Measurement 1	Measurement 2	ICC	p value
	Arterioles			
BDF ₁ (%)	3.6 (2.6)	3.7 (2.6)	0.693	0.900
BDF ₂ (%)	3.6 (2.7)	3 (3.2)	0.390	0.460
BDF ₃ (%)	3.5 (2.2)	3.2 (3.2)	0.315	0.657
<i>Friedman test</i>	0.479	0.717		
MD ₁ (%)	103.7 (3.1)	103.5 (3.2)	0.622	0.478
MD ₂ (%)	103.7 (4.6)	103.7 (3.9)	0.394	0.842
MD ₃ (%)	104.1 (3.9)	103.6 (3.4)	0.522	0.865
<i>Friedman test</i>	0.188	0.836		
MC ₁ (%)	96.5 (2.9)	96.4 (2.4)	0.567	0.918
MC ₂ (%)	97 (2.9)	96.4 (2.8)	0.301	0.796
MC ₃ (%)	96.7 (3.1)	96.9 (2.8)	0.237	0.882
<i>Friedman test</i>	0.226	0.227		
DA ₁ (%)	7.7 (4.8)	6.8 (4.9)	0.688	0.367
DA ₂ (%)	7 (4.6)	7 (5.6)	0.671	0.784
DA ₃ (%)	7 (5.2)	7 (5.4)	0.812	0.690
<i>Friedman test</i>	0.275	0.465		
bFR ₁ (%)	3 (3.3)	2.8 (4)	0.600	0.344
bFR ₂ (%)	3.3 (2.4)	3.6 (2.4)	0.491	0.496
bFR ₃ (%)	3.6 (3)	2.7 (3)	0.572	0.515
<i>Friedman test</i>	0.789	0.619		
ΔD ₁ (%)	3.3 (2.7)	3.8 (4)	0.770	0.871
ΔD ₂ (%)	4.1 (3.9)	4.2 (3.6)	0.583	0.935
ΔD ₃ (%)	3.7 (3.8)	3.3 (3.7)	0.640	0.579
<i>Friedman test</i>	0.614	0.282		
APR ₁	1.9 (1)	1.8 (0.9)	0.115	0.824
APR ₂	1.7 (0.9)	2 (0.9)	0.117	0.415
APR ₃	1.9 (0.9)	1.7 (0.9)	0.317	0.876
<i>Friedman test</i>	0.829	0.588		
Venules				
BDF ₁ (%)	2.7 (1.7)	2.2 (1.7)	0.718	0.169
BDF ₂ (%)	3.2 (1.7)	2.1 (2.4)	0.636	0.160
BDF ₃ (%)	2.7 (2.1)	2.4 (1.5)	0.514	0.297
<i>Friedman test</i>	0.569	0.581		
MD ₁ (%)	104.1 (2.7)	104.2 (3.1)	0.873	0.647
MD ₂ (%)	104.3 (2.9)	104.6 (4.3)	0.913	0.712
MD ₃ (%)	105 (4.1)	104 (3.8)	0.692	0.188
<i>Friedman test</i>	0.006	0.453		
ΔD ₁ (%)	3.9 (2.9)	3.9 (2.6)	0.877	0.723
ΔD ₂ (%)	4.2 (2.5)	3.8 (3.1)	0.866	0.416
ΔD ₃ (%)	4.2 (2.4)	4.3 (4.9)	0.681	0.460
<i>Friedman test</i>	0.581	0.927		

Table 2.12: Independently analysed RVA dynamic flicker response parameters (n=30) compared between measurement sessions. Values are expressed as medians (IQR). Mann Whitney U tests were performed for across measurements comparisons and Friedman tests were performed for within measurements comparisons. For acronyms, see page 114.

2 Retinal Vessel Analyser: Reproducibility

Parameter	Measurement 1	Measurement 2	ICC	p value
	Arterioles			
RT1 (seconds)	18 (8)†	16 (10)¶	0.143	0.495
RT2 (seconds)	16 (6)‡	17 (11)	-0.179	0.398
RT3 (seconds)	17 (11)§	16 (12)	0.172	0.544
<i>Friedman test</i>	0.378	0.869		
CT1 (seconds)	40 (8)	35 (10)	0.341	0.053
CT2 (seconds)	38 (11)	40 (9)	0.327	0.733
CT3 (seconds)	37 (8)	37 (12)	-0.665	0.651
<i>Friedman test</i>	0.378	0.494		
	Venules			
RT1 (seconds)	20 (5)†	20 (7)¶	0.230	0.727
RT2 (seconds)	22 (9)‡	20 (6)	0.013	0.269
RT3 (seconds)	19 (10)§	18 (8)	0.172	0.630
<i>Friedman test</i>	0.849	0.179		

Table 2.13: Independently analysed RVA dynamic response parameters (n=30) compared between measurement sessions. Values are expressed as medians (IQR). Mann Whitney U tests were performed for across measurements and across vessel type (arteries-veins) comparisons and Friedman tests were performed for within measurements comparisons. † signifies statistically significant difference (p=0.017) between arteries and veins for flicker 1, measurement 1. ‡ signifies statistically significant difference (p<0.001) between arteries and veins for flicker 2, measurement 1. § signifies statistically significant difference (p=0.017) between arteries and veins for flicker 3, measurement 1. ¶ signifies statistically significant difference (p=0.006) between arteries and veins for flicker 1, measurement 2. For acronyms, see page 114.

2 Retinal Vessel Analyser: Reproducibility

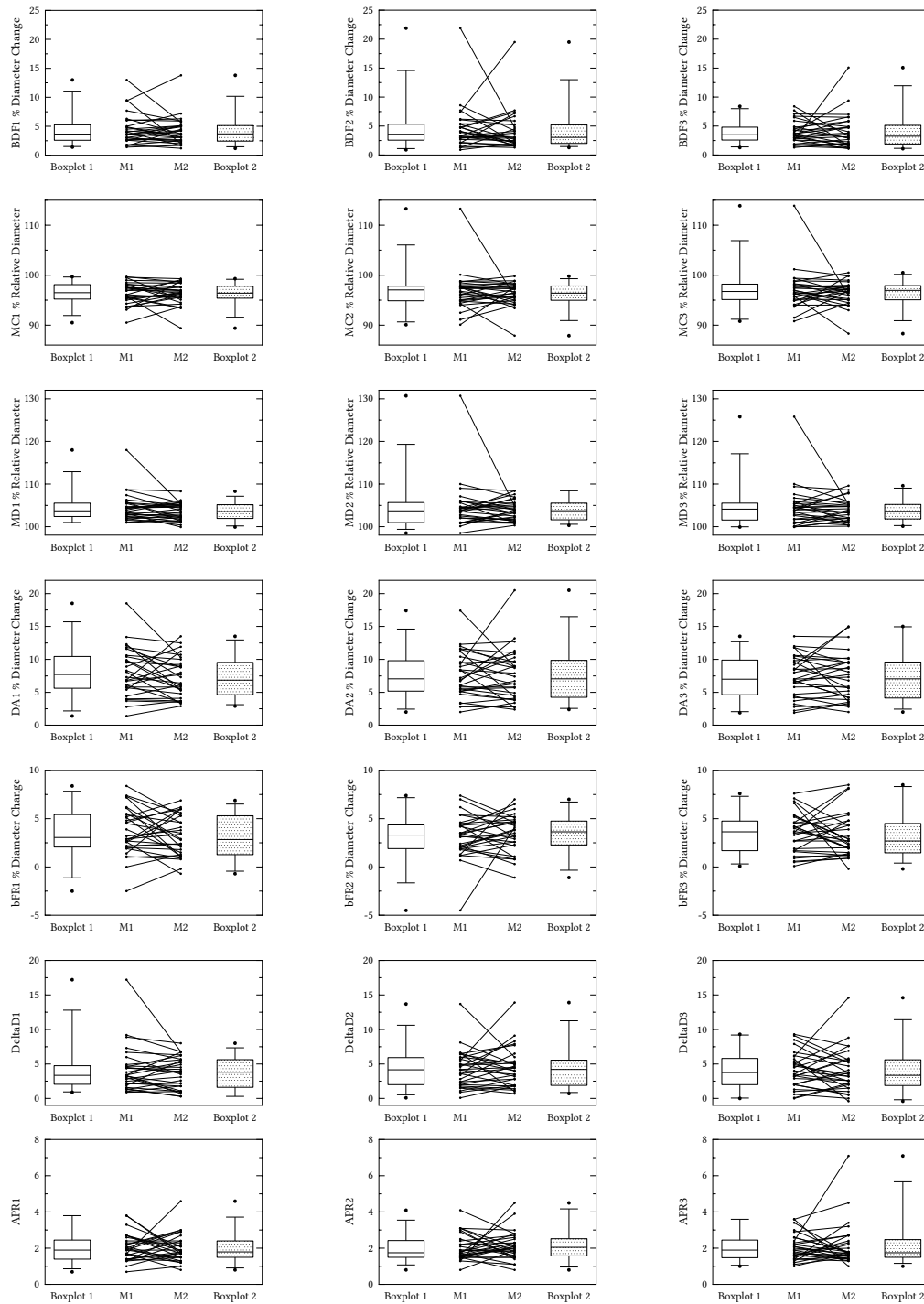


Figure 2.9: Combined box-and-whisker and “Measurement 1 - Measurement 2” comparison scatterplots (joined with straight lines) showing arteriolar diameter fluctuation and responses ($n=30$) across all three flickers. Outliers are depicted as dots. See Table 2.12 for numerical values. For acronyms, see page 114.

2 Retinal Vessel Analyser: Reproducibility

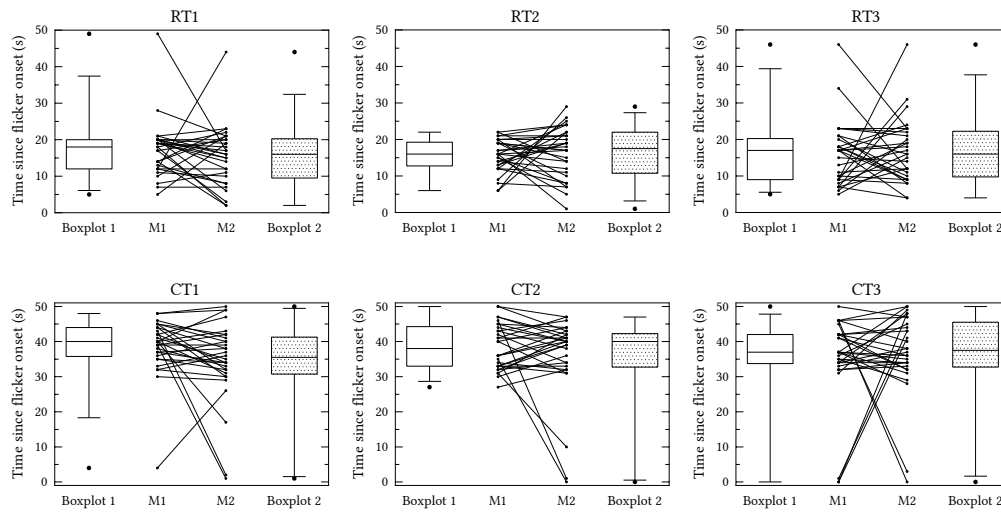


Figure 2.10: Combined box-and-whisker and “Measurement 1 - Measurement 2” comparison scatterplots (joined with straight lines) showing arteriolar reaction and constriction times ($n=30$) across all three flickers. Outliers are depicted as dots. See Table 2.13 for numerical values. For acronyms, see page 114.

2.3.2.5 Comparison Between Inbuilt and Independent Analysis

To compare the inbuilt RVA software analysis with the one independently calculated from raw data, the three flicker responses as per Table 2.12 were averaged. Then, the two were compared using a parametric t -test. Results are shown in Table 2.14. For both measurement sessions, all arterial and venular parameters calculated by means of the vendor-supplied RVA software were underestimated, compared to the respective independently analysed ones. All except one (maximum dilation for measurement session 1) reached statistical significance ($p=0.127$).

Parameter (%)	Measurement 1	p value	Measurement 2	p value
A_{\max}	3.5 (2.3)	0.127	2.9 (2)	0.001
MD (arteries)	4.4 (4.5)		3.7 (2.1)	
A_{\min}	-0.8 (1.3)	<0.001	-0.8 (0.9)	<0.001
MC	-3.2 (3.1)		-3.6 (2.1)	
A_{peak}	4.3 (2.4)	<0.001	3.8 (2.4)	<0.001
DA	7.7 (3.2)		7.3 (3.4)	
V_{\max}	3.9 (2.4)	<0.001	3.7 (2.8)	<0.001
MD (veins)	5.2 (2.6)		4.6 (2.5)	

Table 2.14: Comparison ($n=30$) between inbuilt (see Table 2.11) and independent flicker analysis (see Table 2.12). Values are expressed as means (SD) % change to baseline diameter. Student’s paired t -tests were performed. Statistical significance is denoted in bold. For definitions, see Section 1.8.2.3 on page 37.

2 Retinal Vessel Analyser: Reproducibility

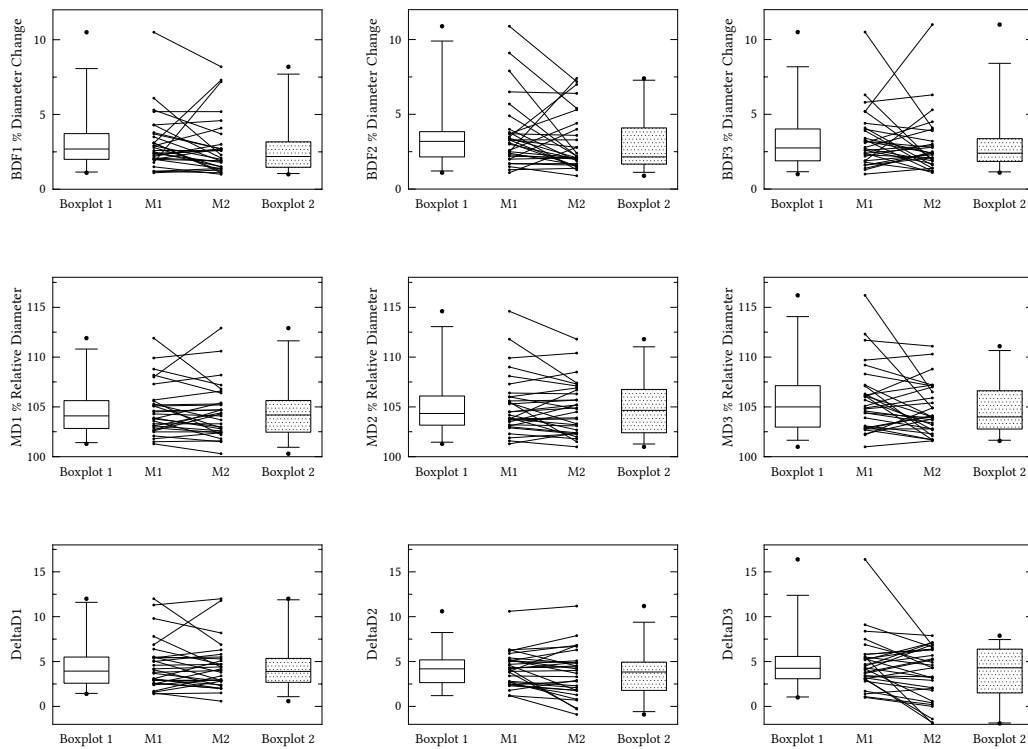


Figure 2.11: Combined box-and-whisker and “Measurement 1 - Measurement 2” comparison scatterplots (joined with straight lines) showing venular diameter fluctuation and responses ($n=30$) across all three flickers. Outliers are depicted as dots. See Table 2.12 for numerical values. For acronyms, see page 114.

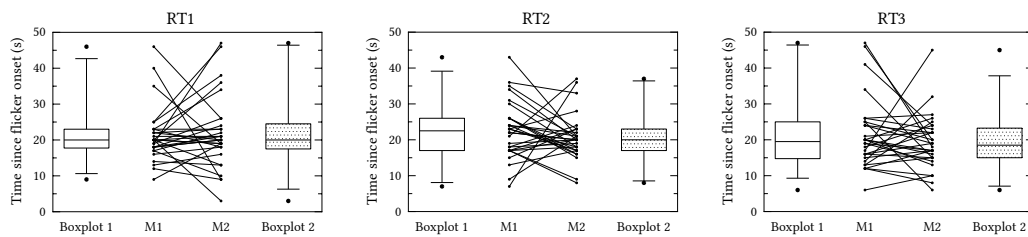


Figure 2.12: Combined box-and-whisker and “Measurement 1 - Measurement 2” comparison scatterplots (joined with straight lines) showing venular reaction times ($n=30$) across all three flickers. Outliers are depicted as dots. See Table 2.13 for numerical values. For acronyms, see page 114.

2.3.2.6 Averaged Flicker Responses

Similarly with results from the interobserver reproducibility analysis, since the majority of research groups are performing averaging across the three flicker cycles, we are also presenting reproducibility results of all previously calculated parameters, this time with averaged values, collapsing data across all flicker repetitions (Tables 2.15 to 2.16). Averaged values followed a normal distribution, hence parametric tests were performed to check for differences.

2.3.2.7 Static Retinal Vessel Parameters

CRAE, CRVE, AVR, tortuosity indices and branching angles values are shown in Table 2.17.

2.3.2.8 Multiple Regression Analysis

Forward stepwise multiple regression analysis was used to test if any of the static and dynamic parameters (averaged across flicker cycles) or any of the measured baseline vessel diameters and IOP or BP values significantly predicted MD (separately for arteries/veins and measurement sessions). For arteries, the dependent variable was arterial MD and the independent variables that were tested whether they predicted MD responses were: absolute arteriolar diameter, IOP, MABP, CRAE, arterial tortuosity, proximal and distal arteriolar bifurcation angles, BDF, bFR, MC, DA, ΔD , APR, RT and CT. For veins, the dependent variable was venular MD and the independent variables that were tested whether they predicted MD responses were: absolute venular diameter, CRVE, venular tortuosity, proximal and distal venular bifurcation angles, BDF, ΔD , and RT.

For measurement 1, the results of the regression for arterial MD indicated that three predictors explained 99.9% of the variance of MD ($R^2=0.999$, $F(3,26)=95861$, $p<0.001$). These were DA ($\beta=1$, $p<0.001$), MC ($\beta=0.99$, $p<0.001$) and CT ($\beta=-0.004$, $p=0.01$). For measurement 2, the results of the regression for arterial MD indicated four predictors that could explain 99.9% of the variance of MD ($R^2=0.999$, $F(4,25)=13585$, $p<0.001$). These were ΔD ($\beta=0.03$, $p=0.003$), bFR ($\beta=0.97$, $p<0.001$), MC ($\beta=0.95$, $p<0.001$) and BDF ($\beta=0.95$, $p<0.001$).

For measurement 1, the results of the regression for venular MD indicated that two predictors explained 80.4% of the variance of MD ($R^2=0.804$, $F(2,27)=55.387$, $p<0.001$). These were ΔD ($\beta=0.76$, $p<0.001$) and BDF ($\beta=0.69$, $p<0.001$). For measurement 2, the results of the regression for venular MD indicated that the same two predictors explained 78% of the variance of MD ($R^2=0.780$, $F(2,27)=47.909$, $p<0.001$). These were ΔD ($\beta=0.66$, $p<0.001$) and BDF ($\beta=0.58$, $p<0.001$).

2 Retinal Vessel Analyser: Reproducibility

Parameter	Measurement 1	Measurement 2	ICC	p value
	Arterioles			
BDF (%)	4.2 (2.4)	4 (2.8)	0.558	0.760
MD (%)	104.4 (4.5)	103.7 (2.1)	0.522	0.305
MC (%)	96.7 (3.1)	96.3 (2.1)	0.363	0.497
DA (%)	7.7 (3.2)	7.3 (3.4)	0.753	0.533
bFR (%)	3.4 (1.7)	3.2 (1.8)	0.739	0.581
Δ D (%)	4.1 (2.5)	4 (2.5)	0.723	0.717
APR	2 (0.5)	2 (0.6)	0.144	0.643
	Venules			
BDF (%)	3.3 (1.7)	2.9 (1.7)	0.802	0.126
MD (%)	105.2 (2.6)	104.6 (2.5)	0.870	0.073
Δ D (%)	4.5 (1.9)	3.9 (2.2)	0.799	0.063

Table 2.15: Independently analysed RVA dynamic flicker response parameters (n=30) compared between measurement sessions, averaged across all three flicker cycles. Values are expressed as means (SD). Student's paired *t*-tests were performed. For acronyms, see page 114.

Parameter	Measurement 1	Measurement 2	ICC	p value
	Arterioles			
RT (seconds)	16 (5)	16 (5)	-0.059	0.941
CT (seconds)	37 (5)	35 (8)	-0.112	0.380
	Venules			
RT (seconds)	21 (5)	20 (4)	0.131	0.369

Table 2.16: Independently analysed RVA dynamic response parameters (n=30) compared between examiners, averaged across all three flicker cycles. Values are expressed as means (SD). Student's paired *t*-tests were performed. For acronyms, see page 114.

Parameter	Arteries	Veins
CRAE (μ m)	175 (14)	N/A
CRVE (μ m)	N/A	216 (21)
AVR	0.82 (0.08)	
Branching Angle 1 (proximal) (degrees)	80.5 (14)	69.1 (17)
Branching Angle 2 (distal) (degrees)	78.9 (19)	75.3 (13)
Tortuosity Index	1.05 (0.05)	1.03 (0.03)

Table 2.17: Static retinal vessel parameters of the healthy, intraobserver cohort (n=30). Values are expressed as means (SD). For acronyms, see page 114.

Lastly, the test of whether arteriolar MD, MABP and IOP predicted the extent of venular MD reached no significance for both measurement sessions.

2.4 Discussion

2.4.1 Interobserver Reproducibility Study

The effect of the strict standardisation procedures during data collection by means of the RVA system is reflected through the high ICC values of absolute arterial and venular diameters selected by the two Examiners (Table 2.2). These confirm that both Examiners selected the same vessel segment. Hence, vessel reaction to flicker stimulation is highly unlikely to be confounded by any (potential) influence on initial absolute vessel diameter.

The inbuilt RVA dynamic response parameters, averaged across all three flicker cycles, exhibit excellent reproducibility across Examiners. As mentioned in Section 1.8.2.3, these values are calculated from an arbitrarily chosen time window, that encompasses 6 seconds: 3 seconds before flicker cessation and 3 seconds after. This means, that the maximal dilation and constriction are “expected” to take place within a fixed time frame, for each flicker cycle: 17-23 seconds after flicker initiation. Recently, this assumption has proven problematic, as reaction times can vary outside this 6 seconds time frame (Heitmar et al., 2010). In line with Heitmar and colleagues, when comparing the two different analyses, statistically significant differences were found for arterial MD and MC when compared with their counterparts (A_{\max} and A_{\min} respectively) (see Table 2.6). Therefore, independently analysing raw RVA data and reporting the maximal dilation and constriction values from a wider time window of 50 seconds (after flicker initiation) eliminates the underestimation or overestimation of flicker responses.

Interobserver reproducibility of the independently analysed parameters generally showed moderate ICC values, similarly for both arteries and veins (Table 2.4). Only the DA parameter, relevant to arteries, showed excellent reproducibility results across all three flicker cycles. These results might be explained by two factors: the relatively small sample size per Examiner ($n=13$) and the inherently variable nature of retinal haemodynamics. Regarding comparisons across the three flicker cycles within Examiners, the non-parametric Friedman test revealed no statistically significant differences. This result gives support to the notion that no comparable differences exist within a single measurement across the three flicker repeats, therefore averaging values would make analysis less complicated without sacrificing information.

Reaction and constriction times for arteries and veins showed moderate reproducibility between Examiners, whereas values did not differ across the three flicker cycles within Examiners. Interestingly, for Examiner 2, veins needed significantly longer time than arteries to reach maximum dilation (Table 2.5). This was the case for two out of three flicker cycles.

A similar “delay” of approximately 3-4 seconds of the venous reaction has been previously reported for healthy subjects (Heitmar et al., 2010, 2011b; Lanzl et al., 2011; Kotliar et al., 2011b) in line to this finding. The fact that this finding was not evident for measurements taken from Examiner 1, might be explained from the relatively small sample size ($n=13$, i.e. low statistical power). Performing an *a priori* power analysis for a two-tailed Wilcoxon signed-rank test (matched pairs) at an alpha level (α) of 0.05 by means of the G*Power software (version 3.1.9) (Faul et al., 2007), revealed that a sample size (n) of 15 would be required for a large effect size (0.8) with 80% statistical power, whereas for a medium effect size (0.5) the sample size would have to be increased to 35. Nevertheless, the range of values for reaction and constriction times reported here, are in very good agreement to the ones obtained from a sample of healthy South Asians and White Europeans (comparable to the sample characteristics of this study) (Patel et al., 2011). The majority of within flicker and across Examiners comparisons did not reveal statistically significant differences, with the exception of arterial RT of the second flicker cycle. This, in conjunction with the results mentioned above, might be proof that different Examiners with similar experience may yield comparable results using the RVA system.

2.4.2 Intraobserver Reproducibility Study

Having a considerably larger sample size of healthy volunteers ($n=30$ versus $n=13$) for the intraobserver reproducibility study, it was possible to overcome the limitations of the interobserver reproducibility study. The baseline characteristics of this cohort (Table 2.9) confirm the healthy status of the participants and that these adhered to the inclusion and exclusion criteria. Contrary to the comparison between Examiners, when all measurements took place on the same day, in this part of the study, measurements took place either on the same day or on a separate visit. Hence, it is important, that prior to both measurements, IOP and BP values showed no significant differences between the two measurement sessions, rendering all subsequent comparisons relevant.

Although, both arterial and venular absolute diameters between measurement sessions had highly reproducible values (shown by ICC values of more than 0.9), the diameter of the selected venular segment was (on average) 3 microns narrower during the repeat measurement (Table 2.10). This difference might have arisen from measurements that took place on separate days, when the repetition feature of the software could not be utilised and manual matching of the vessel segment was performed. Nevertheless, it has been reported that “baseline vessel diameter does not influence relative magnitude of the flicker response” (Gugleta et al., 2006). Assuming that this diameter difference was a defining factor in terms of flicker response, one would expect to find a significant difference in the venular maximum dilation values. In fact, when the two measurement sessions were compared, this was not the case, neither with the

V_{\max} parameter (Table 2.11), nor with the MD parameter (Table 2.12). Results, thus, are in line with previous findings (not influenced by baseline vessel diameter differences).

Similarly to the previous sub-study, the inbuilt RVA dynamic response parameters, averaged across all three flicker cycles, exhibit high reproducibility across measurement sessions. The maximum arterial constriction (A_{\min}) is an exception, with a low ICC value of 0.1 (Table 2.11). Though, as previously mentioned, the validity of the software-generated parameters is more important in this case, rather than how much reproducible they are. As such, comparisons performed between the independently analysed reaction parameters and their counterparts revealed an even stronger difference (compared to the interobserver study) for both measurement sessions (Table 2.14). Namely, the inbuilt analysis consistently underestimated all responses, confirming to a greater extent the same finding as in the smaller cohort of 13 participants.

Regarding reproducibility of the independently analysed dynamic responses, of note is the excellent consistence of values relating to venular parameters (BDF, MD and ΔD) throughout the flicker cycles (Table 2.12) between measurements. On the other hand, arterial parameters show moderate reproducibility in general compared to veins. This could be explained by considering some imaging aspects during data capturing: veins appear darker than arteries and thus exhibit higher contrast to their background. This, in turn, makes veins less susceptible to erroneous diameter estimations and vice versa. Comparisons within measurement sessions, across flicker repeats did not reveal statistically significant differences, with one exception: maximum venular dilation (for measurement 1) showed an increasing trend from flicker to flicker ($p=0.006$).

How do the main outcome measures of this thesis (Table 2.12) compare to the ones found in literature? Since there are few studies that have dealt exclusively with healthy volunteers, to answer this question, one must refer to publications including healthy populations as controls, compared across various pathological states. Arterial BDF and bFR have been reported once on a per flicker basis (Heitmar et al., 2010) in literature. Values fluctuate approximately 1% lower than the ones in the aforementioned study for the former, but are comparable for the latter. There are no reports on venular BDF on a per flicker breakdown, to compare these findings to. On averaged venular BDF values, Patel et al. (2011) report slightly higher values. Arterial and venular MD values are comparable with the ones reported by several studies (Nagel et al., 2006a; Mandecka et al., 2007; Lasta et al., 2013), though these studies have averaged responses across flicker cycles. Approximately 1% lower maximal dilation and 1% larger maximal constriction was found among subjects - for all flickers - compared to the 30 normals (of an older age group) included in Heitmar et al. (2011b). This translates in a comparable arterial DA, despite the age difference. The study (Heitmar et al., 2010) that introduced retinal arteriolar elasticity (defined

as APR) showed similar values to the ones reported here. The index ΔD representing arterial and venular dilatatory capacity shows comparable values between vessel types.

The findings of delayed venular RT compared to arterial RT in the interobserver study, were confirmed with greater power in the intraobserver study. When reaction times of arteries and veins were compared, values from all flicker cycles within the first measurement session reached statistical significance, whereas one cycle did so for the second measurement (the trend that venules took longer to reach maximum dilation, remained though) (Table 2.13). Also it is important to note that both reaction and constriction times have low ICC values, indicating a large fluctuation between sessions and making it debatable whether they are meaningful to calculate. No significant differences were found within measurement sessions. Looking at reaction time values, it is evident that arteries may reach maximum dilation (on average) outside the 17-23 seconds window (for instance on the 16th second). This is essentially the source of underestimation when using the inbuilt RVA parameters. It is even more pronounced when calculating the maximum constriction, as constriction times are well outside this range (ranges of 35-40 seconds). Venular reaction times (on average) fall within the 17-23 seconds window, but not all individual values do so, thus rendering comparisons between the two analyses statistically significant (Table 2.14). The values reported here are comparable with several other studies (Patel et al., 2011; Heitmar et al., 2010, 2011b) highlighting the importance and benefits of standardisation when comparisons across studies are to be performed.

Regression analysis did not reveal any relationship between static (baseline diameters, CRAE, CRVE, tortuosity index, bifurcation angles) and dynamic (MD) parameters, neither in arteries nor in veins. MABP did not predict arteriolar MD in any of the regression models, confirming other studies (Heitmar et al., 2010; Garhöfer et al., 2003). Interestingly, the two measurement sessions did not “agree” in which predictors could explain the variance of arterial MD. This is one more indicator of low agreement among arteriolar calculated parameters. The only common predictor was arteriolar MC, which shows a positive correlation with arteriolar MD. In other words, arteries responding to flicker with large dilation responses exhibit large constriction phases after flicker cessation. Conversely, for veins the two predictors (BDF and ΔD) explained the variance of MD consistently throughout the two measurement sessions. By definition, ΔD is a measure of a vessel’s dilatatory capacity, which explains its relation to MD as shown by the regression analysis results. Of note is that venular BDF, which represents the diameter fluctuation during baseline illumination, can predict MD variation during flicker stimulation. Spontaneous retinal venous pulsation is a well known observation occurring in the proximity of the ONH (Jacks and Miller, 2003). This might contribute to venous BDF despite the considerable distance of the measured vessel segment from the edge of the ONH. Results

support the notion that large baseline fluctuations lead to large dilation responses during flicker stimulation.

2.5 Conclusions

Despite the innovation the RVA system has brought into the field of non-invasive retinal function assessment, research groups do not follow standardised analysis procedures yet and sometimes fail to extensively describe their implemented methods and protocols. Reproducibility of the flicker responses strongly depends on measuring conditions (Seifertl and Vilser, 2002). These should be carefully replicated as carefully as possible, when comparisons are to be made between healthy participants and various disease populations, to ensure the validity of the measurements.

Herewith, results are presented of interobserver and intraobserver reproducibility of a series of parameters that exist to describe the arterial and venular compliance before, during and after flicker provocation. Despite the strict standardisations applied throughout, ICC values are low to moderate for arteries, whereas for veins are moderate to high. Reproducibility is helpful to examine when there is no satisfactory standard against which to compare the validity of a measurement. Studies from other research groups are warranted to compare these results to.

In CVD the delicate balance between vasodilators and vasoconstrictors is disturbed leading to what is commonly referred to as endothelial dysfunction (Nadar et al., 2004). Hence, accurate assessment of vascular function has been investigated as a potential prognostic marker and as a possible therapeutic target. Currently, the golden standard to assess endothelial (dys)function in a non-invasive manner and on a macrovascular level is Flow-Mediated Dilation (FMD). Evaluation of FMD in the brachial artery is performed by means of high-resolution ultrasound recording the physiological response of increased blood flow, following distal forearm induced ischemia. A recent, multi-center reproducibility study has demonstrated that adherence to a rigorous protocol and adequate operator skills improve the reliability of the technique (Ghiadoni et al., 2012). Short-term CVs were ranging from 7.6% to 11.9%, whereas long-term CVs were ranging from 11.6% to 16.1%. Flicker-induced vessel responses were weakly correlated to brachial FMD indicating the absence of a direct analogy between the two vascular beds and possibly between the two mechanisms involved (Pemp et al., 2009).

Current studies employing the RVA system to assess endothelial function are pursuing to explore potential flicker response differences between health and disease. Since these comparisons are naturally cross-sectional, the applicability of the RVA is currently limited to screening or stratification purposes. Lack of longitudinal studies is preventing researchers to

2 Retinal Vessel Analyser: Reproducibility

draw conclusions on the progression of the associations reported. Such studies are needed to explore whether the RVA can be used as a diagnostic tool in the future.

Chapter 3

Location and Length Influence on Vessel Reactivity

3.1 Background

Documents provided by the manufacturer of the RVA system (Imedos AG) describe certain technical limitations as well as certain standardisation procedures which should be followed by end-users. More specifically, on selecting the measurement location and vessel segment's length, the following are advised:

- Measurement location should be at least 0.5 DD away from the ONH.
- Vessel segment's length should have a maximum length of 1 DD, but generally recommended to be kept as long as possible.
- Due to resolution limitations, measurement of vessels with luminal diameter smaller than $90\mu\text{m}$ "may be difficult".

The measurement setup procedure encompasses the following steps. Initially, the camera's objective is adjusted centrally to the dilated pupil to an appropriate distance in order to obtain a uniformly illuminated fundus image on the computer's screen. Then, focus is adjusted to get a sharp image. The fixation needle needs to be placed accordingly so as the subject is able to clearly observe it and at the same time the vessels of interest are central to the image view. The end-user finally places the measurement window on the desired area. An instance of the measuring window is shown in Figure 3.1. The pair of red lines superimposed on an arteriole and a venule indicate the measurement location and length.

How do the aforementioned manufacturer guidelines translate into numerical values? Typically, in a healthy eye, arterioles' diameters are ranging from $90\mu\text{m}$ to $140\mu\text{m}$, whereas venules' diameters from $110\mu\text{m}$ to $180\mu\text{m}$, within a range of 0-3 DD from the edge of the ONH. Hence, there is a substantial range of vessel diameters (i.e. different locations) that can be measured.

Regarding vessel's length, theoretically, the maximum length, that the red lines in Figure 3.1 can be extended to, is 100 pixels (personal communication). Using the Carl Zeiss FF450^{plus} fundus camera at the 30° angle image field, these correspond to 1230 MU or else to 1230 µm for Gullstrand's normal eye (12.3 MU per pixel). Practically, this maximum value cannot possibly be achieved, since the software's algorithm truncates parts of the selection edges, even under ideal conditions. For example, the maximum length that could possibly be selected using a stationary straight target (for testing purposes) yielded a value of 1100 MU.

3.1.1 Motivation and Research Rationale

In addition to the lack of standardisation on dilatory parameter calculations (Chapter 2), currently there is no standardisation regarding the location and the length of the vessel segments selected for retinal endothelial functional assessment by means of the RVA. Although the majority of research groups appear to sample the retina within 1-2 DDs away from the ONH, many others arbitrarily select within a wide range of 0-3 DDs (Nagel et al., 2006a,b; Frederiksen et al., 2006; Bek et al., 2008; Mehlsen et al., 2011). Furthermore, even though the majority of researchers report the location they measured at, they do so without applying any standardisation, but base their selection on visual estimations only. Some do not define their selection at all (Blum et al., 2008; Rueddel et al., 2012).

Similarly for the length of the chosen vessel segments, many studies do not disclose any information (Rickenbacher et al., 2009; Reimann et al., 2009; Pemp et al., 2009; Lott et al., 2012; Lasta et al., 2013), whereas some that do so, report values as long as 1500 µm (Mandacka et al., 2009; Nguyen et al., 2009; Dawczynski et al., 2007; Mandacka et al., 2007) that by definition cannot be true (longer than the theoretical upper limit of 1100 µm). Moreover, no study reports numerical values of absolute vessel segment lengths, despite the fact that this information can be easily extracted from the supplied software. Instead, the values that are reported are qualitative approximations. Also, it is questionable whether values reported are valid, because finding a long straight vessel segment (of an extent of 1500 µm) on *all* measured retinas in a study is improbable.

Understandingly, both vessel location and length selection are governed by individual angioarchitecture. But within the 30° angle image field, retinal blood vessels vary structurally and functionally, as a function of size and location. The use of relative (to the baseline) diameter values to flicker reaction helps to overcome vessel size differences, but vessel dilation and/or constriction might be influenced by locality and/or the extent of segments measured. Herewith, it is investigated whether these two variables - location and length - affect the measuring outcomes.

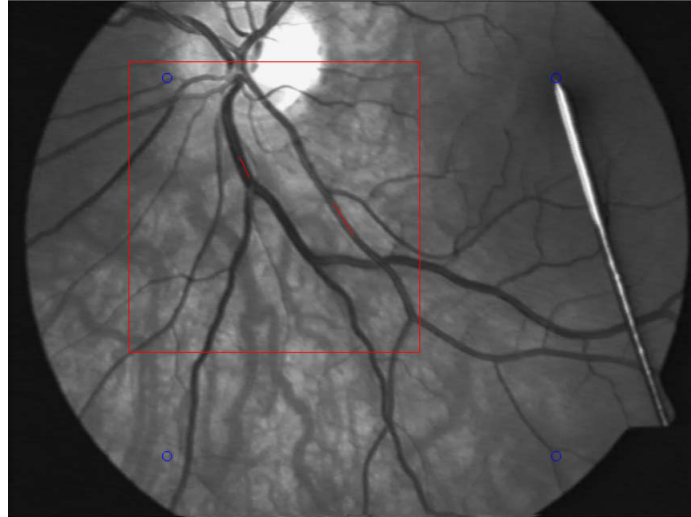


Figure 3.1: RVA's measuring window. The four blue circles at each corner aid the repositioning of the fixation needle (shown at right) for repeated measurements. Here, the superotemporal fundus area of a left eye is shown.

3.2 Subjects and Methods

Measurements were performed by a single examiner for 11 healthy volunteers (5 males, 6 females) in one unselected eye. The same inclusion and exclusion criteria as previously listed (Section 2.2.4), applied.

3.2.1 Data Collection

The same protocol was followed as in Section 2.2.5.3 using three flicker cycles as in Figure 1.11. For every given RVA measurement session, vessel diameters of one pair (arteriole-venule) of operator-selected vessel segments (within an area of 1-2 DD) were recorded across space and time, in real time. These sessions were recorded on S-VHS tapes. This allowed us to replay sessions offline and select two additional measurement locations (0-1 DD and 2-3 DD) as per Figure 3.2. Measurement rings as the ones shown in Figure 3.2 were superimposed on each measurement window according to every individuals' DD to improve standardisation and achieve perfect measurement location accuracy. The use of relative distances to the ONH to describe retinal locations is a standard procedure, as for AVR measurements, for instance. The choice of 1 DD wide rings, on one hand serves for easy comparisons among different groups (because this is what most groups report) and on the other hand satisfies the manufacturer's recommendation for taking vessel segments of a maximum of 1 DD length. Despite the fact that the length of each vessel segment was arbitrarily selected (within the limits of each ring)

prior to the commencement of the measurement session, this was later standardised across subjects, as detailed in the next Section.

3.2.2 Data Processing

Data were analysed independently of the vendor-supplied software. Custom-built scripts were used to process raw data output from the RVA software in a versatile way. These scripts were written by Dr. Robert J. Summers. Excel data matrices containing both the artery and vein flicker reaction across space (one diameter recording every 10 MU, extending to a variable amount of columns, depending on segment length) and time (25 diameter recordings per second, for 350 seconds equalling to a total maximum of 8750 rows of diameter data) were split into two Comma-separated Values (CSV) files using a *bash* script, by means of the *xls2csv* and *csplit* utilities. Further *awk* scripts:

- removed any potential outliers (eliminating irregularly high or low values due to e.g. blinks), data outside ± 2 SDs from the mean, similarly to others (Jensen et al., 2011)
- filled in any potential missing data blocks, using linear interpolation, in line with Kotliar et al. (2011a)
- binned values over 1 second intervals (each containing 25 data points), in line with Nagel et al. (2004); Gugleta et al. (2006)
- normalised vessel diameter values to the mean of the 30 seconds of baseline diameter values, in line with Polak et al. (2002); Kotliar et al. (2010)

3.2.2.1 Analysis per Location

Further to the real-time recordings of one arteriole and one venule within the area of 1-2 DD (designated as Segment 2) distal to the ONH, two additional pairs of vessel segments were measured offline from the video tape recordings. These were within a range of 0-1 DD (designated as Segment 1) and 2-3 DD (designated as Segment 3) distal to the ONH. Hence, a total of 33 arteriolar vessel segments and 33 venular segments went into the analysis. To eliminate any potential bias of vessel length selection, an equally long vessel segment (240 MU, corresponding to 24 columns of data), was processed for all segments across subjects with the aid of the aforementioned scripts. Absolute arteriolar and venular diameters were recorded in MU and compared across measurement locations.

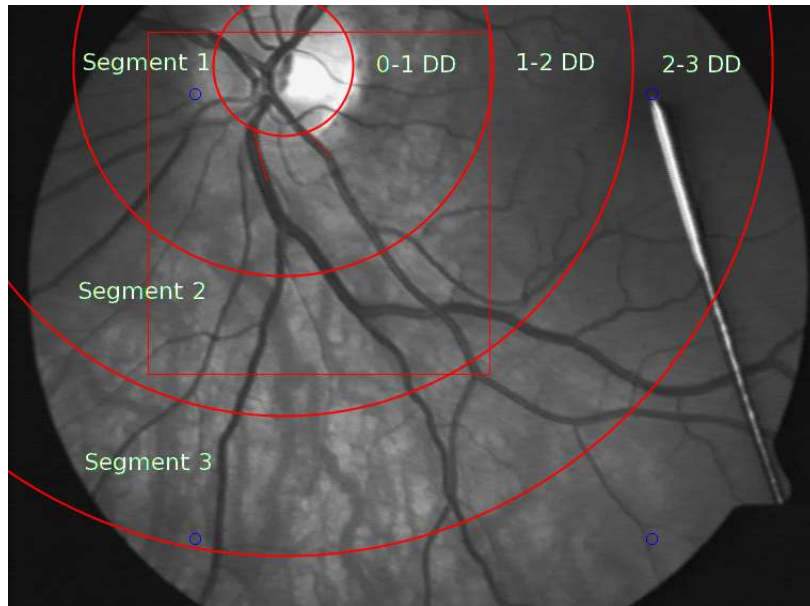


Figure 3.2: Illustration of measured locations in relation to the distance from the ONH. The segment taken out from the area of 0-1 DD distal to the ONH is designated as Segment 1, from the area of 1-2 DD as Segment 2 and from the area of 2-3 DD as Segment 3.

3.2.2.2 Analysis per Segment's Length

For the purpose of comparing vessel diameter's flicker responses of different lengths all vessel segment pairs measured from the 1-2 DD area were re-analysed. During that re-analysis, instead of truncating the vessel lengths to 240 MU, their full length was utilised as initially selected during the real-time measurement session. Depending on individual angioarchitecture, these lengths ranged from 440 MU to 920 MU for arteries and from 350 MU to 1230 MU for veins. Detailed breakdown on a per individual basis is shown in the Results section (Table 3.7). The diameter recordings during flicker stimulation of these longer segments went into a comparison with the previously standardised lengths of 240 MU.

3.2.3 Data and Statistical Analysis

SPSS (Version 13.0 Chicago, SPSS Inc.) was used for statistical analysis and for plotting purposes. Normality tests were performed on all continuous data by means of the Shapiro-Wilk test, to determine distribution. For the case of absolute vessel diameters, values were normally distributed, thus one-way Analysis of Variance (ANOVA) was used with the measurement location as the categorical independent variable and vessel diameter as the continuous variable. For all other outcome parameters calculated, which were non-normally distributed, Kruskal-Wallis H tests were performed, with the measurement location as the grouping variable. For

all calculations, a P value of < 0.05 was considered significant. Associations of the outcome parameters (where applicable) with vessel diameter and MABP were examined by means of linear regression analysis. Finally, a graphical representation for comparing long and short segments was used by plotting the difference of the vessel diameter flicker response of each of the longest vessel segments minus their 240 MU long counterparts.

3.3 Results

3.3.1 Baseline Characteristics

Data from 11 healthy volunteers (5 males, 6 females) were analysed and included in this study. Values of baseline parameters (vessel diameters across all measured segments, age, SBP, DBP, MABP, HR and IOP) are shown in Table 3.1. A one-way ANOVA was used to test for vessel diameters differences among the three measurement locations. Values did not differ significantly across the three measurement locations, neither for arterioles ($F(2, 30) = 1.386$, $p = 0.266$), nor for venules ($F(2, 30) = 1.871$, $p = 0.172$).

3.3.2 Comparison Across Vessel Segments

The following parameters (as defined in Section 1.8.2.3) were calculated and compared (across three measurement locations) for all three flicker cycles by means of raw RVA output data processing: BDF, bFR, MD, MC, DA, RT, CT, ΔD and APR. Kruskal-Wallis H tests showed no statistically significant differences across any of the RVA dynamic flicker responses between the three measurement locations: neither in a flicker per flicker analysis (Table 3.2), nor when all flicker cycles were averaged together (Table 3.4).

Parameters	Segment 1 (0-1 DD)	Segment 2 (1-2 DD)	Segment 3 (2-3 DD)	p-value
Arteriolar Diameters (MU)	117 (11)	114 (14)	108 (13)	0.266
Venular Diameters (MU)	160 (31)	144 (21)	128 (40)	0.172
Age (years)		29 (9)		
SBP (mmHg)		113 (11)		
DBP (mmHg)		68 (11)		
MABP (mmHg)		83 (10)		
HR (pulses/min)		69 (9)		
IOP (mmHg)		13 (3)		

Table 3.1: Absolute arteriolar and venular diameters ($n=11$) across three measurement locations and baseline characteristics of the cohort. Values are expressed as means (SD). For acronyms, see page 114.

3 Location and Length Influence on Vessel Reactivity

Parameter	Arterioles			p value
	Segment 1 (0-1 DD)	Segment 2 (1-2 DD)	Segment 3 (2-3 DD)	
BDF1 (%)	4.5 (5.3)	5.5 (4.8)	4.3 (3.2)	0.826
BDF2 (%)	5.6 (4.6)	4.8 (3.1)	5.5 (4.4)	0.782
BDF3 (%)	4.8 (5.9)	4.1 (2.3)	4.5 (3.8)	0.518
MD1 (%)	103.6 (4.4)	104.1 (1.9)	103.6 (4.0)	0.926
MD2 (%)	103.3 (3.7)	104.1 (2.6)	102.9 (3.0)	0.733
MD3 (%)	104.1 (3.8)	103 (2.2)	104.7 (4.0)	0.465
MC1 (%)	96.4 (3.7)	96 (4.2)	96 (4.3)	0.867
MC2 (%)	97.1 (3.2)	95.7 (2.6)	95.9 (4.2)	0.462
MC3 (%)	97 (2.7)	96.5 (1.7)	97 (4.0)	0.582
DA1 (%)	8.4 (8.7)	8.3 (5.6)	8.1 (7.0)	0.892
DA2 (%)	8.8 (8.3)	8.1 (3.6)	9.2 (8.0)	0.926
DA3 (%)	10.1 (7.4)	7.6 (3.8)	8.3 (6.8)	0.540
bFR1 (%)	3.4 (3.9)	2.4 (2.2)	4 (4.4)	0.227
bFR2 (%)	2.2 (3.9)	3.1 (2.7)	2.8 (3.1)	0.494
bFR3 (%)	2.6 (4.0)	2.9 (3.7)	3.1 (3.8)	0.651
Δ D1 (%)	4.3 (7.2)	4.1 (3.2)	4.9 (4.2)	0.874
Δ D2 (%)	3.7 (8.3)	4.7 (5.0)	3.1 (4.5)	0.982
Δ D3 (%)	3.8 (3.4)	3.2 (2.4)	3.6 (4.3)	0.421
APR1	1.7 (0.6)	1.5 (0.4)	1.7 (1.1)	0.257
APR2	1.3 (0.6)	1.6 (0.6)	1.5 (0.4)	0.106
APR3	1.4 (0.6)	1.6 (1.4)	1.8 (0.5)	0.318
	Venules			
BDF1 (%)	4.2 (2.2)	2.7 (1)	3.5 (4.1)	0.077
BDF2 (%)	4.8 (2.4)	3.3 (3.4)	3.9 (4.1)	0.675
BDF3 (%)	3.6 (1.5)	3.5 (3.8)	4.3 (3.2)	0.499
MD1 (%)	105.3 (5.3)	104.1 (3.8)	105.3 (2.8)	0.982
MD2 (%)	105.3 (6.5)	105 (6)	105.6 (4.9)	0.864
MD3 (%)	105.7 (5.6)	105.3 (4)	106.5 (5.9)	0.937
Δ D1 (%)	5.8 (2.6)	4.6 (5.3)	5.8 (4.9)	0.716
Δ D2 (%)	4.7 (3.6)	5.5 (2.5)	4.4 (6.9)	0.713
Δ D3 (%)	5.8 (3)	4.9 (2.9)	5.5 (3.2)	0.562

Table 3.2: RVA dynamic flicker response parameters across three fundus locations (n=11) in a flicker by flicker analysis. Values are expressed as medians (IQR). Kruskal-Wallis H tests were performed for comparisons across measurement locations. For acronyms, see page 114.

3 Location and Length Influence on Vessel Reactivity

Arteriolar reaction times showed a trend of slower reaction (time needed to reach maximum dilation) for larger vessels (closer to the ONH) compared to smaller ones (further away from the ONH). This was the case when individual flicker analysis was performed (Table 3.3) and when flickers were averaged (Table 3.5). A Kruskal-Wallis test revealed that this trend reached statistical significance in the case of averaged flickers (Table 3.5): there was a statistically significant difference between the different measurement locations ($H(2,n=33) = 7.388$, $p = 0.025$), with a mean rank of 23.32 seconds for Segment 1, 12.77 seconds for Segment 2 and 14.91 seconds for Segment 3. A post-hoc test using Dunn's multiple comparisons showed a significant difference in arteriolar reaction times between Segment 1 and Segment 2 ($p = 0.0304$). Segment 1 compared to Segment 3 followed a similar trend, however failed to reach statistical significance ($p = 0.1211$).

Since the previous non-parametric Kruskal-Wallis H tests showed no significant differences across the three measurement locations for all outcome parameters (as shown in Table 3.2), all measurement sites ($n=33$) were pooled together for linear regression analysis. Exploring potential associations of the outcome parameters with absolute vessel diameters did not show statistically significant correlations. For example, neither absolute arteriolar diameter ($r=-0.15$, $p=0.4$), nor absolute venular diameter ($r=-0.05$, $p=0.7$) correlated with maximum arteriolar and venular dilation, respectively. On the contrary, there was a significant positive correlation between MABP of subjects and arteriolar diameter response induced by flickering light ($r=0.4148$, $p=0.0164$; Figure 3.3).

3.3.3 Flicker Responses Variability as a Function of Location

To assess whether the measurement location influences the variability of the outcome measures, coefficients of variation were calculated across all three flicker cycles and then averaged across participants ($n=11$). Results for both arterioles and venules are summarised in Table 3.6.

3.3.4 Comparison Between Segment Lengths

Output from continuous diameter recordings as per the standard flicker protocol were extracted from the same vessel selection, twice: once for the longest possible selection and a second time from the truncation of this long segment to a 240 MU long segment. The point by point subtraction of each diameter value derived from the long and short segments are plotted in Figure 3.4 for arteries and Figure 3.5 for veins, for all subjects ($n=11$). The analysis was constrained only within a 1-2 DD range from the edge of the ONH (i.e. only "Segments 2" were analysed).

3 Location and Length Influence on Vessel Reactivity

Parameter	Arterioles			p value
	Segment 1 (0-1 DD)	Segment 2 (1-2 DD)	Segment 3 (2-3 DD)	
RT ₁ (seconds)	18 (11)	12 (11)	17 (5)	0.295
RT ₂ (seconds)	20 (6)	18 (9)	17 (6)	0.170
RT ₃ (seconds)	22 (10)	14 (5)	14 (8)	0.175
CT ₁ (seconds)	37 (13)	35 (41)	33 (11)	0.643
CT ₂ (seconds)	33 (20)	33 (36)	32 (11)	0.960
CT ₃ (seconds)	39 (46)	37 (10)	42 (18)	0.364
		Venules		
RT ₁ (seconds)	18 (8)	21 (10)	20 (9)	0.902
RT ₂ (seconds)	19 (5)	22 (20)	20 (10)	0.318
RT ₃ (seconds)	16 (12)	21 (8)	20 (11)	0.343

Table 3.3: RVA dynamic flicker reaction and constriction times across three fundus locations (n=11) in a flicker by flicker analysis. Values are expressed as medians (IQR). Kruskal-Wallis H tests were performed for comparisons across measurement locations. For acronyms, see page 114.

Parameter	Arterioles			p value
	Segment 1 (0-1 DD)	Segment 2 (1-2 DD)	Segment 3 (2-3 DD)	
BDF (%)	5.4 (4.6)	4.8 (2.4)	5.1 (3.8)	0.800
MD (%)	103.5 (3.6)	104 (2.9)	103.7 (3.9)	0.832
MC (%)	97.2 (3.2)	96 (3)	96.1 (3.2)	0.507
DA (%)	9.2 (7.4)	8.4 (3.9)	9.9 (6.9)	0.742
bFR (%)	3.2 (3.1)	3.2 (1.5)	3.8 (3.8)	0.514
Δ D (%)	4.7 (6)	3.8 (1.9)	4.3 (4)	0.789
APR	1.5 (0.3)	1.6 (0.5)	1.8 (0.6)	0.163
		Venules		
BDF (%)	3.9 (1.8)	3.5 (2.3)	4.6 (3.8)	0.668
MD (%)	105.3 (6.2)	105.1 (4.8)	105.7 (4.5)	0.899
Δ D (%)	5.3 (3.6)	5 (2.1)	5.6 (5.1)	0.785

Table 3.4: RVA dynamic flicker response parameters across three fundus locations (n=11), averaged across three flicker cycles. Values are expressed as medians (IQR). Kruskal-Wallis H tests were performed for comparisons across measurement locations. For acronyms, see page 114.

3 Location and Length Influence on Vessel Reactivity

Parameter	Arterioles			p value
	Segment 1 (0-1 DD)	Segment 2 (1-2 DD)	Segment 3 (2-3 DD)	
RT (seconds)	19 (5) [†]	15 (4) [†]	16 (3)	0.025
CT (seconds)	38 (21)	35 (17)	34 (11)	0.788
	Venules			
RT (seconds)	18 (7)	20 (12)	20 (5)	0.609

Table 3.5: RVA dynamic flicker reaction and constriction times across three fundus locations (n=11), averaged across three flicker cycles. Values are expressed as medians (IQR). Kruskal-Wallis H tests were performed for comparisons across measurement locations. Statistical significance is denoted in bold. † signifies post-hoc test's statistically significant differences between Segment 1 and Segment 2 (p = 0.0304). For acronyms, see page 114.

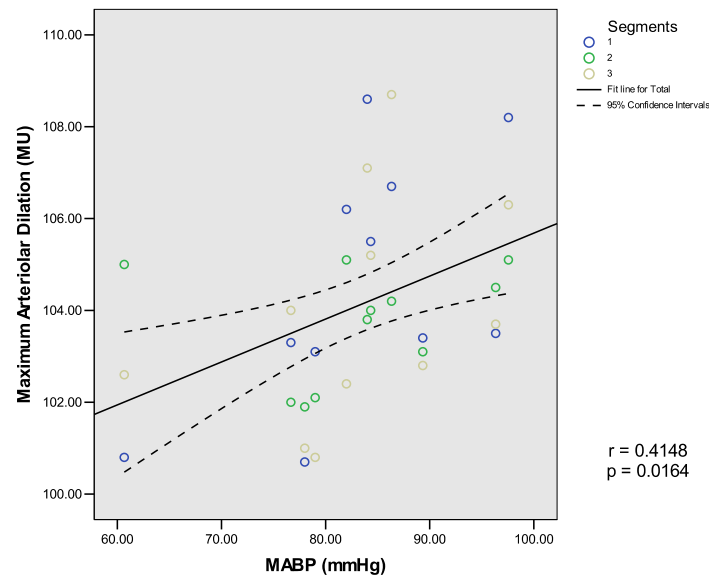


Figure 3.3: Correlation between the maximum arteriolar dilation response and MABP for all segments (33) of all subjects (n=11). The solid line corresponds to the regression line and the dashed line corresponds to the 95% confidence interval. Segment 1 corresponds to an area of 0-1 DD, Segment 2 to an area of 1-2 DD and Segment 3 to an area of 2-3 DD distal to the ONH.

3 Location and Length Influence on Vessel Reactivity

Parameter	Arterioles		
	Segment 1 (0-1 DD)	Segment 2 (1-2 DD)	Segment 3 (2-3 DD)
BDF	24.3%	25.0%	24.0%
MD	0.8%	0.6%	0.9%
MC	0.6%	0.9%	1.1%
DA	13.1%	13.8%	16.3%
bFR	68.7%	35.2%	43.1%
ΔD	40.9%	46.4%	41.2%
APR	24.5%	21.1%	24.8%
RT	33.7%	38.6%	27.6%
CT	49.6%	43.7%	31.4%
	Venules		
BDF	24.4%	30.7%	27.5%
MD	0.6%	0.7%	0.9%
ΔD	32.3%	33.2%	38.4%
RT	36.0%	31.3%	32.1%

Table 3.6: Mean coefficients of variation across flicker cycles as a function of location for each outcome parameter. Smallest variability per parameter is highlighted in bold. For acronyms, see page 114.

Subjects	Arteries			Veins		
	Short MU	Long MU	Difference MU	Short MU	Long MU	Difference MU
1	240	840	600	240	350	110
2	240	890	650	240	390	150
3	240	820	580	240	1230	990
4	240	440	200	240	570	330
5	240	920	680	240	980	740
6	240	710	470	240	940	700
7	240	770	530	240	860	620
8	240	680	440	240	880	640
9	240	630	390	240	610	370
10	240	620	380	240	760	520
11	240	860	620	240	690	450

Table 3.7: Vessel segments lengths that went into the comparison. The extent of the long segments was only restricted by individual angioarchitecture (selection was always kept as long as possible). The extent of the short segments was truncated to an arbitrary length of 240 MU in order to compare two distinctly different lengths.

To quantify the graphical representation of the differences as shown in Figures 3.4 to 3.5, the area under the curve (positive deviation from zero), the area above the curve (negative deviation from zero) and their sums (total deviation from zero) were calculated (Table 3.8) for arteries and veins individually per subject. Since the subtraction was (arbitrarily) calculated as the long segment minus the short one, larger positive deviations from zero compared to their negative counterparts means that longer segments showed higher amount of dilation (on average, across the 350 seconds) compared to the shorter segments and vice versa. For arteries, the best agreement (i.e. total deviation values closer to zero) between the two lengths selections is found for Subjects 4, 6 and 10. For veins, the best agreement between the two lengths selections is found for Subjects 4, 6 and 7. This leaves the majority of participants (8 out of 11) with considerable deviations from the theoretical value of zero, indicating an influence of vessel segment's length on diameter recordings.

No correlation was found (neither for arteries, nor for veins) between the absolute length difference between the long and the short vessel segments (Table 3.7) and the induced total deviation from zero (Table 3.8).

3.4 Discussion

3.4.1 Measurement Location Considerations

Retinal vessels have varying structural and functional properties as they extend along space. Smooth muscle cells provide structural support to the vasculature and mediate the myogenic mechanism for vascular autoregulation of blood flow. As shown by electron microscopy, the arterial wall consists of five to seven layers of smooth muscle cells (tunica media) near the optic disk (Pournaras et al., 2008). Towards the equator, these decrease to two or three layers. An additional variable parameter when examining different locations along the retina is vessel branching. Depending on individual angioarchitecture an arteriole belonging to the area of 2-3 DD away from the edge of the ONH may belong to a third order bifurcation, since it is quite common for feeding arterioles to branch off towards the macula in the area prior to that (1-2 DD). Consequently, there is a pressure drop between arterioles of differing branching order, which may affect the potential of each vessel segment to dilate, accordingly (Gafiychuk and Lubashevsky, 2001). This is corroborated from the fact that axial velocity of red blood cells in the major retinal arteries and veins of normal human and primate monkey eyes has been found to increase linearly with vessel diameter by means of bidirectional laser Doppler velocimetry (Pournaras et al., 2008).

Regarding functional heterogeneity along the retinal microvasculature structural differences on a cellular level in endothelial cells have been identified in the pig retina *in vitro* by means of

3 Location and Length Influence on Vessel Reactivity

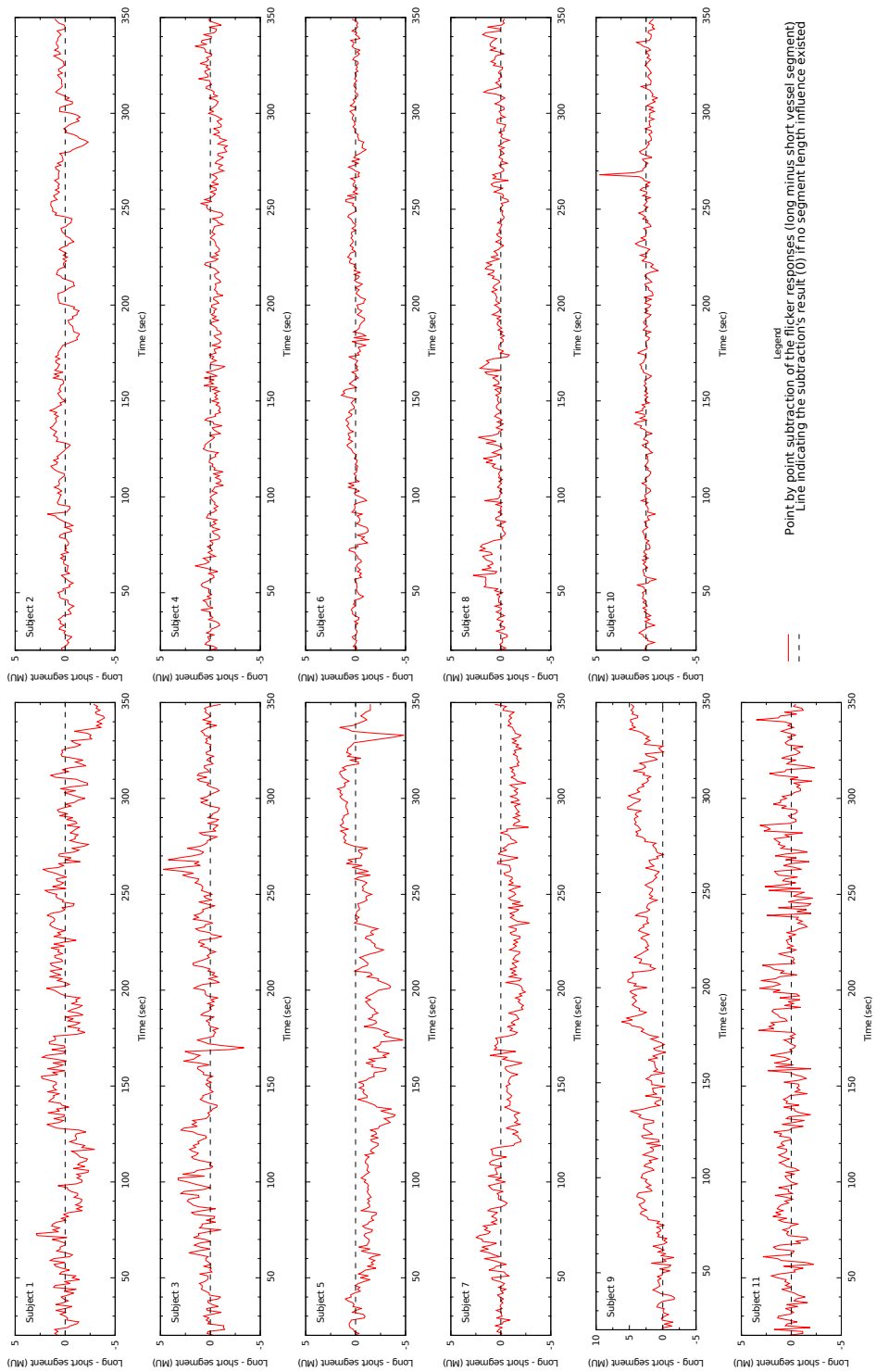


Figure 3.4: Plots of the flicker response difference between the longest possible segment measured and a truncated shorter segment of 240 MU for all subjects for arteries. Vessel segments belonged to an area of 1-2 DD distal to the ONH.

3 Location and Length Influence on Vessel Reactivity

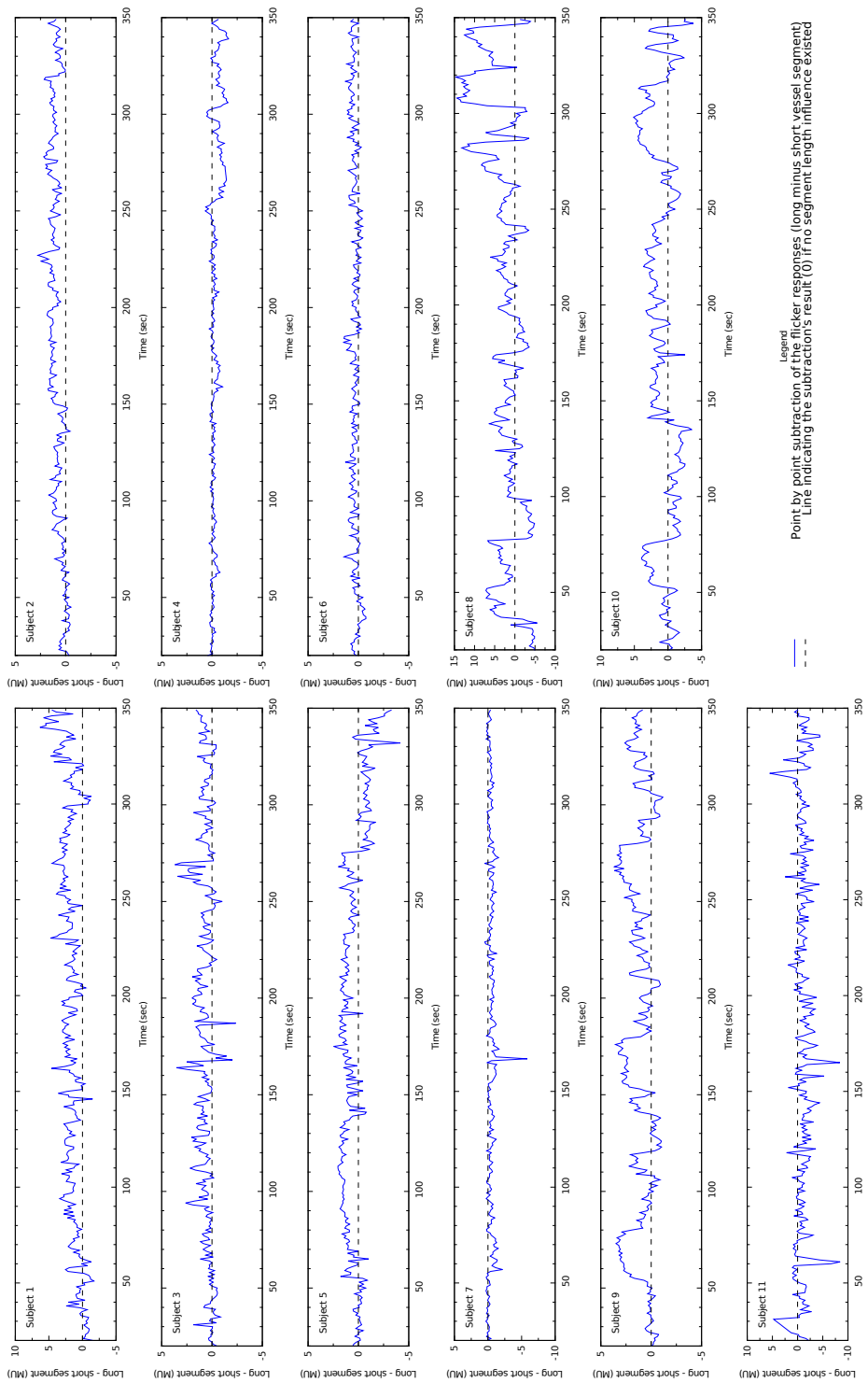


Figure 3.5: Plots of the flicker response difference between the longest possible segment measured and a truncated shorter segment of 240 MU for all subjects for veins. Vessel segments belonged to an area of 1-2 DD distal to the ONH.

3 Location and Length Influence on Vessel Reactivity

Subjects	Arteries			Veins		
	Deviation from zero					
	Positive	Negative	Total	Positive	Negative	Total
1	140.6	203.2	343.8	583.1	25.5	608.6
2	131.9	65.5	197.4	306.4	6.8	313.3
3	226.3	42.6	269	228.9	20	248.9
4	35.7	134	169.7	10.7	113.9	124.6
5	67.1	361.8	428.9	259.7	86.4	346.2
6	56.5	56.1	112.6	131	12	143
7	60.9	291.6	352.5	8	153.5	161.5
8	136.5	24.4	160.9	1047.7	223.9	1271.6
9	733	18.7	751.7	400.4	27.9	428.3
10	45.5	59	104.5	443.7	139.3	583
11	192.5	98	290.5	73.9	387.6	461.5

Table 3.8: Values of positive, negative and total deviation from the theoretical value of zero, if the long and short segments had no influence on output of diameter recordings for arteries (Figure 3.4) and veins (Figure 3.5). Essentially, positive values represent the area under the curve, negative values the area above the curve and total deviation their sum.

confocal microscopy (Yu et al., 1997). The distribution of F-actin, endothelial cell size and shape, nucleus size, shape and position within the cell were determined as a function of location along the vascular tree.

Exploration of retinal vascular reactivity over a range of locations is not a recent concept. Despite the lack of cutting edge technology at the time, Lanigan et al. (1988) demonstrated the variability of retinal vessel responses at 18 different sites using isometric muscle contractions as a stimulus. Responses differed by at least 1% in various arteriolar sites and at least 2% in various venular sites.

Prior to the incorporation of the embedded flicker module in the RVA at a flicker frequency of 12.5 Hz, flicker stimulation was achieved using an external lamp, which shone light onto a rotating sector disc (Polak et al., 2002). In their study, their main motivation was to investigate the optimisation of the diameter response in terms of different flicker frequencies (2-64 Hz). At the same time though, they measured offline multiple locations using the video recordings: a major vessel trunk proximally (0-1 DD), the same major vessel trunk distally (1-2 DD) and a distal branch. Using two different flicker frequencies (8 and 16 Hz), they found comparable diameter flicker responses for arteries across all locations. In retinal veins, the response in branches (i.e. the smaller venules) had a tendency to be higher, but this effect was not significant for their healthy cohort of nine subjects. Results in this work, although, not directly comparable due the protocol differences, are in agreement, since no differences were found in arteriolar or

3 Location and Length Influence on Vessel Reactivity

venular responses across the three different locations. They also observed negative correlation between baseline diameters and maximum dilation values in veins, but not in arteries. Here, results showed a similar negative trend, but this was very weak and did not reach statistical significance.

In a sample of 12 healthy, non-vasospastic females, Gugleta and colleagues found no significant differences in maximum dilation amplitude between proximal (0-1 DD) and distal (2-3 DD) retinal vessels (arteries and veins), with the three flicker cycles being analysed separately (Gugleta et al., 2006). Similarly to the results reported in this thesis, they reported no influence of the measurement site on vessel responses.

Another study investigated the influence of measurement location in 10 healthy males in arterial diameter response by means of the RVA (Jeppesen et al., 2007). Their participants were subjected to isometric exercise, which induced an increase to systemic BP, while arteriolar diameters were continuously recorded. While this was a completely different experimental protocol (pressure autoregulation) compared to that of flicker stimulation (metabolic autoregulation), which induces arterial contraction instead of dilation, it is of interest to note their findings: distal retinal arterioles (of smaller calibre) contracted significantly more than their proximal counterparts.

A recent study investigated differences in the response of arterioles supplying two different areas; the macular and the peripheral retina (Jensen et al., 2011). They applied three different provocation protocols: isometric exercise, flickering light and a combination of the two. With flickering light alone, no differences were observed between the response in macular and peripheral arterioles within their 17 healthy subjects.

The findings in this thesis extend current knowledge and certain methodological standardisations are proposed. To implement the location-dependent comparisons, measurement rings analogous to the concept of AVR measurement rings (Figure 1.10) were introduced. In this way, the three measurement sites are fully standardised across subjects, rather than using visual judgement to describe the approximate measurement location as the case is with current studies. For instance, Gugleta et al. (2013) clearly show an example of vessel location selection to belong to an area of 0-1 DD, but it is not clear whether this location was kept for all of their subjects, since they mention that “vascular geometry governed the exact location of the measurement”. Moreover, splitting the areas in 1 DD wide rings (0-1 DD, 1-2 DD and 2-3 DD) fulfils the manufacturer’s recommendation to obtain vessel segments of a maximum length of 1 DD.

The main outcome parameter, maximum arteriolar and venular dilation in response to flickering light, did not differ significantly across the three measuring sites. This was the case both for

3 Location and Length Influence on Vessel Reactivity

individual flicker analysis and for averaged flicker responses. The same applied for BDF, MC, DA, bFR, ΔD , APR and CT. Statistically, this is a direct implication that one could select any measurement location within a 3 DD radius from the edge of the ONH without this having any impact on outcome parameters. The only outcome parameter that is an exception, according to results herein, is arteriolar reaction time between Segment 1 and 2. When the three reaction times were averaged, proximal arterioles were slower to reach maximum dilation compared to their immediate neighbouring arterioles. There are no other studies to have measured within a 0-1 DD area and to report reaction time values to compare this finding to.

Present data lend further support to previous observations (Polak et al., 2002; Nagel et al., 2004) that baseline absolute vessel diameters do not correlate with relative amplitude of flicker response, as confirmed by linear regression analysis, pooling all 33 vessel segments together. Also, a positive correlation between MABP and maximum arteriolar dilation was found. A 10 mmHg difference in MABP showed approximately a 1% difference in maximum arteriolar dilation induced by flicker provocation (within a range of normal BP values). Of course, correlation does not imply causation and since there are no relevant data in literature to compare this finding to, no further assumptions can be made at this point. A comparison between 26 normotensives with MABP of 96 mmHg and 15 hypertensives with MABP of 110 mmHg, showed an inverse relationship of diminishing maximum arteriolar dilation (6.4% versus 3.9%, respectively), but used a longer protocol of 5 flicker repeats (Nagel et al., 2004).

Despite the aforementioned structural and functional heterogeneities along the retinal microvasculature, measurements of vascular reactivity in three distinct locations in arterioles and venules did not differ. There could be various reasons for that. First, the vessels' characteristics may not vary enough within 0-3 DD for the RVA's resolving capabilities to be able to capture these differing vessel properties. Second, retinal diameters are inherently fluctuating even under constant illumination during the cardiac cycle. Reliable detection of small diameter changes (1.4%) was only possible by taking fundus photographs synchronised to an electrocardiograph, while other methods either failed to detect changes or were unreliable (Dumskyj et al., 1996). As the pulse wave travels along the microvasculature, flicker initiation may coincide with the crest, the trough or anywhere in between of the wave at a given vessel segment. Therefore, responses may be blunted or augmented accordingly, masking any potential differences across different measuring locations. Lastly, the sample size might not suffice to detect significant differences. By all means, further studies on this topic are warranted to explore the influence of measurement location on retinal vessel reactivity by means of flicker stimulation.

3.4.2 Measurement Length Considerations

Selecting the extent of the measuring vessel segment using the RVA system is primarily governed by individual angioarchitecture. Tortuous retinal vessels, bifurcations and closely situated arteries and veins are segments that cannot be considered for inclusion. Given that the software's algorithm automatically truncates parts of the segment selection in case of quality issues (for instance, low contrast between vessels and surrounding tissue), end-users should always attempt to select segments that are as long as possible.

For the first time, results on the effect of different vessel segment lengths on flicker provocation diameter recordings of both arterioles and venules are reported. So far, a large body from the RVA-related publications has given little or no attention to systematic reporting of the extent of their vessel selection. From the analysis in this thesis, it is evident that for the majority of cases (8 out of 11 for arteries and 8 out of 11 for veins) the measurement length is a factor that induces variability to the final outcome. For both arteries and veins, there was substantial variability in the diameter responses when two distinctly different in length vessel segments were compared. This implies that including additional (or less) "information" from adjacent locations, yields a different diameter recording. One could argue that fluctuations are a consequence of noise or insufficient measurement quality (for instance, due to low contrast). However, this is highly unlikely, since all recordings were carefully selected prior to inclusion in this analysis. As a matter of fact, this is the reason for the relatively small sample size: only measurements with even illumination across the full 30° field and high quality recordings could be fully analysed up to the 2-3 DD measurement ring. This was achieved by extracting the brightness course graphs by means of the vendor-supplied software and validating that fluctuations were kept to a minimum along the measurement duration. It is also known, that optical distortions may add up to errors of measuring sensitivity up to 4% if the measuring location is located near the margins of the image area (Seifertl and Vilser, 2002). Hence, for added confidence, only vessel segments belonging to the central 1-2 DD measurement ring were included into the analysis. Another interesting observation is that in the case of veins (specifically for Subjects 9 and 10) the long segment selections exhibit consistently higher amounts of dilation (since the subtraction of long minus short selections are above zero) due to flickering light (time ranges of 50-70, 150-170 and 250-270 seconds) by a factor of 3-4 MU.

Nevertheless, the implications of this novel finding do not necessarily have a negative impact to the reliability of the RVA system, if certain standardisations are enforced. Firstly, all relevant studies should be reporting the actual measurement location and the exact vessel length of their analysis. Unfortunately, a considerable amount of publications so far have not disclosed any such information. Secondly, comparisons within subjects (for example, from multiple

visit measurements) should always be made with equally long segment selections. Of course, this is practically not feasible to achieve in real time, but truncating offline vessel segments accordingly, prior to data analysis, can be easily accomplished.

3.5 Conclusions

The vulnerability of the retina to vascular related diseases and the substantial reliance on local regulation of the retinal vasculature renders an improved understanding of such local regulatory mechanisms of significant clinical importance. Multi-segment analysis may indeed show comparable responses in healthy volunteers, but this may not be the case in various retinal manifestations of systemic disease, including diabetic retinopathy, glaucoma and hypertensive retinopathy.

Standardisation of measurement conditions is a necessity when utilising the RVA system. The magnitude of the induced responses by means of retinal flicker provocation is small and many factors can potentially suppress or augment those responses. Both measurement location and the extend of the vessel segment sampled should be taken into account to be able to control for these factors and should always be reported in future publications. Agreement between research groups on standardisation protocols needs to be reached, before the RVA can be considered clinically useful in detecting or predicting vascular dysfunction.

Chapter 4

Essential Hypertension: Case Reports

4.1 Introduction and Motivation

Imaging the retinal microvasculature offers a surrogate view of systemic vascular health, allowing non-invasive and longitudinal assessment of vascular pathology. In order to discuss the strengths and weaknesses of utilising the RVA system to assess metabolic autoregulation in the retina in treated essential hypertensives three essential hypertensives were invited that were previously (5 years ago) subjected to the protocol detailed below, as a follow-up, longitudinal, small case report study.

4.2 Ethical Approval

The study adhered to the tenets of the declaration of Helsinki and the protocol was peer reviewed from Aston University as well as undergone through a separate second peer review by the Aston Optometry and Audiology Research Ethics Committee, which subsequently approved it. Furthermore, this study has undergone R&D and NHS ethics review prior to its commencement (Research Ethics Committee Reference: 12/EM/0080).

4.3 Methods and Subjects

One previously diagnosed and two newly diagnosed essential hypertensives had been initially examined as part of a research study in 2008 and returned for a follow-up examination in 2013. Both the initial and the follow-up assessments were split into two research appointments, held on two consecutive days as follows.

4.3.1 Day 1 - Ambulatory BP and ECG Monitoring

Participants were invited to attend their first research appointment after fasting from midnight of the preceding day. A 24 hour BP and ECG monitor (Cardiotens, Meditech, PMS Instruments,

UK) was fitted to assess both systemic circulation and autonomic function. BP measurements were obtained every 15 minutes during the day period and every 30 minutes during the night period. Given - for instance - a typical 8 hour sleep period the total number of BP measurements obtained amounted to 80. Patients recorded a standardised patient diary on the monitoring day with information on their daily routine, physical activities undertaken and time and type of antihypertensive medication taken. Then, subjects were dismissed.

4.3.1.1 Outcome Measures

At completion of the 24 hour period the BP and ECG monitor was removed. Data were downloaded onto a personal computer and were analysed using the vendor-supplied software, namely CardioVisions (Version 1.18.22). Outcome variables were SBP, DBP, HR, LF, HF, HRV triangular index, each for day, night and 24 hour periods.

4.3.2 Day 2 - Eye examinations

The following day, patients returned for their second research appointment. At least 12 hours prior to their morning visits, participants were asked to abstain from smoking, from consuming products containing alcohol or caffeine, as well as from taking up any sort of considerable physical activity, whereas they were instructed not to fast. Room temperature was maintained constant during all measurements (21-24 °C). Only right eyes were tested.

4.3.2.1 Intraocular Pressure Measurement

Non-contact tonometry was performed to assess IOP by means of a validated (Ogbuehi and Almubrad, 2008) device (Pulsair EasyEye, Keeler Ltd., UK). Three consecutive readings were obtained from the experimental eye and the average value was recorded.

4.3.2.2 Retinal Functional Analysis

Details on the RVA measuring principle have been extensively described (Section 2.2.5.3). One drop of Tropicamide (1% w/v, Bausch & Lomb, UK) was instilled to achieve pupil dilation necessary for getting unobstructed view of the posterior pole. As soon as full pupil dilation was reached, the dynamic retinal vessel assessment commenced. One retinal arteriole and one retinal venule from the superotemporal fundus area 1-2 DD away from the edge of the ONH were examined.

4.3.2.3 Outcome Measures

The following parameters (as defined in Section 1.8.2.3) were obtained (from both initial and follow-up sessions) averaged across the three flicker cycles by means of raw RVA output data

processing: BDF, bFR, MD, MC, DA, RT, CT, Δ D and APR. Absolute arteriolar and venular diameters were recorded in MU.

4.3.3 Data Analysis

Longitudinal results are reported per individual. Due to the nature of the study (case report) no statistical analyses have been performed. For visualisation of the RVA diameter recordings, graphs were plotted comparing initial and follow-up measurements.

4.4 Results

4.4.1 Sample

Three male Caucasians, non-smokers, essential hypertensives took part in this case reports series. JW had been previously diagnosed prior to the initial examination (treatment with combination of beta-blockers and Angiotensin Converting Enzyme (ACE) inhibitors). JH was diagnosed shortly after the initial examination and had been under treatment (ACE inhibitors) ever since the follow-up examination. TR was undiagnosed at the time point of the initial examination and was under treatment for a few months only (ACE inhibitors and Latanoprost) prior to the follow-up visit. At the time point of their initial visit JH was 59, JW was 37 and TR was 47 years old.

4.4.2 24hr BP and ECG Monitoring

Values of 24 hour BP monitoring parameters and frequency-domain HRV parameters from 24 hour ECG monitoring are shown in Table 4.1. For the case of JH, sympatho-vagal balance as defined by the LF/HF ratio (for both day and night) has dropped, between the two time points, to values signifying equal sympathetic and parasympathetic activity. This was mediated from a combined drop in LF and increase in HF components. SBP and DBP values have dropped substantially, whereas HR has remained stable. Day time BP values for JW and TR have largely remained stable. Conversely, improvement on BP values due to antihypertensive medication is clearly visible in the night time values which have been lowered. Regarding frequency domain HRV parameters, the younger subject of the three (JW) shows directly opposite sympatho-vagal activity when compared to the older subject (JH) (approximately two decades of age difference). No specific pattern of sympatho-vagal changes is observed in the case of TR.

4.4.3 Retinal Functional Assessment

Averaged values across the three flicker provocation cycles were calculated and reported in Table 4.2. Both arteriolar and venular MD dropped between the two time points for JH

Parameter	JH, 59		JW, 37		TR, 47	
	Initial	Follow-up	Initial	Follow-up	Initial	Follow-up
SBP/DBP day (mmHg)	150/92	126/75	130/79	131/83	132/78	132/84
SBP/DBP night (mmHg)	147/78	126/75	127/71	107/60	119/67	111/64
SBP/DBP 24h (mmHg)	149/86	121/69	128/76	123/75	127/74	126/78
HR day	78	76	83	84	76	73
HR night	61	61	77	58	64	58
HR 24h	70	70	81	75	71	69
LF day (NU)	69	49	79	81	86	79
LF night (NU)	64	54	76	84	71	75
HF day (NU)	27	44	20	18	13	20
HF night (NU)	40	45	23	15	29	25
LF/HF day (NU)	2.6	1.1	3.9	4.4	6.4	4
LF/HF night (NU)	1.6	1.2	3.3	5.6	2.5	3.1
Day/night LF (NU)	65	51	78	83	81	77
Day/night HF (NU)	37	46	21	16	18	21
Day/night LF/HF (NU)	1.8	1.1	3.8	5.1	4.5	3.6
HRV TI	30	34	53	42	37	44

Table 4.1: BP, HR and frequency-domain HRV parameters for the initial and follow-up examinations of the three hypertensives. Noted years of age for each participant are at the time point of their initial visit. Follow-up period was five years. TI, Triangular Index; NU, Normalised Units.

and JW, contrary to TR who showed increased arteriolar reactivity in both vessels. Despite the increased reactivity for the case of TR, arteriolar dilatory capacity as described by DA shows similar values across the two visits. This is corroborated by the arteriolar MC values. Apparently, antihypertensive medication across all subjects has a positive effect in arteriolar RT. Arteries take substantially less time to reach maximum dilation, although the value reached is lower for the cases of JH and JW (101.6 MU and 100.8 MU, respectively).

Graphical representations of the diameter responses induced by flickering light by means of the RVA for the three hypertensives are shown in Figures 4.1 to 4.3. Arteries and veins are plotted separately for easier comparisons between the initial and follow-up examinations.

4.5 Discussion

In both hospitalised and non-hospitalised subjects electrocardiograms were recorded for 24 hours and the main finding was that in both groups the markers of sympathetic and vagal regulation of HR underwent circadian changes (Furlan et al., 1990). Namely sympathetic predominance (LF component) was apparent during the day and vagal predominance (HF component) during the night. For 9 out of 12 instances this was true for subjects in this study as well (day LF higher than night LF and night HF higher than day HF, Table 4.1). A more

4 Essential Hypertension: Case Reports

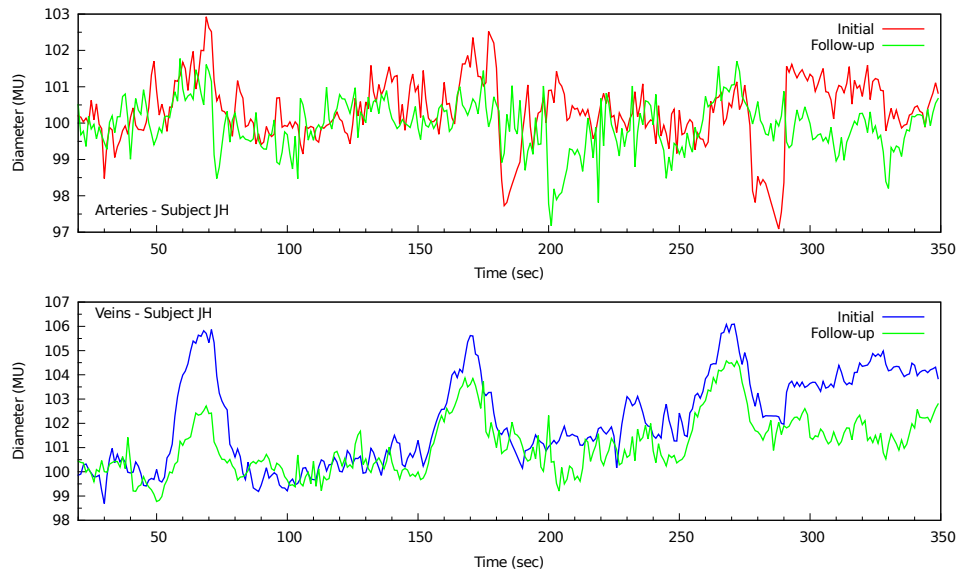


Figure 4.1: Retinal vascular reactivity by means of the RVA across a 5 year period for Subject JH. Green lines represent the follow-up measurement.

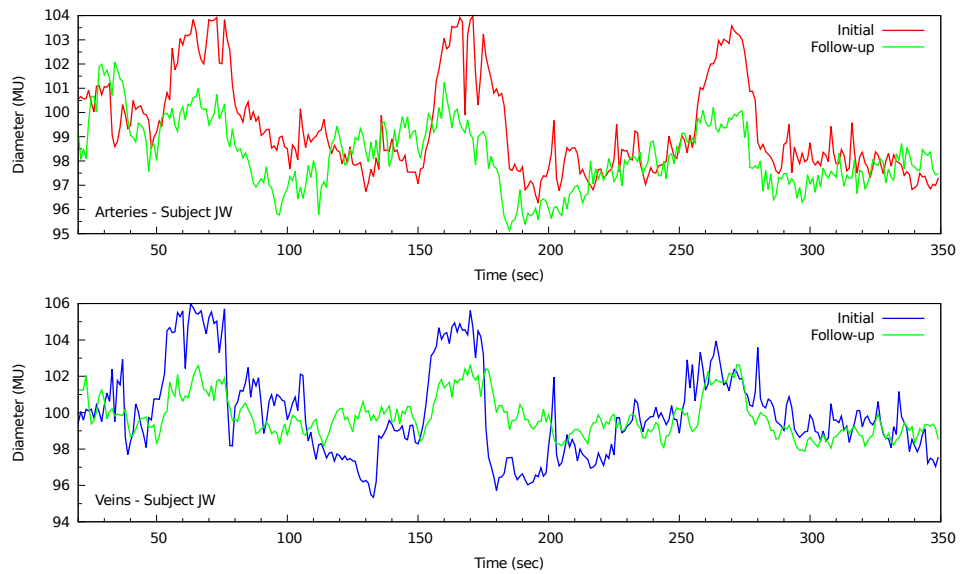


Figure 4.2: Retinal vascular reactivity by means of the RVA across a 5 year period for Subject JW. Green lines represent the follow-up measurement.

4 Essential Hypertension: Case Reports

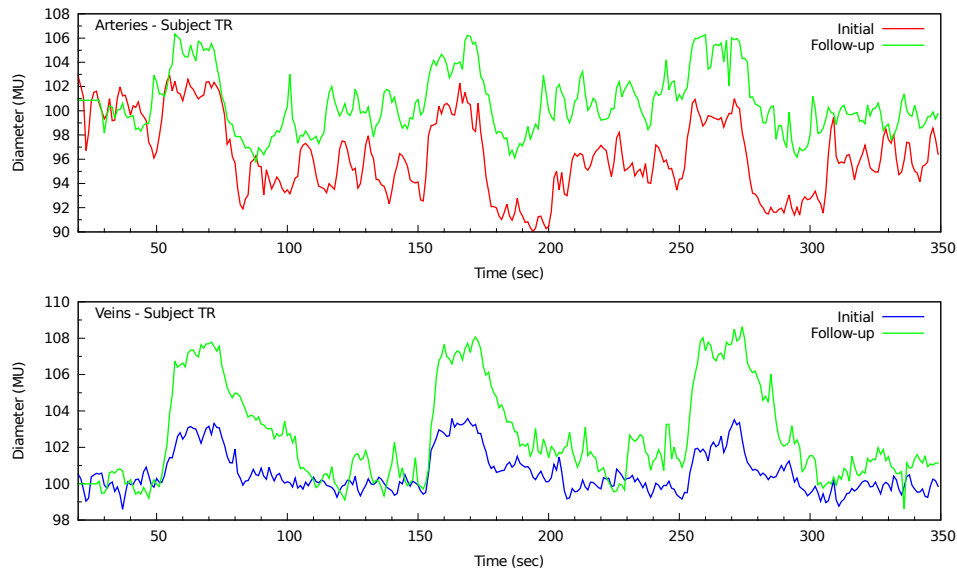


Figure 4.3: Retinal vascular reactivity by means of the RVA across a 5 year period for Subject TR. Green lines represent the follow-up measurement.

Parameter	JH, 59		JW, 37		TR, 47	
	Initial	Follow-up	Initial	Follow-up	Initial	Follow-up
Arteries						
BDF (%)	2.4 (0.7)	1.9 (0.6)	3.7 (1.6)	2.8 (1.5)	5.7 (1)	4.8 (0.9)
MD (%)	102.4 (0.7)	101.6 (0.2)	103.8 (0.2)	100.8 (0.5)	102.1 (1)	106.3 (0.1)
MC (%)	98.1 (1.2)	98.2 (1)	97.1 (0.8)	95.7 (0.6)	91.1 (1)	96 (0.2)
DA (%)	4.3 (0.7)	3.4 (0.8)	6.7 (0.9)	5.1 (1.1)	10.9 (1.3)	10.3 (0.3)
bFR (%)	1.8 (1.4)	1.5 (1.4)	2.9 (2)	2.3 (1.7)	5.2 (1.2)	5.5 (1)
Δ D (%)	1.8 (0.6)	1.9 (0.8)	5.6 (0.8)	2 (0.3)	7.5 (0.7)	4.8 (1.2)
APR	1.9 (0.7)	2 (1.1)	2 (0.8)	2.1 (0.9)	1.9 (0.3)	2.2 (0.4)
RT (s)	30 (12.2)	19 (8.5)	21 (1.5)	13 (3)	14 (8.2)	12 (6.2)
CT (s)	37 (3.6)	25 (24.1)	43 (4.6)	43 (6.9)	41 (7)	40 (4.4)
Veins						
BDF (%)	2.3 (0.6)	2 (0.3)	4.4 (0.8)	2.4 (0.9)	1.7 (0.6)	2.8 (1.1)
MD (%)	105.9 (0.2)	103.7 (0.9)	105.2 (1)	102.6 (0.1)	103.5 (0.1)	108.2 (0.4)
Δ D (%)	5.3 (0.8)	4 (0.3)	5.6 (1.5)	2.9 (0.5)	3.7 (0.3)	7.1 (0.5)
RT (s)	21 (0.6)	18 (0.6)	16 (3.8)	19 (3.1)	21 (1.5)	22 (1.5)

Table 4.2: RVA dynamic flicker response parameters and reaction times, averaged across all three flicker cycles. Noted years of age for each participant are at the time point of their initial visit. Follow-up period was five years. Values are expressed as means (SD). For acronyms, see page 114.

recent study reported significant alterations in markers of SA regulation (increased LF and reduced HF) both in pre-hypertensives and to a larger extent in hypertensives (Lucini et al., 2002). Also, they noted that “hypertensive autonomic dysregulation was particularly apparent in the youngest group”.

As it can be seen from the limited amount of data of this small case report study, the interactions between factors, such as, disease onset and duration, treatment type and duration, age and others are creating a highly diverse clinical picture. An additional limitation of the case reports presented here is the long follow-up period of 5 years with no in between repeat visits. Although data shown here include a temporal element, more frequent examinations should ideally be performed (e.g. on a yearly basis). Similar studies to the concept of Nagel et al. (2006b) but with sufficiently large sample sizes and well stratified hypertensive groups would enable fruitful comparisons across varying pathological and physiological states. Nevertheless, the combination of macrovascular with microvascular information is the necessary step for the ultimate goal for risk stratification or treatment monitoring.

Each year CVD causes more than 4.3 million deaths in Europe, accounting for nearly half of all deaths (48%) (Allender et al., 2008). Major advances in prevention have led to improved hypertension-related mortality and morbidity figures over the last three decades; nevertheless essential hypertension is still the most prevalent among cardiovascular disorders. The pathophysiology of essential hypertension involves a multitude of factors, including the central nervous system, endocrine factors, the large arteries and the microcirculation. Large scale population-based studies pioneered in identifying the relationships between impaired microvascular perfusion, autoregulation or structure and subsequent target organ damage. The limitation of such studies is that they are cross-sectional in nature. This allows only assumptions to be made on the time course of the various disease manifestations: does microvascular damage precede CVD or vice versa, or is it a complex two-way interaction?

No single modality is able to give definitive answers. The techniques as well as the strategies for investigating microcirculatory function have evolved almost exponentially over the last 50 years. The RVA technology is definitely a piece of the puzzle. It may serve as a complementary research tool to help answer unresolved questions in both physiologic and pathological conditions. Existing data demonstrate that visual stimulation is a powerful modulator of retinal and optic nerve blood flow. Much work has been accomplished thus far in exploring neurovascular/neurometabolic coupling in the human retina but there are still many open questions that remain to be elucidated. Technical limitations in imaging methods of low spatial and temporal resolution can now be overcome making the reliable tracking of retinal capillaries feasible (Bedgood and Metha, 2012).

Bibliography

- Abramoff, M., Magalhaes, P., and Ram, S. (2004). Image processing with ImageJ. *Biophotonics international*, 11(7):36–43.
- Allender, S., Scarborough, P., Peto, V., Rayner, M., Leal, J., Luengo-Fernandez, R., and Gray, A. (2008). *European cardiovascular disease statistics*. European Heart Network London.
- Antonios, T. F. T., Singer, D. R. J., Markandu, N. D., Mortimer, P. S., and MacGregor, G. A. (1999). Structural Skin Capillary Rarefaction in Essential Hypertension. *Hypertension*, 33(4):998–1001.
- Anuradha, S., Healy, G. N., Dunstan, D. W., Klein, R., Klein, B. E., Cotch, M. F., Wong, T. Y., and Owen, N. (2011). Physical Activity, Television Viewing Time, and Retinal Microvascular Caliber. *American Journal of Epidemiology*, 173(5):518–525.
- Azegrouz, H., Trucco, E., Dhillon, B., MacGillivray, T., and MacCormick, I. (2006). Thickness dependent tortuosity estimation for retinal blood vessels. In *Engineering in Medicine and Biology Society, 2006. EMBS '06. 28th Annual International Conference of the IEEE*, volume 1, pages 4675 – 4678.
- Barna, I., Keszei, A., and Dunai, A. (1998). Evaluation of Meditech ABPM-04 ambulatory blood pressure measuring device according to the British Hypertension Society protocol. *Blood Press Monitoring*, 3(6):363–368.
- Barold, S. (2005). Norman J. “Jeff” Holter—“Father” of Ambulatory ECG Monitoring. *Journal of Interventional Cardiac Electrophysiology*, 14(2):117–118.
- Bedggood, P. and Metha, A. (2012). Direct visualization and characterization of erythrocyte flow in human retinal capillaries. *Biomed. Opt. Express*, 3(12):3264–3277.
- Beevers, G., Lip, G. Y., and O’Brien, E. (2001). Blood pressure measurement: Part I—Sphygmomanometry: factors common to all techniques. *BMJ*, 322(7292):981–985.
- Bek, T., Hajari, J., and Jeppesen, P. (2008). Interaction between flicker-induced vasodilatation and pressure autoregulation in early retinopathy of type 2 diabetes. *Graefe’s Archive for*

Bibliography

- Clinical and Experimental Ophthalmology*, 246(5):763–769.
- Berne, R. M. and Levy, M. N. (1997). *Cardiovascular Physiology*. Mosby, 7th edition.
- Bevan, J. A., Bevan, R. D., Hwa, J. J., Owen, M. P., and Tayo, F. M. (1986). Calcium Regulation in Vascular Smooth Muscle: Is There a Pattern to Its Variability Within the Arterial Tree? *Journal of Cardiovascular Pharmacology*, 8:S71–S75.
- Blum, M., Bachmann, K., Wintzer, D., Riemer, T., Vilser, W., and Strobel, J. (1999). Noninvasive measurement of the Bayliss effect in retinal autoregulation. *Graefe's Archive for Clinical and Experimental Ophthalmology*, 237(4):296–300.
- Blum, M., Kloos, C., Günther, S., Hunger-Dathe, W., and Müller, U. (2008). Improved metabolic control results in better myogenic response of retinal arterioles in patients with diabetes mellitus type 1. *Ophthalmologica*, 222(6):373–377.
- Blum, M., Scherf, C., Bachmann, K., and Strobel, J. (2001). Alterskorrelierte Kontraktilität retinaler Arteriolen bei Sauerstoffatmung. *Der Ophthalmologe*, 98:265–268.
- Bracher, D. (1982). Changes in peripapillary tortuosity of the central retinal arteries in newborns. *Graefe's Archive for Clinical and Experimental Ophthalmology*, 218:211–217.
- Brown, S. M. and Jampol, L. M. (1996). New Concepts of Regulation of Retinal Vessel Tone. *Arch Ophthalmol*, 114(2):199–204.
- Chapman, N., Dell'omo, G., Sartini, M. S., Witt, N., Hughes, A., Thom, S., and Pedrinelli, R. (2002). Peripheral vascular disease is associated with abnormal arteriolar diameter relationships at bifurcations in the human retina. *Clin. Sci.*, 103(2):111–116.
- Chapman, N., Haines, G., Stanton, A. V., Thom, S. A., and Hughes, A. D. (2000). Acute effects of oxygen and carbon dioxide on retinal vascular network geometry in hypertensive and normotensive subjects. *Clin. Sci.*, 99(6):483–488.
- Chasis, H. (1974). Appreciation of the Keith, Wagener, and Barker classification of hypertensive disease. *The American Journal of the Medical Sciences*, 268(6):347.
- Chen, H., Patel, V., Wiek, J., Rassam, S., and Kohner, E. (1994). Vessel diameter changes during the cardiac cycle. *Eye (London, England)*, 8:97–103.
- Cheung, C. Y., Hsu, W., Lee, M. L., Wang, J. J., Mitchell, P., Lau, Q. P., Hamzah, H., Ho, M., and Wong, T. Y. (2010). A New Method to Measure Peripheral Retinal Vascular Caliber over an Extended Area. *Microcirculation*, 17(7):495–503.
- Clifford, G. D., Azuaje, F., and McSharry, P. (2006). *Advanced Methods And Tools for ECG Data Analysis*. Artech House, Inc.

Bibliography

- Dart, A. M. and Kingwell, B. A. (2001). Pulse pressure—a review of mechanisms and clinical relevance. *Journal of the American College of Cardiology*, 37(4):975–984.
- Dawczynski, J., Mandecka, A., Blum, M., Müller, U. A., Ach, T., and Strobel, J. (2007). Endotheliale Dysfunktion zentraler Netzhautgefäße als Prognoseparameter der diabetischen Retinopathie? *Klin Monatsbl Augenheilkd*, 224(11):827–831.
- Delles, C., Michelson, G., Harazny, J., Oehmer, S., Hilgers, K. F., and Schmieder, R. E. (2004). Impaired Endothelial Function of the Retinal Vasculature in Hypertensive Patients. *Stroke*, 35(6):1289–1293.
- Dolan, E., Li, Y., Thijs, L., McCormack, P., Staessen, J. A., O'Brien, E., and Stanton, A. (2006). Ambulatory arterial stiffness index: rationale and methodology. *Blood Pressure Monitoring*, 11(2):103–105.
- Dorion, T. (1998). *Manual of ocular fundus examination*. Butterworth-Heinemann.
- Dougherty, G., Johnson, M., and Wiers, M. (2010). Measurement of retinal vascular tortuosity and its application to retinal pathologies. *Medical and Biological Engineering and Computing*, 48(1):87–95.
- Dougherty, G. and Varro, J. (2000). A quantitative index for the measurement of the tortuosity of blood vessels. *Medical Engineering & Physics*, 22(8):567 – 574.
- Dumskyj, M. J., Aldington, S. J., Doré, C. J., and Kohner, E. M. (1996). The accurate assessment of changes in retinal vessel diameter using multiple frame electrocardiograph synchronised fundus photography. *Current Eye Research*, 15(6):625–632.
- Faul, F., Erdfelder, E., Lang, A.-G., and Buchner, A. (2007). G*power 3: a flexible statistical power analysis program for the social, behavioral, and biomedical sciences. *Behav Res Methods*, 39(2):175–191.
- Formaz, F., Riva, C., and Geiser, M. (1997). Diffuse luminance flicker increases retinal vessel diameter in humans. *Current Eye Research*, 16(12):1252–1257.
- Frederiksen, C., Jeppesen, P., Knudsen, S., Poulsen, P., Mogensen, C., and Bek, T. (2006). The blood pressure-induced diameter response of retinal arterioles decreases with increasing diabetic maculopathy. *Graefe's Archive for Clinical and Experimental Ophthalmology*, 244(10):1255–1261.
- Furlan, R., Guzzetti, S., Crivellaro, W., Dassi, S., Tinelli, M., Baselli, G., Cerutti, S., Lombardi, F., Pagani, M., and Malliani, A. (1990). Continuous 24-hour assessment of the neural regulation of systemic arterial pressure and RR variabilities in ambulant subjects. *Circulation*, 81(2):537–47.

Bibliography

- Gafiychuk, V. V. and Lubashevsky, I. A. (2001). On the Principles of the Vascular Network Branching. *Journal of Theoretical Biology*, 212(1):1 – 9.
- Garhöfer, G., Bek, T., Boehm, A. G., Gherghel, D., Grunwald, J., Jeppesen, P., Kergoat, H., Kotliar, K., Lanzl, I., Lovasik, J. V., Nagel, E., Vilser, W., Orgul, S., and Schmetterer, L. (2010). Use of the retinal vessel analyzer in ocular blood flow research. *Acta Ophthalmologica*, 88(7):717–722.
- Garhöfer, G., Resch, H., Weigert, G., Lung, S., Simader, C., and Schmetterer, L. (2005). Short-Term Increase of Intraocular Pressure Does Not Alter the Response of Retinal and Optic Nerve Head Blood Flow to Flicker Stimulation. *Investigative Ophthalmology & Visual Science*, 46(5):1721–1725.
- Garhöfer, G., Zawinka, C., Huemer, K.-H., Schmetterer, L., and Dorner, G. T. (2003). Flicker Light-Induced Vasodilatation in the Human Retina: Effect of Lactate and Changes in Mean Arterial Pressure. *Investigative Ophthalmology & Visual Science*, 44(12):5309–5314.
- Gasser, P. and Bühler, F. R. (1992). Nailfold microcirculation in normotensive and essential hypertensive subjects, as assessed by video-microscopy. *Journal of Hypertension*, 10(1):83–86.
- Ghiadoni, L., Faita, F., Salvetti, M., Cordiano, C., Biggi, A., Puato, M., Di Monaco, A., De Siati, L., Volpe, M., Ambrosio, G., Gemignani, V., Muiesan, M. L., Taddei, S., Lanza, G. A., and Cosentino, F. (2012). Assessment of flow-mediated dilation reproducibility: a nationwide multicenter study. *Journal of Hypertension*, 30(7):1399–1405.
- Gugleta, K., Kochkorov, A., Katamay, R., Zawinka, C., Flammer, J., and Orgul, S. (2006). Analysis of Retinal Vasodilation after Flicker Light Stimulation in Relation to Vasospastic Propensity. *Investigative Ophthalmology & Visual Science*, 47(9):4019–4025.
- Gugleta, K., Kochkorov, A., Waldmann, N., Polunina, A., Katamay, R., Flammer, J., and Orgul, S. (2012). Dynamics of retinal vessel response to flicker light in glaucoma patients and ocular hypertensives. *Graefe's Archive for Clinical and Experimental Ophthalmology*, 250(4):589–594.
- Gugleta, K., Waldmann, N., Polunina, A., Kochkorov, A., Katamay, R., Flammer, J., and Orgul, S. (2013). Retinal neurovascular coupling in patients with glaucoma and ocular hypertension and its association with the level of glaucomatous damage. *Graefe's Archive for Clinical and Experimental Ophthalmology*, 251:1577–1585.
- Gunn, M. (1898). On ophthalmoscopic evidence of general arterial disease. *Trans Ophthalmol Soc UK*, 18:356–381.
- Guzzetti, S., Dassi, S., Pecis, M., Casat, R., Masu, A. M., Longoni, P., Tinelli, M., Cerutti, S., Pagani, M., and Malliani, A. (1991). Altered pattern of circadian neural control of heart

Bibliography

- period in mild hypertension. *Journal of Hypertension*, 9(9):831–838.
- Haefliger, I., Flammer, J., and Luscher, T. (1993). Heterogeneity of endothelium-dependent regulation in ophthalmic and ciliary arteries. *Investigative Ophthalmology & Visual Science*, 34(5):1722–1730.
- Hammer, M., Vilser, W., Riemer, T., and Schweitzer, D. (2008). Retinal vessel oximetry-calibration, compensation for vessel diameter and fundus pigmentation, and reproducibility. *Journal of Biomedical Optics*, 13(5):054015–1–054015–7.
- Harper, R. N., Moore, M. A., Marr, M. C., Watts, L. E., and Hutchins, P. M. (1978). Arteriolar rarefaction in the conjunctiva of human essential hypertensives. *Microvascular Research*, 16(3):369–372.
- Hart, W. E., Goldbaum, M., Côté, B., Kube, P., and Nelson, M. R. (1999). Measurement and classification of retinal vascular tortuosity. *International Journal of Medical Informatics*, 53(2-3):239 – 252.
- Heitmar, R., Blann, A., Cubbidge, R. P., Lip, G., and Gherghel, D. (2010). Continuous retinal vessel diameter measurements - the future of retinal vessel assessment? *Investigative Ophthalmology & Visual Science*, 51(11):5833–5839.
- Heitmar, R., Blann, A., Cubbidge, R. P., Lip, G., and Gherghel, D. (2011a). Author Response: Can Vascular Function Be Assessed by the Interpretation of Retinal Vascular Diameter Changes? *Investigative Ophthalmology & Visual Science*, 52(1):636–638.
- Heitmar, R., Cubbidge, R. P., Lip, G. Y. H., Gherghel, D., and Blann, A. D. (2011b). Altered Blood Vessel Responses in the Eye and Finger in Coronary Artery Disease. *Investigative Ophthalmology & Visual Science*, 52(9):6199–6205.
- Heitmar, R. and Summers, R. (2012). Assessing vascular function using dynamic retinal diameter measurements: A new insight on the endothelium. *Thrombosis and Haemostasis*, 107(6):1019–1026.
- Hemminki, V., Kähönen, M., Tuomisto, M., Turjanmaa, V., and Uusitalo, H. (2007). Determination of retinal blood vessel diameters and arteriovenous ratios in systemic hypertension: comparison of different calculation formulae. *Graefe's Archive for Clinical and Experimental Ophthalmology*, 245:8–17.
- Hnatkova, K., Copie, X., Staunton, A., and Malik, M. (1995). Numeric processing of Lorenz plots of R-R intervals from long-term ECGs: Comparison with time-domain measures of heart rate variability for risk stratification after myocardial infarction. *Journal of Electrocardiology*, 28, Supplement 1(0):74 – 80.

Bibliography

- Houben, A., Canoy, M., Paling, H., Derhaag, P., and de Leeuw, P. (1995). Quantitative analysis of retinal vascular changes in essential and renovascular hypertension. *J Hypertens*, 13(12):1729–1733.
- Hubbard, L., Ehrhardt, B., and Klein, R. (1992). The association between generalized arteriolar narrowing and blood pressure. *Investigative Ophthalmology & Visual Science*, 33:804.
- Hubbard, L. D., Brothers, R. J., King, W. N., Clegg, L. X., Klein, R., Cooper, L. S., Sharrett, A. R., Davis, M. D., and Cai, J. (1999). Methods for evaluation of retinal microvascular abnormalities associated with hypertension/sclerosis in the Atherosclerosis Risk In Communities study. *Ophthalmology*, 106(12):2269 – 2280.
- Hughes, A. D., Martinez-Perez, E., Jabbar, A. S., Hassan, A., Witt, N. W., Mistry, P. D., Chapman, N., Stanton, A. V., Beevers, G., Pedrinelli, R., Parker, K. H., and Thom, S. A. (2006). Quantification of topological changes in retinal vascular architecture in essential and malignant hypertension. *J Hypertens*, 24(5):889–894.
- Jacks, A. S. and Miller, N. R. (2003). Spontaneous retinal venous pulsation: aetiology and significance. *Journal of Neurology, Neurosurgery & Psychiatry*, 74(1):7–9.
- Jean-Louis, S., Lovasik, J., and Kergoat, H. (2005). Systemic hyperoxia and retinal vasomotor responses. *Investigative Ophthalmology & Visual Science*, 46(5):1714–1720.
- Jensen, S. P., Jeppesen, P., and Bek, T. (2011). Differential diameter responses in macular and peripheral retinal arterioles may contribute to the regional distribution of diabetic retinopathy lesions. *Graefe's Archive for Clinical and Experimental Ophthalmology*, 249:407–412.
- Jeppesen, P., Sanye-Hajari, J., and Bek, T. (2007). Increased Blood Pressure Induces a Diameter Response of Retinal Arterioles that Increases with Decreasing Arteriolar Diameter. *Investigative Ophthalmology & Visual Science*, 48(1):328–331.
- Johnson, P. (1986). Autoregulation of blood flow. *Circulation research*, 59(5):483–495.
- Kagan, A., Aurell, E., and Tibblin, G. (1967). Signs in the fundus oculi and arterial hypertension: unconventional assessment and significance. *Bulletin of the World Health Organization*, 36(2):231–241.
- Kalitzeos, A. A., Lip, G. Y., and Heitmar, R. (2013). Retinal vessel tortuosity measures and their applications. *Experimental Eye Research*, 106(0):40 – 46.
- Kamath, M. and Fallen, E. (1993). Power spectral analysis of heart rate variability: a noninvasive signature of cardiac autonomic function. *Crit Rev Biomed Eng*, 21(3):245–311.

Bibliography

- Keith, N. M. M., Wagener, H. P. M., and Barker, N. W. M. (1939). Some different types of essential hypertension: their course and prognosis. *The American Journal of the Medical Sciences*, 197(3):332–343.
- King, L., Stanton, A., Sever, P., Thom, S., and Hughes, A. (1996). Arteriolar length-diameter (L:D) ratio: a geometric parameter of the retinal vasculature diagnostic of hypertension. *Journal of Human Hypertension*, 10(6):417–418.
- Kiss, B., Polska, E., Dorner, G., Polak, K., Findl, O., Mayrl, G. F., Eichler, H.-G., Wolzt, M., and Schmetterer, L. (2002). Retinal Blood Flow during Hyperoxia in Humans Revisited: Concerted Results Using Different Measurement Techniques. *Microvascular Research*, 64(1):75 – 85.
- Klabunde, R. E. (2011). *Cardiovascular physiology concepts*. Wolters Kluwer Health.
- Knudtson, M. D., Klein, B. E. K., Klein, R., Wong, T. Y., Hubbard, L. D., Lee, K. E., Meuer, S. M., and Bulla, C. P. (2004). Variation associated with measurement of retinal vessel diameters at different points in the pulse cycle. *British Journal of Ophthalmology*, 88(1):57–61.
- Knudtson, M. D., Lee, K. E., Hubbard, L. D., Wong, T. Y., Klein, R., and Klein, B. E. (2003). Revised formulas for summarizing retinal vessel diameters. *Current Eye Research*, 27(3):143–149.
- Kotliar, K., Nagel, E., Vilser, W., and Lanzl, I. (2008). Functional in vivo assessment of retinal artery microirregularities in glaucoma. *Acta Ophthalmologica*, 86(4):424–433.
- Kotliar, K., Nagel, E., Vilser, W., Seidova, S.-F., and Lanzl, I. M. (2010). Microstructural alterations of retinal arterial blood column along the vessel axis in systemic hypertension. *Investigative Ophthalmology & Visual Science*, 51(4):2165–2172.
- Kotliar, K. E., Baumann, M., Vilser, W., and Lanzl, I. M. (2011a). Pulse wave velocity in retinal arteries of healthy volunteers. *British Journal of Ophthalmology*, 95:675–679.
- Kotliar, K. E., Lanzl, I. M., Schmidt-Trucksäss, A., Sitnikova, D., Ali, M., Blume, K., Halle, M., and Hanssen, H. (2011b). Dynamic retinal vessel response to flicker in obesity: A methodological approach. *Microvascular Research*, 81(1):123 – 128.
- Kotliar, K. E., Vilser, W., Nagel, E., and Lanzl, I. (2004). Retinal vessel reaction in response to chromatic flickering light. *Graefe's Archive for Clinical and Experimental Ophthalmology*, 242:377–392.
- Kylstra, J., Wierzbicki, T., Wolbarsht, M., Landers, M., and Stefansson, E. (1986). The relationship between retinal vessel tortuosity, diameter, and transmural pressure. *Graefe's Archive for Clinical and Experimental Ophthalmology*, 224:477–480.

Bibliography

- La Rovere, M. T., Specchia, G., Mortara, A., and Schwartz, P. J. (1988). Baroreflex sensitivity, clinical correlates, and cardiovascular mortality among patients with a first myocardial infarction. A prospective study. *Circulation*, 78(4):816–24.
- Langewitz, W., Rüdgel, H., and Schächinger, H. (1994). Reduced parasympathetic cardiac control in patients with hypertension at rest and under mental stress. *American Heart Journal*, 127(1):122 – 128.
- Lanigan, L., Clark, C., and Hill, D. (1988). Retinal circulation responses to systemic autonomic nerve stimulation. *Eye (London, England)*, 2:412–417.
- Lanzl, I., Seidova, S., Maier, M., Lohmann, C., Schmidt-Trucksäss, A., Halle, M., and Kotliar, K. (2011). Dynamic retinal vessel response to flicker in age-related macular degeneration patients before and after vascular endothelial growth factor inhibitor injection. *Acta Ophthalmologica*, 89:472–479.
- Lasta, M., Palkovits, S., Boltz, A., Schmidl, D., Kaya, S., Cherecheanu, A. P., Garhöfer, G., and Schmetterer, L. (2012). Reproducibility of retinal vessel oxygen saturation measurements in healthy young subjects. *Acta Ophthalmologica*, 90:e616–e620.
- Lasta, M., Pemp, B., Schmidl, D., Boltz, A., Kaya, S., Palkovits, S., Werkmeister, R., Howorka, K., Popa-Cherecheanu, A., Garhöfer, G., and Schmetterer, L. (2013). Neurovascular Dysfunction Precedes Neural Dysfunction in the Retina of Patients with Type 1 Diabetes. *Investigative Ophthalmology & Visual Science*, 54(1):842–847.
- Leatham, A. (1949). The retinal vessels in hypertension. *QJM*, 18(3):203–215.
- Lee, B. B., Pokorny, J., Smith, V. C., Martin, P. R., and Valberg, A. (1990). Luminance and chromatic modulation sensitivity of macaque ganglion cells and human observers. *JOSA A*, 7(12):2223–2236.
- Li, Y., Wang, J.-G., Dolan, E., Gao, P.-J., Guo, H.-F., Nawrot, T., Stanton, A. V., Zhu, D.-L., O'Brien, E., and Staessen, J. A. (2006). Ambulatory Arterial Stiffness Index Derived From 24-Hour Ambulatory Blood Pressure Monitoring. *Hypertension*, 47(3):359–364.
- Lombardi, F., Malliani, A., Pagani, M., and Cerutti, S. (1996). Heart rate variability and its sympatho-vagal modulation. *Cardiovascular research*, 32(2):208–216.
- Lotmar, W., Freiburghaus, A., and Bracher, D. (1979). Measurement of vessel tortuosity on fundus photographs. *Graefe's Archive for Clinical and Experimental Ophthalmology*, 211:49–57.
- Lott, M. E. J., Slocomb, J. E., Shivkumar, V., Smith, B., Gabbay, R. A., Quillen, D., Gardner, T. W., and Bettermann, K. (2012). Comparison of retinal vasodilator and constrictor responses in

Bibliography

- type 2 diabetes. *Acta Ophthalmologica*, 90(6):e434–e441.
- Lucini, D., Mela, G. S., Malliani, A., and Pagani, M. (2002). Impairment in cardiac autonomic regulation preceding arterial hypertension in humans: Insights from spectral analysis of beat-by-beat cardiovascular variability. *Circulation*, 106(21):2673–2679.
- Luscher, T. F. (1994). The Endothelium and Cardiovascular Disease – A Complex Relation. *N Engl J Med*, 330(15):1081–1083.
- Mahler, F., Saner, H., Boss, C., and Annaheim, M. (1987). Local cold exposure test for capillaroscopic examination of patients with Raynaud's syndrome. *Microvascular research*, 33(3):422–427.
- Malik, M., Bigger, J. T., Camm, A. J., Kleiger, R. E., Malliani, A., Moss, A. J., and Schwartz, P. J. (1996). Heart rate variability: Standards of measurement, physiological interpretation, and clinical use. *European Heart Journal*, 17(3):354–381.
- Malliani, A. (2005). Heart rate variability: from bench to bedside. *European Journal of Internal Medicine*, 16(1):12 – 20.
- Man, R. E. K., Kawasaki, R., Wu, Z., Luu, C. D., Wang, J. J., Wong, T. Y., and Lamoureux, E. L. (2013). Reliability and Reproducibility of Retinal Oxygen Saturation Measurements using a Predefined Peri-papillary Annulus. *Acta Ophthalmologica*, 91:e590–e594.
- Mancia, G., De Backer, G., Dominiczak, A., Cifkova, R., Fagard, R., Germano, G., Grassi, G., Heagerty, A. M., Kjeldsen, S. E., Laurent, S., Narkiewicz, K., Ruilope, L., Rynkiewicz, A., Schmieder, R. E., Struijker Boudier, H. A., Zanchetti, A. t., Vahanian, A., Camm, J., De Caterina, R., Dean, V., Dickstein, K., Filippatos, G., Funck-Brentano, C., Hellems, I., Kristensen, S. D., McGregor, K., Sechtem, U., Silber, S., Tendera, M., Widimsky, P., Zamorano, J. L., Kjeldsen, S. E., Erdine, S., Narkiewicz, K., Kiowski, W., Agabiti-Rosei, E., Ambrosioni, E., Cifkova, R., Dominiczak, A., Fagard, R., Heagerty, A. h. M., Laurent, S., Lindholm, L. H., Mancia, G., Manolis, A., Nilsson, P. M., Redon, J., Schmieder, R. E., Struijker-Boudier, H. A., Viigimaa, M., Filippatos, G., Adamopoulos, S., Agabiti-Rosei, E., Ambrosioni, E., Bertomeu, V., Clement, D., Erdine, S., Farsang, C., Gaita, D., Kiowski, W., Lip, G., Mallion, J.-M., Manolis, A. J., Nilsson, P. M., O'Brien, E., Ponikowski, P., Redon, J., Ruschitzka, F., Tamargo, J., van Zwieten, P., Viigimaa, M., Waeber, B., Williams, B., and Zamorano, J. L. (2007). 2007 Guidelines for the management of arterial hypertension. *European Heart Journal*, 28(12):1462–1536.
- Mandecka, A., Dawczynski, J., Blum, M., Müller, N., Kloos, C., Wolf, G., Vilser, W., Hoyer, H., and Müller, U. A. (2007). Influence of Flickering Light on the Retinal Vessels in Diabetic Patients. *Diabetes Care*, 30(12):3048–3052.

Bibliography

- Mandecka, A., Dawczynski, J., Vilser, W., Blum, M., Müller, N., Kloos, C., Wolf, G., and Müller, U. A. (2009). Abnormal retinal autoregulation is detected by provoked stimulation with flicker light in well-controlled patients with type 1 diabetes without retinopathy. *Diabetes Research and Clinical Practice*, 86(1):51 – 55.
- Mehlsen, J., Jeppesen, P., Erlandsen, M., Poulsen, P. L., and Bek, T. (2011). Lack of effect of short-term treatment with Amlodipine and Lisinopril on retinal autoregulation in normotensive patients with type 1 diabetes and mild diabetic retinopathy. *Acta Ophthalmologica*, 89:764–768.
- Millar-Craig, M., Bishop, C., and Raftery, E. (1978). Circadian variation of blood pressure. *The Lancet*, 311(8068):795 – 797.
- Moore, R. F. (1916). The Retinitis of Arterio-Sclerosis, and Its Relation to Renal Retinitis and to Cerebral Vascular Disease. *QJM*, 08-10(37-38):29–77.
- Muench, K., Vilser, W., and Senff, I. (1995). Adaptive Algorithms for the Automatic Measurement of Retinal Vessel Diameters. *Biomedizinische Technik*, 40(11):322–325.
- Murray, C. (1926). The physiological principle of minimum work applied to the angle of branching of arteries. *Proc Natl Acad Sci U S A*, 12(3):835–841.
- Nadar, S., Blann, A. D., and Lip, G. Y. (2004). Endothelial Dysfunction: Methods of Assessment and Application to Hypertension. *Current Pharmaceutical Design*, 10(29):3591–3605.
- Nagel, E. and Vilser, W. (2004). Autoregulative behavior of retinal arteries and veins during changes of perfusion pressure: a clinical study. *Graefe's Archive for Clinical and Experimental Ophthalmology*, 42:13–17.
- Nagel, E., Vilser, W., Fink, A., and Riemer, T. (2006a). Varianz der Netzhautgefäßreaktion auf Flickerlicht. *Der Ophthalmologe*, 103(2):114–119.
- Nagel, E., Vilser, W., Fink, A., Riemer, T., and Lanzl, I. (2006b). Blood pressure effects on retinal vessel diameter and flicker response: A 1.5-year follow-up. *European Journal of Ophthalmology*, 16(4):560–565.
- Nagel, E., Vilser, W., and Lanzl, I. (2004). Age, Blood Pressure, and Vessel Diameter as Factors Influencing the Arterial Retinal Flicker Response. *Investigative Ophthalmology & Visual Science*, 45(5):1486–1492.
- Nagel, E., Vilser, W., and Lanzl, I. (2005). Vergleich der Durchmesserreaktion retinaler Arterien und Venen auf Flickerlicht. *Der Ophthalmologe*, 102(8):787–793.

Bibliography

- Nguyen, T. T., Kreis, A. J., Kawasaki, R., Wang, J. J., Seifert, B.-U., Vilser, W., Nagel, E., and Wong, T. Y. (2009). Reproducibility of the Retinal Vascular Response to Flicker Light in Asians. *Current Eye Research*, 34(12):1082–1088.
- Nickla, D. L. and Wallman, J. (2010). The multifunctional choroid. *Progress in Retinal and Eye Research*, 29(2):144 – 168.
- Noon, J. P., Walker, B. R., Webb, D. J., Shore, A. C., Holton, D. W., Edwards, H. V., and Watt, G. C. (1997). Impaired microvascular dilatation and capillary rarefaction in young adults with a predisposition to high blood pressure. *J Clin Invest*, 99(8):1873–1879.
- Ogbuehi, K. C. and Almubrad, T. M. (2008). Accuracy and Reliability of the Keeler Pulsair EasyEye Non-Contact Tonometer. *Optometry & Vision Science*, 85(1):61–66.
- Pache, M., Nagel, E., and Flammer, J. (2002). Reproduzierbarkeit der Messungen mit dem Retinal Vessel Analyzer unter Optimalbedingungen Reproducibility of measurements with the retinal vessel analyzer under optimal conditions. *Klinische Monatsblätter für Augenheilkunde*, 219:523–527.
- Pagani, M., Lombardi, F., Guzzetti, S., Rimoldi, O., Furlan, R., Pizzinelli, P., Sandrone, G., Malfatto, G., Dell’Orto, S., and Piccaluga, E. (1986). Power spectral analysis of heart rate and arterial pressure variabilities as a marker of sympatho-vagal interaction in man and conscious dog. *Circulation Research*, 59(2):178–93.
- Panza, J. A., Quyyumi, A. A., Brush, J. E., and Epstein, S. E. (1990). Abnormal Endothelium-Dependent Vascular Relaxation in Patients with Essential Hypertension. *New England Journal of Medicine*, 323(1):22–27.
- Parr, J. (1974). Hypertensive generalised narrowing of retinal arteries. *Transactions of the Ophthalmological Society of New Zealand*, 26(0):55–60.
- Parr, J. and Spears, G. (1974a). General caliber of the retinal arteries expressed as the equivalent width of the central retinal artery. *American journal of ophthalmology*, 77(4):472–477.
- Parr, J. and Spears, G. (1974b). Mathematic relationships between the width of a retinal artery and the widths of its branches. *American journal of ophthalmology*, 77(4):478–483.
- Patel, S. R., Bellary, S., Qin, L., Gill, P., Taheri, S., Heitmar, R., Gibson, J. M., and Gherghel, D. (2011). Abnormal retinal vascular function and lipid levels in a sample of healthy UK South Asians. *British Journal of Ophthalmology*, 95:1573–1576.
- Patton, N., Aslam, T., MacGillivray, T., Dhillon, B., and Constable, I. (2006). Asymmetry of Retinal Arteriolar Branch Widths at Junctions Affects Ability of Formulæ to Predict Trunk Arteriolar Widths. *Investigative Ophthalmology & Visual Science*, 47(4):1329–1333.

Bibliography

- Patton, N., Maini, R., MacGillivray, T., Aslam, T. M., Deary, I. J., and Dhillon, B. (2005). Effect of Axial Length on Retinal Vascular Network Geometry. *American Journal of Ophthalmology*, 140(4):648.e1 – 648.e7.
- Pemp, B., Weigert, G., Karl, K., Petzl, U., Wolzt, M., Schmetterer, L., and Garhöfer, G. (2009). Correlation of Flicker-Induced and Flow-Mediated Vasodilatation in Patients With Endothelial Dysfunction and Healthy Volunteers. *Diabetes Care*, 32(8):1536–1541.
- Pickering, T. G., Gerin, W., and Schwartz, A. R. (2002). What is the white-coat effect and how should it be measured? *Blood pressure monitoring*, 7(6):293–300.
- Polak, K., Dorner, G., Kiss, B., Polska, E., Findl, O., Rainer, G., Eichler, H.-G., and Schmetterer, L. (2000). Evaluation of the Zeiss retinal vessel analyser. *British Journal of Ophthalmology*, 84(11):1285–1290.
- Polak, K., Schmetterer, L., and Riva, C. E. (2002). Influence of Flicker Frequency on Flicker-Induced Changes of Retinal Vessel Diameter. *Investigative Ophthalmology & Visual Science*, 43(8):2721–2726.
- Pournaras, C. J., Rungger-Brändle, E., Riva, C. E., Hardarson, S. H., and Stefansson, E. (2008). Regulation of retinal blood flow in health and disease. *Progress in Retinal and Eye Research*, 27(3):284 – 330.
- Quyyumi, A. A., Crake, T., Mockus, L. J., Wright, C. A., Rickards, A. F., and Fox, K. M. (1986). Value of the bipolar lead CM₅ in electrocardiography. *British Heart Journal*, 56(4):372–376.
- Reimann, M., Prieur, S., Lippold, B., Bornstein, S. R., Reichmann, H., Julius, U., and Ziemssen, T. (2009). Retinal vessel analysis in hypercholesterolemic patients before and after LDL apheresis. *Atherosclerosis Supplements*, 10(5):39 – 43. Proceedings from the 1st Dresden International Symposium on Therapeutic Apheresis: Recent progress in Therapeutic Apheresis.
- Resch, H., Zawinka, C., Weigert, G., Schmetterer, L., and Garhöfer, G. (2005). Inhaled Carbon Monoxide Increases Retinal and Choroidal Blood Flow in Healthy Humans. *Investigative Ophthalmology & Visual Science*, 46(11):4275–4280.
- Rickenbacher, I., Gugleta, K., Zawinka, C., Schötzau, A., Katamay, R., Flammer, J., and Orgül, S. (2009). Flickerlichtprovokation bei Vasospastikern verglichen mit gesunden Kontrollpersonen. *Klinische Monatsblätter für Augenheilkunde*, 226:305–309.
- Riva, C. E., Logean, E., and Falsini, B. (2005). Visually evoked hemodynamical response and assessment of neurovascular coupling in the optic nerve and retina. *Progress in Retinal and Eye Research*, 24(2):183 – 215.

Bibliography

- Rogers, K. (2010). *Blood: Physiology and Circulation*. The Rosen Publishing Group.
- Rogoza, A. N., Pavlova, T. S., and Sergeeva, M. V. (2000). Validation of A&D UA-767 device for the self-measurement of blood pressure. *Blood Pressure Monitoring*, 5(4):227–231.
- Rueddel, T., Kneser, M., and Tost, F. (2012). Impact of exercise on retinal microvascular regulation measured by dynamic vessel analysis in healthy individuals. *Clinical Physiology and Functional Imaging*, 32(2):158–161.
- Scheie, H. (1953). Evaluation of Ophthalmoscopic changes of Hypertension and Arteriolar Sclerosis. *AMA Arch Ophthalmol*, 49(2):117–138.
- Seifertl, B. U. and Vilser, W. (2002). Retinal Vessel Analyzer (RVA)–design and function. *Biomed Tech*, 47 Suppl 1 Pt 2:678–681.
- Serne, E. H., Gans, R. O., ter Maaten, J. C., Tangelder, G.-J., Donker, A. J., and Stehouwer, C. D. (2001). Impaired Skin Capillary Recruitment in Essential Hypertension Is Caused by Both Functional and Structural Capillary Rarefaction. *Hypertension*, 38(2):238–242.
- Shantsila, A., Shantsila, E., and YH Lip, G. (2010). Malignant Hypertension: A Rare Problem or is it Underdiagnosed? *Current Vascular Pharmacology*, 8(6):775–779.
- Shrout, P. and Fleiss, J. (1979). Intraclass correlations: uses in assessing rater reliability. *Psychological bulletin*, 86(2):420–428.
- Staessen, J. A., Wang, J., Bianchi, G., and Birkenhäger, W. H. (2003). Essential hypertension. *The Lancet*, 361(9369):1629 – 1641.
- Stanton, A., Wasan, B., Cerutti, A., Ford, S., Marsh, R., Sever, P., Thom, S., and Hughes, A. (1995). Vascular network changes in the retina with age and hypertension. *J Hypertens*, 13(12 Pt 2):1724–1728.
- Stokoe, N. and Turner, R. (1966). Normal retinal vascular pattern. Arteriovenous ratio as a measure of arterial calibre. *British Medical Journal*, 50(1):21–40.
- Stücker, M., Baier, V., Reuther, T., Hoffmann, K., Kellam, K., and Altmeyer, P. (1996). Capillary blood cell velocity in human skin capillaries located perpendicularly to the skin surface: measured by a new laser Doppler anemometer. *Microvascular research*, 52:188–192.
- Taarnhøj, N. C. B. B., Larsen, M., Sander, B., Kyvik, K. O., Kessel, L., Hougaard, J. L., and Sorensen, T. I. A. (2006). Heritability of Retinal Vessel Diameters and Blood Pressure: A Twin Study. *Investigative Ophthalmology & Visual Science*, 47(8):3539–3544.
- Taarnhøj, N. C. B. B., Munch, I. C., Sander, B., Kessel, L., Hougaard, J. L., Kyvik, K., Sørensen, T. I. A., and Larsen, M. (2008). Straight versus tortuous retinal arteries in relation to blood

Bibliography

- pressure and genetics. *British Journal of Ophthalmology*, 92(8):1055–1060.
- Taylor, J. A., Carr, D. L., Myers, C. W., and Eckberg, D. L. (1998). Mechanisms Underlying Very-Low-Frequency RR-Interval Oscillations in Humans. *Circulation*, 98(6):547–555.
- Verberk, W., Kroon, A., Jongen-Vancraybex, H., and De Leeuw, P. (2007). The applicability of home blood pressure measurement in clinical practice: A review of literature. *Vascular Health and Risk Management*, 3(6):959–966.
- Verdecchia, P. (2000). Prognostic Value of Ambulatory Blood Pressure: Current Evidence and Clinical Implications. *Hypertension*, 35(3):844–851.
- Waeber, B., Genoud, M., Feihl, F., Hayoz, D., and Waeber, G. (2007). Ambulatory blood pressure monitoring: a mean to stratify cardiovascular risk. *Blood Pressure Monitoring*, 12(4):263–265.
- Wallace, D. (2007). Computer-assisted quantification of vascular tortuosity in retinopathy of prematurity (an American Ophthalmological Society thesis). *Transactions of the American Ophthalmological Society*, 105:594–615.
- Walsh, J. (1982). Hypertensive retinopathy. Description, classification, and prognosis. *Ophthalmology*, 89(10):1127–1131.
- White, W. B., Berson, A. S., Robbins, C., Jamieson, M. J., Prisant, L. M., Roccella, E., and Sheps, S. G. (1993). National standard for measurement of resting and ambulatory blood pressures with automated sphygmomanometers. *Hypertension*, 21(4):504–509.
- Whitworth, J. (2003). 2003 World Health Organization (WHO)/International Society of Hypertension (ISH) statement on management of hypertension. *Journal of hypertension*, 21(11):1983–1992.
- Williams, B., Poulter, N., Brown, M., Davis, M., McInnes, G., Potter, J., Sever, P., and Thom, S. (2004). Guidelines for management of hypertension: report of the fourth working party of the British Hypertension Society, 2004–BHS IV. *Journal of Human Hypertension*, 18(3):139–185.
- Williams, T. (1982). Quantification of arteriolar tortuosity in two normotensive age groups. *American journal of optometry and physiological optics*, 59(8):675–679.
- Wimpissinger, B., Resch, H., Berisha, F., Weigert, G., Schmetterer, L., and Polak, K. (2004). Response of choroidal blood flow to carbogen breathing in smokers and non-smokers. *British Journal of Ophthalmology*, 88(6):776–781.
- Witt, N. W., Chapman, N., Thom, S. A. M., Stanton, A. V., Parker, K. H., and Hughes, A. D. (2010). A novel measure to characterise optimality of diameter relationships at retinal vascular

Bibliography

- bifurcations. *Artery Research*, 4(3):75 – 80.
- Wong, T. Y., Wang, J. J., Rochtchina, E., Klein, R., and Mitchell, P. (2004). Does refractive error influence the association of blood pressure and retinal vessel diameters? The Blue Mountains Eye Study. *American Journal of Ophthalmology*, 137(6):1050 – 1055.
- Yu, P. K., Yu, D.-Y., Alder, V. A., Seydel, U., Su, E.-N., and Cringle, S. J. (1997). Heterogeneous Endothelial Cell Structure Along the Porcine Retinal Microvasculature. *Experimental Eye Research*, 65(3):379 – 389.
- Yvonne-Tee, G. B., Rasool, A. H. G., Halim, A. S., and Rahman, A. R. A. (2006). Noninvasive assessment of cutaneous vascular function in vivo using capillaroscopy, plethysmography and laser-Doppler instruments: Its strengths and weaknesses. *Clinical Hemorheology and Microcirculation*, 34(4):457-473.
- Zamir, M., Medeiros, J. A., and Cunningham, T. K. (1979). Arterial bifurcations in the human retina. *The Journal of General Physiology*, 74(4):537-548.

Acronyms

AASI	Ambulatory Arterial Stiffness Index	17
ABPM	Ambulatory Blood Pressure Monitoring	17
ACE	Angiotensin Converting Enzyme	94
AECG	Ambulatory Electrocardiography	19
ANOVA	Analysis of Variance	77
ANS	Autonomic Nervous System	13
APR	Average Peak Ratio	38
ARIC	Atherosclerosis Risk In Communities	30
AV	Atrioventricular	12
AVR	Arterio-Venous Ratio	30
BDF	Baseline Diameter Fluctuation	38
bFR	Baseline-Corrected Flicker Response	38
BP	Blood Pressure	12
CCD	Charged-Coupled Device	34
CO	Cardiac Output	12
CRA	Central Retinal Artery	26
CRAE	Central Retinal Artery Equivalent	29
CRV	Central Retinal Vein	26
CRVE	Central Retinal Vein Equivalent	30
CSV	Comma-separated Values	76
CT	Constriction Time	38
CV	Coefficient of Variation	43
CVD	Cardio-Vascular Disease	36
DA	Dilation Amplitude	38
DBP	Diastolic Blood Pressure	14
DD	Disk Diameter	30
ECG	Electrocardiogram	17
FMD	Flow-Mediated Dilation	71

Acronyms

HRV	Heart Rate Variability	19
HF	High Frequency	22
HR	Heart Rate	12
HT	Hypertension	17
ICC	Intraclass Correlation Coefficient	35
IOP	Intraocular Pressure	27
IQR	Inter-Quartile Range	50
LDR	Length-to-Diameter Ratio	34
LED	Light-emitting Diode	47
LF	Low Frequency	22
MABP	Mean Arterial Blood Pressure	15
MC	Maximum Constriction	38
MD	Maximum Dilation	38
MU	Measuring Units	35
NN	Normal-to-Normal	21
NO	Nitric Oxide	13
OD	Optical Density	40
ODR	Optical Density Ratio	40
ONH	Optic Nerve Head	26
OPP	Ocular Perfusion Pressure	27
PNS	Parasympathetic Nervous System	12
PP	Pulse Pressure	15
PSD	Power Spectral Density	22
RT	Reaction Time	38
RVA	Retinal Vessel Analyser	34
SA	Sinoatrial	11
SBP	Systolic Blood Pressure	14
SD	Standard Deviation	37
SITA	Swedish Interactive Thresholding Algorithm	40
SNS	Sympathetic Nervous System	12
OSat	Oxygen Saturation	35
SV	Stroke Volume	15
SVR	Systemic Vascular Resistance	12
TIFF	Tagged Image File Format	47
VF	Visual Field	40
VLF	Very Low Frequency	22

Page removed for copyright restrictions.